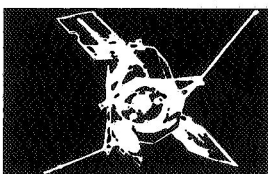
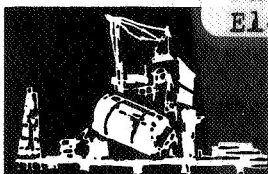
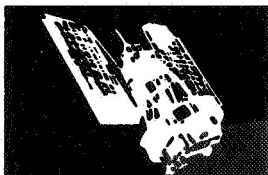
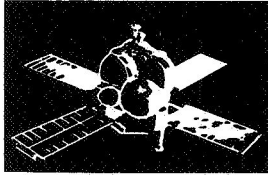
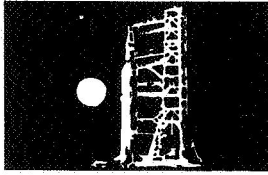
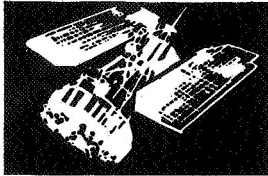


SPACE DIVISION



DEVELOPMENT OF CONTAINERLESS PROCESS FOR PREPARATION OF TUNGSTEN WITH IMPROVED SERVICE CHARACTERISTICS

FINAL REPORT

Contract No. NAS8-29879

November, 1975

Prepared For

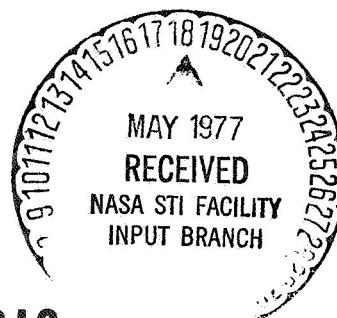
National Aeronautics and Space Administration
George C. Marshall Space Flight Center

(NASA-CR-150256) DEVELOPMENT OF
CONTAINERLESS PROCESS FOR PREPARATION OF
TUNGSTEN WITH IMPROVED SERVICE
CHARACTERISTICS Final Report (General
Electric Co.) 109 p

N77-77629

Unclas
00/26 26069

Space Sciences Laboratory
General Electric Space Division
P.O. Box 8555, Philadelphia, Pa. 19101



GENERAL  ELECTRIC

DEVELOPMENT OF CONTAINERLESS PROCESS
FOR PREPARATION OF TUNGSTEN WITH
IMPROVED SERVICE CHARACTERISTICS

FINAL REPORT

Contract No. NAS8-29879

November 1975

Prepared for

National Aeronautics and Space Administration
George C. Marshall Space Flight Center

Prepared by

G. Wouch, Principle Investigator
R. T. Frost, Manager - Earth Orbit
Applications Programs

D. J. Rutecki
N. Beser
E.C. Okress

Space Sciences Laboratory
General Electric Space Division
P.O. Box 8555, Philadelphia, Pa. 19101

TABLE OF CONTENTS

Foreword-----	vii
Abstract-----	ix
1.0 Introduction-----	1
1.1 Objectives-----	1
1.2 Containerless Processing Of Tungsten And Other Metals And Alloys-----	3
1.3 Contribution Of The Work-----	7
1.4 Factors Influencing The Service Properties Of Tungsten-----	9
1.4.1 The Metal Tungsten And Its Applications-----	9
1.4.2 Service Properties Of Tungsten-----	10
1.4.3 Origin Of Undesirable Service Properties Of Tungsten At Temperatures Below The Ductile-Brittle Transition Temperature-----	11
1.4.4 Extrinsic Factors Below The DBTT-----	12
1.4.5 Intrinsic Factors and Temperatures Below the DBTT---	22
1.4.6 Controlling Mechanisms in Tungsten Below the DBT----	25
1.4.7 Service Properties of Tungsten Above the DBTT-----	26
1.4.8 Enhancing the Service Properties Of Unalloyed Tungsten-----	30
2.0 Levitation System Apparatus-----	32
2.1 Glass Levitation System -----	33
2.2 Stainless Steel Levitation System-----	40
3.0 Levitation Experiments: Solid State-----	47
3.1 High Temperature Vacuum Degassing-----	47
3.2 Levitation of Solid Tungsten-----	53
3.2.1 Procedure-----	54
3.2.2 Experimental Results-----	55
3.3 Experiments With Solid Tungsten In The Stainless Steel System-----	60
4.0 Levitation Experiments: Molten State-----	62
4.1 Procedure-----	65
4.2 Specimens Solidified While Levitated-----	66
4.2.1 Characterization of Single Crystals Produced By Solidification While Levitated-----	70

	<u>Page</u>
4.3 Specimens Solidified Through Falling Onto A Water Cooled Copper Plate While Molten-----	77
4.4 Specimens Solidified By Dropping Into Molten Tin-----	77
4.5 Specimens Freely Falling-----	84
4.6 Containerless Vapor Deposition-----	84
5.0 Evaluation and Analysis-----	87
5.1 Re-evaluation Of BUS Study Of Tungsten Targets Produced In Space-----	90
5.2 General Electric Effort On Specimens Characterization-----	92
5.3 Conclusions-----	93
5.4 Recommendations-----	94
References-----	95

FIGURES

	<u>Page</u>
Figure 1 Effect Of Temperature On Flow And Fracture Characteristics Of Tungsten. Powder-Metallurgy Tungsten (200 PPM C; 80 PPM N)	13
Figure 2 Variation Of Yield Stress And Fracture Stress For Melted Tungsten	13
Figure 3 Effect Of Temperature And Intentionally Induced Microcracks On The Deformation Behavior Of Tungsten	15
Figure 4 Effect Of Temperature On Yield Stress Of Tungsten Single Crystals Having Various Orientations	15
Figure 5 Effect Of Strain Rate On Yield Stress Of Tungsten At 525 K ($0.14T_M$)	18
Figure 6 Effect Of Strain Rate On Ductile-Brittle Transition Temperature Of Tungsten	18
Figure 7 Strain Rate Sensitivity Of Unalloyed, Arc-Melted Tungsten	19
Figure 8 Effect Of Grain Size On The Ductile-Brittle Transition Temperature Of Tungsten	19
Figure 9 Variation Of Yield Stress With Grain Size At 500K	20
Figure 10 Effects Of Oxygen And Carbon On Ductile-Brittle Transition Temperature Of Single-Crystal And Polycrystalline Tungsten	20
Figure 11 Effects Of Oxygen And Carbon On Yield Stress Of Single-Crystal And Polycrystalline Tungsten	21
Figure 12 Stress-Strain Curves For Single-Crystal Tungsten At 300K	21
Figure 13 An Increase In Dislocation Density With Plastic Strain For Single-Crystal Tungsten Having Various Orientations	23
Figure 14 Variation Of Dislocation Density With Strain For Polycrystalline Tungsten	23
Figure 15 Strength Of High Temperature Metals	27
Figure 16 Ultimate Tensile Stress Of Refractory Metals	27

	<u>Page</u>
Figure 17 Stress-Rupture Strength For 10-hr Life	28
Figure 18 Summary Of High-Temperature Deformation Of The Group VI _A Refractory Metals (Melted Material Only)	28
Figure 19 Stress At $= 10^{-6} \text{ Sec}^{-1}$ vs T/T_M For Group V _A And Group VI _A Metals (Melted Material Only)	29
Figure 20 Stress At 10^{-6} Sec^{-1} vs T/T_M For Arc-Cast And Metallurgy Group VI _A Metals	29
Figure 21 Glass Levitation System	34
Figure 22 Copper End Plate With Coil Assembly And Pedastal Assembly	36
Figure 23 Pedastal Assembly With Specimen Inserted In Levitation Coil	37
Figure 24 Copper End Plate Exterior View	38
Figure 25 Levitated Solid Tungsten Specimen (2600°C)	39
Figure 26 Stainless Steel Levitation Chamber With Electron Beam Heating Unit	41
Figure 27 Four Foot Drop Tube	42
Figure 28 Solid State Imaging Array	43
Figure 29 Stainless Steel Levitation System (Video Display Of Levitated Specimen)	44
Figure 30 Melting Sequence With Progressive Elongation Of Levitated Molten Tungsten Specimen. Electron Beam Strikes Specimen At Its Top And Melting Progresses Downward	46
Figure 31 Micrograph Of Starting Tungsten Material. Magnification Is 150x	49
Figure 32 Micrograph Of Tungsten Specimen Held At 1800°C For One Hour.	49
Figure 33 Micrograph Of Tungsten Specimen Held at 1900°C For Two Hours. Magnification 150x	51

	<u>Page</u>
Figure 34 Micrograph Of Tungsten Specimen Held At 2000°C For One Hour. Magnification 150X	51
Figure 35a X-ray Laue Pattern Of Initial Starting Tungsten Material By Back Reflection	52
Figure 35b X-ray Laue Pattern Of Recrystallized Tungsten After Being Held At 2000°C For One Hour.	52
Figure 36 Pressure Rise Curves For Outgassing Solid Tungsten At 2600°C	56
Figure 37 Recrystallization At The Melting Point. Partial Melting Observed At Tor.	61
Figure 38 Exterior Of Specimen Solidified While Levitated. The Grid Is A Millimeter Grid To Show True Size	67
Figure 39 Single Crystal With Low Angle Grain Boundary. Orientation Determined By Single Crystal Orienter. Single Crystal Determined By X-ray Diffractometry And Back Reflection A Cross Low Angle Grain Boundary.	68
Figure 40 Single Crystal With No Macroscopic Subgrain Structure Evident	69
Figure 41a Bicrystal With Evidence Of Nucleation Starting At Tip	71
Figure 41b Polycrystalline Specimen Solidified By Impacting Stabilizing Ring	71
Figure 42 Micrograph Of Figure 39 Specimen Showing Subgrain Structure After Etching And Polishing. Magnification 1000x	73
Figure 43 Micrograph Of Figure 40 Specimen After Further Electro Polishing And Etching Showing Low Angle Grain Boundary Magnification 1230x	73
Figure 44 Single Crystal Laue Patterns By Back Reflection.	74
Figure 45a Asterism In Laue Pattern After Deformation By Compression	75
Figure 45b Slip Produced By Same Compressive Deformation	75
Figure 46 Stress-Strain Curve Incompression For Starting Material And Single Crystal Produced By Levitation	76

	<u>Page</u>
Figure 47 Specimen Solidified Through Falling Onto A Water Cooled Copper Plate While Molten	78
Figure 48a Small Satellite Drop Sectioned, Etched, And Polished Magnification 50x	79
Figure 48b Small Satellite Drop Sectioned, Etched, And Polished Magnification 50x	79
Figure 49 Specimen Solidified By Falling Into Molten Tin	80
Figure 50 Specimen Solidified By Falling Into Molten Tin	81
Figure 51 Fine Grained Regions Of Specimen Solidified By Falling Into Molten Tin	82
Figure 52 Fine Grained Regions Of Specimen Solidified By Falling Into Molten Tin	83
Figure 53 Vapor Deposited Tungsten Onto Molybdeum Substrate From Containerless Melt	85
Figure 54 Molten Drop With Electron Beam Impinging At Top	87
Figure 55 Solid-Liquid Interface Shape Which Prevents Stray Nuclei From Growing Into Melt	88
Figure 56 Nucleation and Grain Growth Versus Degree of Supercooling	89

FOREWORD

Prior work by Walker*, Stuhr**, and Frawley and Childs*** indicated that by achieving a high degree of supercooling in melts of metals and alloys and with initiation of nucleation at these supercooled temperatures, significant grain refinement would occur upon solidification and a fine grained structure would be produced.

In light of the desirable mechanical properties resulting from this fine grained structure such as enhanced ductility and fabricability at room temperatures the achievement of this goal would be extremely important.

Achievement of this goal is very difficult terrestrially and has only been achieved for metals of relatively low melting point such as nickel. With the high temperature refractory metals such as tungsten with a melting point of 3410°C this goal has not been achieved terrestrially with bulk melts of tungsten.

The driving factor for achieving this goal is the new or better products that would result from the availability of refractory metals such as tungsten with enhanced room temperature ductility coupled with high temperature strength. One such product is a more ductile tungsten for use as targets in x-ray tubes. A highly interested and involved user is GE's X-ray Systems Product Department, one of the largest x-ray tube manufacturers in the country.

It was postulated that with a levitated melt of tungsten, free from contamination by crucible walls and free from sites of heterogenous nucleation on crucible walls that this goal could be obtained with small specimens of one centimeter in diameter and with larger specimens in the weightless environment of space,

large enough to be fabricated into x-ray targets.

It was in that spirit that this work was begun. As reported herein, many surprises resulted during the work and the results show that serendipity in research can often lead to entirely unexpected progress. It is felt that the results obtained to date require further investigation and that the need to conduct such work in the weightless environment of space has been definitely established to obtain the desired goal.

* Walker, J. L., Physical Chemistry of Process Metallurgy, St. Pierre, G.R., editor, Interscience, New York, 1959, p 845

** Stuhr, D. M. S. Thesis, Rennselaer Polytechnic Institute, New York, 1962

*** Frawley, J. J. and Childs, W. J., Trans Met Soc., AIME, 242, pp 256, 1968

ABSTRACT

Reported herein is the completion of a unique facility combining electromagnetic levitation and electron beam melting to levitation melt tungsten, not heretofore reported in the literature. The results of experiments performed with levitated molten tungsten and with molten tungsten freely falling are reported. A new technique for the growth of single crystals of tungsten, which may have application to other materials is also reported. A new technique for vapor deposition of tungsten onto molybdenum substrates from a levitated, superheated melt is described. The rationale for development of these techniques in the weightless environment of space in terms of scale up in size and stability of terrestrially levitated, superheated melts is discussed. Three routes to the production of tungsten x-ray targets with enhanced service properties are presented. The rationale for improvements in the service properties of tungsten as an x-ray target material as well as for other applications is reviewed.

From the results obtained to date, the necessity of continuing this work terrestrially and in the weightless environment of space is discussed.

Significant differences in the behavior of molten tungsten while freely falling or while cooling while levitated have been observed, demonstrating that experiments in the weightless environment of space may yield significant differences in solidification structures by achievement of large amounts of supercooling.

That production of tungsten x-ray targets from large single crystals, from fine grained material obtained by grain refinement through solidification of super-cooled melts, or by vapor deposition onto molybdenum substrates from a super-heated tungsten melt requires the weightless environment of space in terms of scale up and obtainable superheats is considered and recommendations for further work are presented.

DEVELOPMENT OF CONTAINERLESS PROCESS
FOR PREPARATION OF TUNGSTEN WITH
IMPROVED SERVICE CHARACTERISTICS

1.0 INTRODUCTION AND CONTRIBUTION

1.1 OBJECTIVES

The objectives of the work reported herein were:

1. To investigate the improvement of the service properties of tungsten through a process involving the steps of vacuum purification, vacuum melting, supercooling the melt, and initiation of nucleation at the desired nucleation temperature to achieve grain refinement.
2. Establishment of the limitations of ground based levitation heating and melting of tungsten in order to evaluate the advantages of processing in the weightless environment of space.
3. To supply the necessary knowledge for conceptual development of a space processing experiment to produce tungsten with improved service qualities.

At the beginning of this effort, it was not known whether or not tungsten could be levitation melted and what the results of such a process would be.

It was hoped that through purification of the tungsten and by achieving a high degree of undercooling that a high purity, fine grained tungsten could be produced which could be worked at room temperature to fabricate such components as tungsten x-ray targets. Prior research by the General Electric Medical X-ray Division had indicated three routes to production of a better x-ray target. These were.

1. Monocrystal x-ray targets
2. Vapor deposited x-ray targets
3. Fine grained high purity x-ray targets

A great deal of research has gone into the first two of these routes without success. Single crystal tungsten tended to fracture catastrophically and good vapor deposited targets had yet to be made. The third route was new and had yet to be investigated.

During the performance of the work reported herein, the possibility of enhancing the service properties of tungsten through each of these three routes and the rationale for processing based on each route was investigated experimentally with a unique facility constructed for this purpose, to be described below and, conceptually from the standpoint of economic viability, high success probability, and the rationale for zero-g processing. At the beginning of this work, the possibility of growing single crystals of tungsten of high perfection or the possibility of vacuum vapor deposition of tungsten onto molybdenum was not considered. As the work progressed, it became apparent that these routes were both accessible from containerless processing and also desirable from the standpoint of fabricating better tungsten x-ray targets.

At the same time, it also became apparent that a new and unique technique for the growth of single crystals had been demonstrated with the metal tungsten and that a new technique for vacuum vapor deposition onto substrates from superheated levitated melts had been demonstrated also. These techniques may be extended to grow large single crystals of other materials or to produce thin films of materials of very high purity and desirable grain size for device applications.

That ground based containerless processing is limited as to the specimen size, the available superheat before specimen loss from the levitation coil, and the amount of supercooling attainable was delineated during the work performed. With the work in the 4-foot section of drop tube it was readily demonstrated that in the weightless environment, free from the constraints imposed by terrestrial levitation, large amounts of supercooling could be obtained. Thus the work reported herein leads to the conclusion that processing in the weightless environment of space may be desirable to achieve the goal of producing tungsten x-ray targets with enhanced service properties through any of the three routes discussed

1.2 CONTAINERLESS PROCESSING OF TUNGSTEN AND OTHER METALS AND ALLOYS

Containerless processing of metals via electromagnetic levitation melting was first suggested by Muck in 1923 (Ref. 1). The first successful electromagnetic levitation of a solid conducting body was accomplished by Peer and Tonks of the General Electric Company in 1936 (Ref. 2). The first successful electromagnetic levitation melting of metals was accomplished by Okress, et. al., of the Westinghouse Electric Corporation in 1952 (Ref. 3). Since that time electromagnetic levitation melting of metals has become a standard laboratory tool used for:

1. the preparation of metals and alloys of high purity and uniformity for laboratory investigations.
2. the study of liquid metal-gas interactions
3. the study of the solidification of metals and alloys
4. the measurement of the physical properties of metals and alloys

Limitations in the size of the metal charge that can be levitated terrestrially have prevented containerless processing of metals from being applied to commercial processes. With the advent of the NASA Space Processing Program,

which can exploit the weightless environment of space, where objects are naturally levitated in free fall, large charges of material can be processed. The restriction to materials having metallic conductivity is also removed. During the NASA contract NAS8-29680, the General Electric Company Space Sciences Laboratory investigated the capabilities of electromagnetic containerless processing in the weightless environment of space and delineated the prospects for processing new materials presently not accessible to terrestrial containerless processing (Ref. 4). The extension of containerless processing to materials of resistivity 5 decades above metallic conductors or those which could be preheated to resistivities within 5 decades of metallic conductors appears to have opened up an entirely new era for containerless processing.

The advantages of containerless processing of metals, especially for the high melting temperature and/or reactive metals are:

1. elimination of sources of contamination from the crucible by elimination of the crucible.
2. elimination of sites for heterogenous nucleation by elimination of crucible walls, thus enabling achievement of large amounts of supercooling in very pure melts.
3. Achieving homogeneity of the melt due to very efficient electromagnetic stirring in terrestrial levitation.
4. retention of homogeneity in the melt due to the rapidity of solidification.
5. rapid attainment of equilibrium in gas-liquid metal systems.
6. rapid purification in high vacuum conditions.
7. rapid heating and melting permitting a large number of melts per day with a large number of varied melt parameters.
8. rapid consolidation of compacts of pressed and/or sintered powders.

The disadvantages of terrestrial containerless processing have been:

1. limited temperature control of the levitated melt
2. difficulties with temperature measurement
3. Rapid vaporization of vapor pressure elements due to large surface to

to volume ratio and rapid stirring.

4. small size of charge that can be levitated

5. limited amount of superheating that can be obtained for vapor deposition. During the work reported herein the first disadvantage has been eliminated for the high melting temperature metals such as tungsten by a unique combination of electromagnetic levitation and electron beam heating.

The development of this unique facility and the first successful levitation melting of tungsten was reported to the scientific community during the work reported herein(Ref. 5). During the work reported herein, some progress was made in overcoming the second difficulty. The fourth difficulty can be overcome by processing in the weightless environment of space. The third difficulty is fundamental in the preparation of many important compounds, such as the III-V semiconductors. It appears likely that this can be overcome by containerless processing under high pressure of the volatile component or a combination of volatile and inert gas to reduce evaporation of the volatile component. In many instances, when considering vapor deposition from a containerless melt onto a substrate, superheating the melt to attain a high vaporization rate is highly desirable. From the work on tungsten, it appears that there is a limit to the amount of superheating that can be obtained in terrestrial levitation before the specimen is lost. In the weightless environment of space no such limitation would exist.

The consolidation of tungsten by arc casting or electron beam melting has generally proved inferior to powder metallurgical techniques. The material is more pure but, because of its coarse grained nature, is brittle and requires primary working before it can be used commercially (Ref. 6). Casting into water cooled copper crucibles has also proved unsatisfactory (ref. 7) producing very brittle ingots. As there are no other crucible materials which can contain molten tungsten, which melts at 3410°C (6170°F), without severe contamination to the tungsten, containerless processing offers the best possibility of controlling the microstructure of tungsten by varying the conditions under which it is solidified. By suitably controlling the conditions, a large variety of microstructures from fine grained to single crystal may be obtained, and it is this prospect which was the driving factor in the work reported herein. The terrestrial limitations in achieving this wide variety of microstructures became apparent as the work progressed and the work in the drop tube provided convincing evidence that only in the weightless environment of space could this complete control of microstructure be realized.

Through powder metallurgical techniques, a variety of refractory metals and alloys have been produced with useful service properties. In order to successfully compete with this technique, containerless processing must offer some definite advantages. It appears likely that this is indeed the case in several areas. The particular case in point is the production of x-ray targets with enhanced service characteristics. There control of microstructure to achieve enhanced ductility and high temperature strength without addition of costly alloying agents such as rhenium would significantly simplify the fabrication and increase the exposure lifetime of the target. This

will be discussed fully below. As has been discussed above, three routes to achieve this were proposed. As the work has progressed, it appears likely that the vapor deposition method is the favored technique with the single crystal method a close second. The high recrystallization rate of tungsten at the temperature of operation of the x-ray target observed during the work reported herein raise definite problems for the fine grained material approach.

1.3 CONTRIBUTION OF THE WORK

The contributions of the work reported herein are:

1. The successful levitation melting of tungsten, heretofore not possible.
2. The development of a new technique to grow single crystals of metals and alloys.
3. The development of a new technique for vapor deposition of high purity metals and alloys onto suitable substrates.
4. The development of a unique apparatus combining electromagnetic levitation and electron beam melting for containerless processing of high temperature materials.
5. The investigation of the limitations of terrestrial levitation for producing materials of controlled microstructure and for vapor deposition of materials onto substrates.
6. Through work in the drop tube, verification that in the weightless environment of space, large amounts of supercooling can be achieved.
7. Verification that electron beam heating and melting of levitated solids of high melting temperature is feasible.
8. Progress in observation of containerless processing through television viewing and videotape recording.

9. Progress in temperature measurement through observation with an imaging solid state array.

It is felt that these contributions have both advanced the state of terrestrial levitation and have shown the necessity for space processing of materials in terms of the basic limitations of terrestrial levitation.

1.4 FACTORS INFLUENCING THE SERVICE PROPERTIES OF TUNGSTEN

1.4.1 The Metal Tungsten and Its Applications

The metal tungsten, one of the "less-common metals," is found in group VI-A of the Periodic Table of Elements. Its behavior is most closely related to molybdenum, which is another member of that group. Tungsten has the highest melting point of all metals (3410°C) and few other compounds have higher melting temperatures. The metal has excellent conductivity for heat and electricity and exhibits good high temperature mechanical properties.

The high melting point of tungsten and its good electrical conductivity made possible the efficient production of visible light via the incandescent electric light bulb, once ductile tungsten wire became available. The present largest users of tungsten are in the steel industry as an alloying element and in the hard metals industry for cemented carbides. These industries consume about two-thirds of the tungsten produced in this country each year.

Although the amount of tungsten produced each year is small, the applications of tungsten are essential to our society. The principal applications of tungsten at the present time other than the steel industry and the hard metals industry are:

1. Lamp filaments and strips
2. Cathodes and anticathodes
3. X-ray targets and grids
4. X-ray protection
5. Interrupters and contacts
6. Nozzles and heat shields for rockets
7. Thermocouple-elements
8. Field Ion microscope
9. Laboratory equipment; high temperature structures

10. welding electrodes
11. Automobile and airplane ignition systems
12. Emitter surface for thermionic diodes
13. Cladding for fuel elements for nuclear power generation in space
14. Spark plug points

and many other applications. For these applications high purity even when alloyed with other metals such as rhenium, fabricability, and good mechanical properties at high temperature are essential. Generally the device applications of tungsten make use of the following properties of the metal:

1. High melting temperature
2. Good heat conductivity
3. Good electrical conductivity
4. High atomic number

Ideally, for the production of tungsten medical x-ray targets and other devices, the tungsten material should be:

1. Fabricable at room temperature without special techniques
2. Have good high temperature strength (creep, rupture, etc.)

The present state of the art in fabricating medical x-ray targets is an expensive tungsten/10% rhenium layer bonded to a molybdenum substrate. It has been postulated that improvements in the fabrication of tungsten x-ray targets and enhancement in exposure lifetime would result from the development of a more ductile tungsten with good high temperature properties.

1.4.2 Service Properties of Tungsten

The metal tungsten has the following desirable service properties:

1. High strength to weight ratio at temperatures above 1500°C
2. Good ductility above the ductile to brittle transition temperature (DBTT)

3. High melting point (3410°C)
4. Good electrical conductivity ($5.5 \mu\Omega\text{-cm}$) at room temperature and at temperatures up to the melting point ($150 \mu\Omega\text{-cm}$) at the melting point)
5. High atomic number (74) for production of x-rays
6. High thermionic emission at 2000°C and above when thoriated
7. Low vapor pressure at extremely high temperatures

The major undesirable properties of tungsten are:

1. High ductile - brittle transition temperature (DBTT)
2. Low oxidation resistance at elevated temperatures.

Even where oxidation resistance is not a factor, as in the application of tungsten for medical x-ray targets, the brittle behavior of tungsten at room temperature results in difficulty in fabrication without special techniques and poor mechanical strength at low temperatures. The development of a structure with enhanced ductility at room temperature coupled with good mechanical strength at high temperatures would be a significant development for technological applications of tungsten.

1.4.3 Origin of Undesirable Service Properties of Tungsten at Temperatures Below the Ductile-Brittle Transition Temperature

Tungsten single crystals with close to (100) orientation prepared by electron beam zone refining have an elongation to fracture of approximately 22% while single crystals with the same orientation prepared by the older strain anneal

method have an elongation to fracture of only 2% (Ref. 8). The high ductility exhibited by electron beam zone refined single crystals is attributed to the reduction of impurities in solid solution (Ref. 9).

The factors influencing the mechanical properties of tungsten at temperatures less than 500°C can be categorized into two major categories. These are:

1. Extrinsic factors
2. Intrinsic factors

The extrinsic factors are the thermodynamic variables of temperature and pressure and the factors of strain rate, surface condition, grain size and impurity content. The intrinsic factors are those of the crystal lattice of tungsten such as crystal structure, stacking fault energy, twinning stress, and dislocation mobility.

1.4.4 Extrinsic Factors Below the DBTT

The dependence of the mechanical properties of polycrystalline tungsten at temperatures less than 500°C on any one extrinsic factor is difficult to unravel. For different grain sizes, impurity content and surface conditions, the behavior can be markedly different. Tungsten has a body centered cubic crystal structure. Characteristic of the BCC crystals, the yield stress rises sharply with decreasing temperature below the DBTT. Below the DBTT, the brittle fracture stress for powder metallurgy tungsten is independent of the temperature and when the yield stress is above the fracture stress, brittle fracture occurs and failure is by intercrystalline fracture (Ref. 10). This is illustrated in Figure 1. With polycrystalline rod prepared from single-crystal ingots swaged to rod (Ref. 11), the brittle fracture stress below the DBTT is approximately equal to the yield stress and both rise sharply with decreasing temperature. This and the similar behavior for arc-melted tungsten (Ref. 11) is shown in Figure 2. With intentionally introduced microcracks (Ref. 12), the fracture stress is either independ-

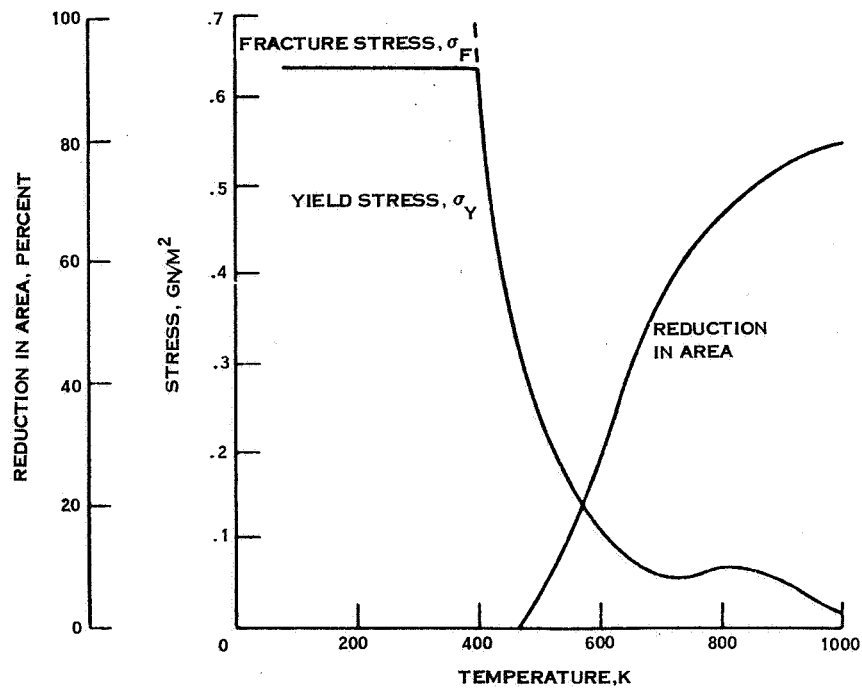
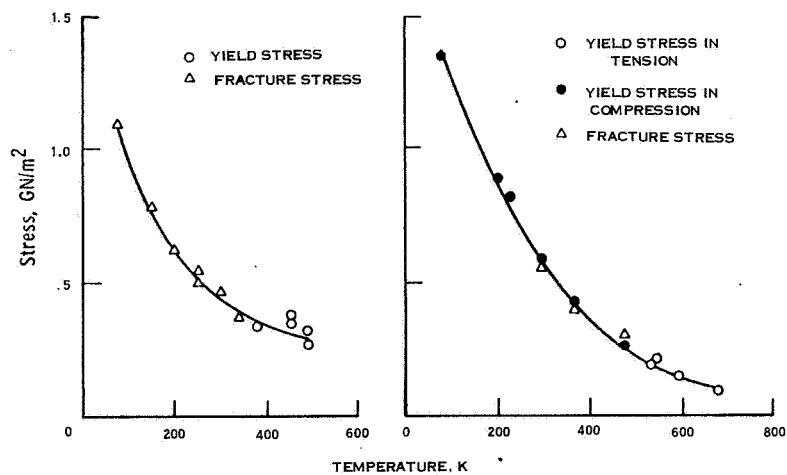


Figure 1 - Effect of Temperature on Flow and Fracture Characteristics of Tungsten. Powder-Metallurgy Tungsten (200 ppm C; 80 ppm N).



(A) SINGLE-CRYSTAL TUNGSTEN SWAGED AND RECRYSTALLIZED (10 TO 200 PPM C; 10 TO 300 PPM O)

(B) ARC-MELTED TUNGSTEN (4 PPM C; 2 PPM O)

Figure 2 - Variation of Yield Stress and Fracture Stress for Melted Tungsten

ent of temperature below the DBTT or decreases with decreasing temperature. Brittle fracture for both uncracked and cracked specimens was by cleavage. This is shown in Figure 3. The difference in behavior for two types of cracks was explained as due to the relative sharpness of the cracks. (Ref. 12)

On the basis of these references, the best curves representing the behavior of the yield and fracture stress of tungsten is that shown in Figure 2. For powder metallurgy tungsten this behavior is not realized, for below the DBTT, the fracture stress is below the yield stress.

It is thought that the brittle fracture stress of tungsten (Ref. 13) can be represented by (1) $\sigma_F = \sigma_{FI} + \sigma_{FP}$, where σ_F is the brittle ~~crack~~ fracture stress, σ_{FI} the crack initiation dependence term and σ_{FP} the crack propagation dependence term. Interstitials segregated at grain boundaries provide an easy path for crack propagation (Ref. 14) and hence lower σ_{FP} while the introduction of microcracks lowers σ_{FI} .

That below the DBTT the yield and fracture stress are the same is not encouraging for promoting ductility. It is the high DBTT of tungsten ($\sim 200^\circ\text{C}$) that prevents the enhancement of room temperature ductility in tungsten. Lowering the DBTT of tungsten to room temperature would achieve this goal.

The sharp DBTT which characterizes polycrystalline tungsten is not evident in high purity single crystal tungsten (Ref. 15). The yield stress rises sharply with decreasing temperature as shown in Figure 4, but the single crystal evidences considerable ductility even at 4.2°K (-268.8°C) (Ref. 16), provided surface scratches are kept to a minimum. Thus, tungsten is not inherently brittle in the absence of grain boundaries.

There is a pressure-dependence of the ductile-brittle transition temperature also (Ref. 17) and pressures of at least 8 to 12 kilobars are necessary for an increase in the ductility of tungsten at room temperature. At 14 kilobars, the ductility is at least 50% at room temperature and at 28 kilobars at least 75%

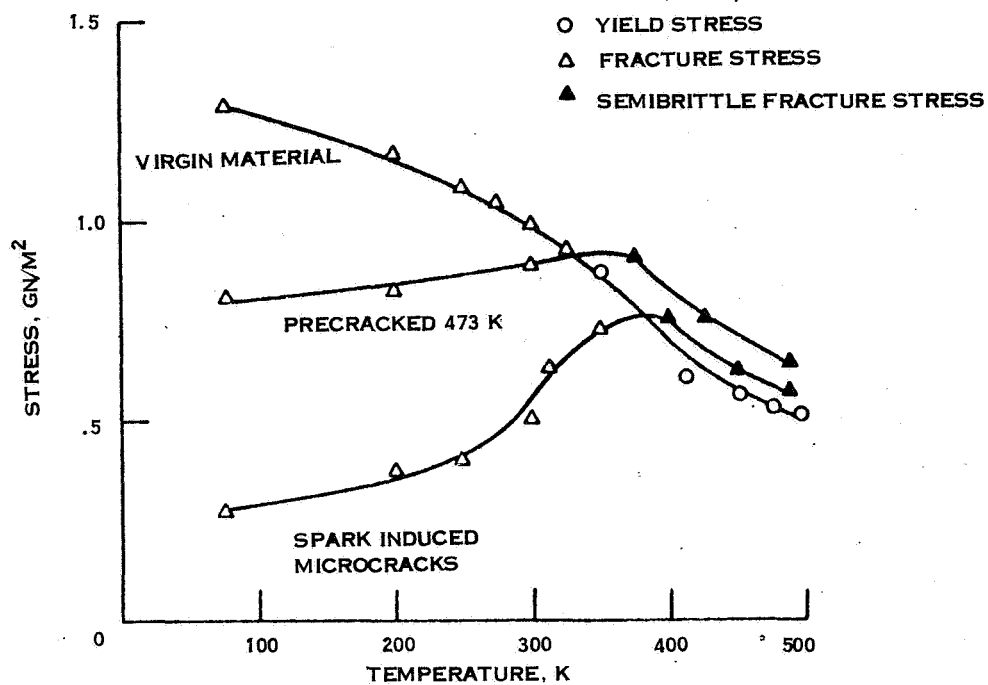


Figure 3 - Effect of Temperature and Intentionally Induced Microcracks on the Deformation Behavior of Tungsten

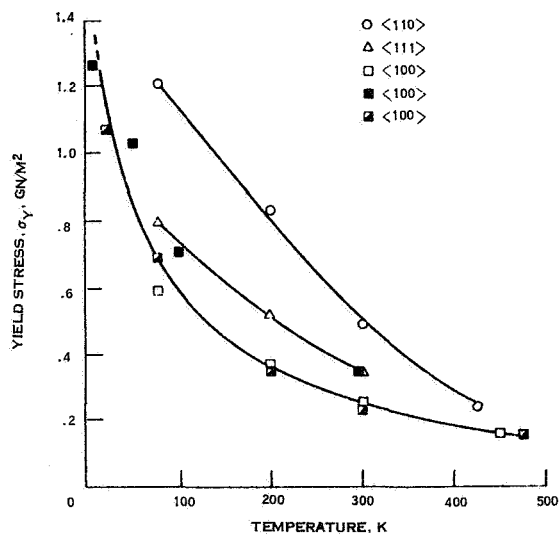


Figure 4 - Effect of Temperature on Yield Stress of Tungsten Single Crystals Having Various Orientations

(Ref. 17). Pressurization of tungsten to 40 kilobars (Ref. 18) produced no irreversible changes in the yield stress and fracture stress of polycrystalline tungsten of good purity. At high pressures, the same type of temperature dependence for yield stress and fracture stress is shown below the DBTT (Ref. 19). High hydrostatic pressures then reduce the ductile brittle transition temperature and, hence, promote ductility in tungsten. Fabrication techniques based on high pressure behavior are of great interest (Ref. 20). However, in service at one atmosphere (one bar), the service properties are not enhanced by the prior application of high pressure and it is these service properties which are of interest herein.

The surface condition of the tungsten piece can play a large role in its deformation behavior at temperatures less than 500°C. Electropolishing the surface (Ref. 21) appears to improve the transverse rupture stress and bend ductility of wrought tungsten. There are two postulated (Ref. 21) reasons for the improvement. These are:

1. The removal of surface notches and cracks resulting from processing
2. Removal of a carbon contaminated layer

Removal of surface defects by oxidation (Ref. 22) also improves the ductility and lowers the DBTT.

The effect of strain rate on the low temperature deformation properties of tungsten is important and is discussed in many references (Ref. 23,24).

The DBTT decreases with decreasing strain rate and the yield stress decreases with decreasing strain rate. The effect of strain rate on the tensile properties of tungsten is much greater than that observed for the more common metals aluminum, copper and iron (Ref. 23). The strain rate exponent for tungsten is some twelve times that of iron. It is important to test at low strain rate to determine the tensile properties of tungsten. In service, the control of this extrinsic

factor is not always possible and, hence, there may be little that can be done in this case except to insure that the strain rate does not exceed a minimal level. Figures 5, 6 and 7 show typical curves for strain rates of the variation of yield stress, DBTT and strain rate sensitivity.

The extrinsic factors of temperature, pressure and strain rate are not directly controllable for most service applications. The extrinsic factors of grain size and purity and, possibly, surface condition, are accessible to control. Thus, they are the most important extrinsic factors for direct control. The effect of grain size on the DBTT of tungsten is shown in Figure 8 (Ref. 25) and on the yield stress in Figure 9 Ref. 26). It is interesting to note that there is a peak in DBTT at about 0.2 mm grain size (200 microns); the DBTT is between 500°K and 700°K (227°C and 427°C). At 0.001 mm or 1 micron it is between 190°K and 273°K, or -83°C and 0°C. Above 1 mm or 1000 microns it could be as low as 27°C but also it could be very high. In the limit of large grain size, the DBTT does not apparently exist and single crystals are ductile at very low temperatures (4.2°K). It would appear from these curves of Figure 8 that there are two directions to go to obtain a low DBTT. These are toward fine grained or toward single crystal tungsten.

The effect of interstitial impurities on the DBTT and yield stress of polycrystalline and single crystal tungsten is shown in Figures 10 and 11 (Ref. 27,28). For single crystal tungsten, the effect of impurities on the DBTT is moderate but for polycrystalline tungsten the effects are dramatic. With single crystal tungsten, the effects of carbon on the yield stress are dramatic, but for polycrystalline tungsten they are only moderate. In Figure 12, the temperature dependence of the yield stress of tungsten single crystals with different impurities is shown. The yield stress of the less pure tungsten is higher but the temperature dependence is similar for all cases, indicating that this is controlled by an intrinsic factor. It is evident that for both

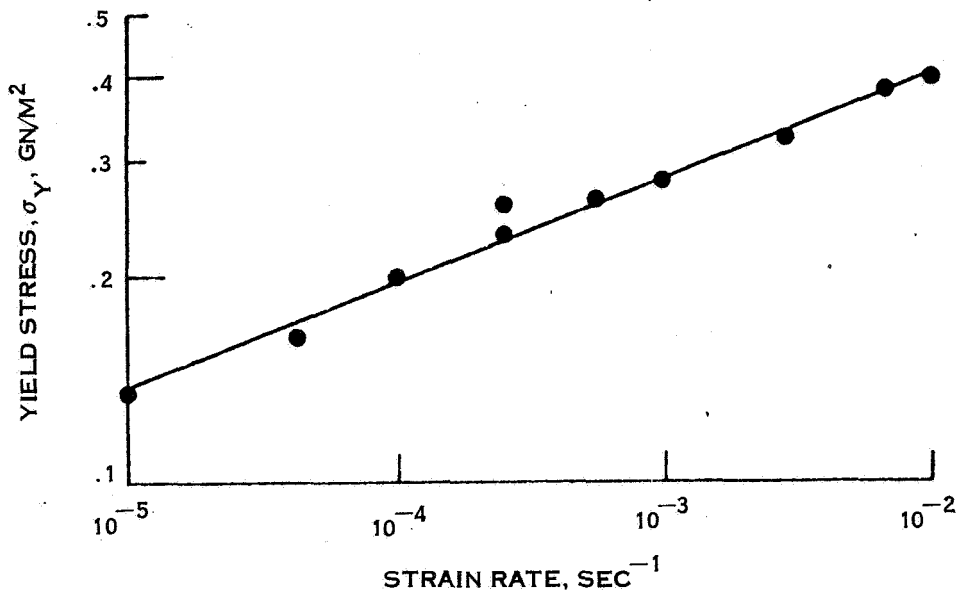


Figure 5 - Effect Of Strain Rate On Yield Stress Of Tungsten at 525 K ($0.14 T_m$)

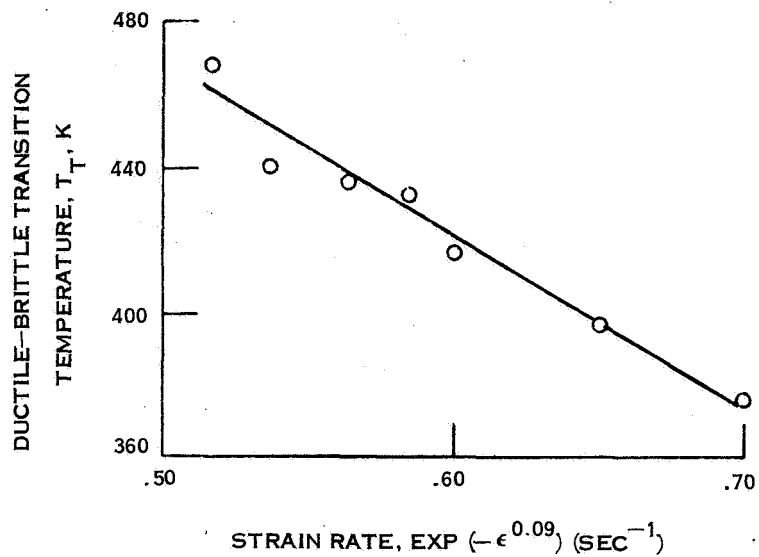


Figure 6 - Effect of Strain Rate On Ductile-Brittle Transition Temperature Of Tungsten

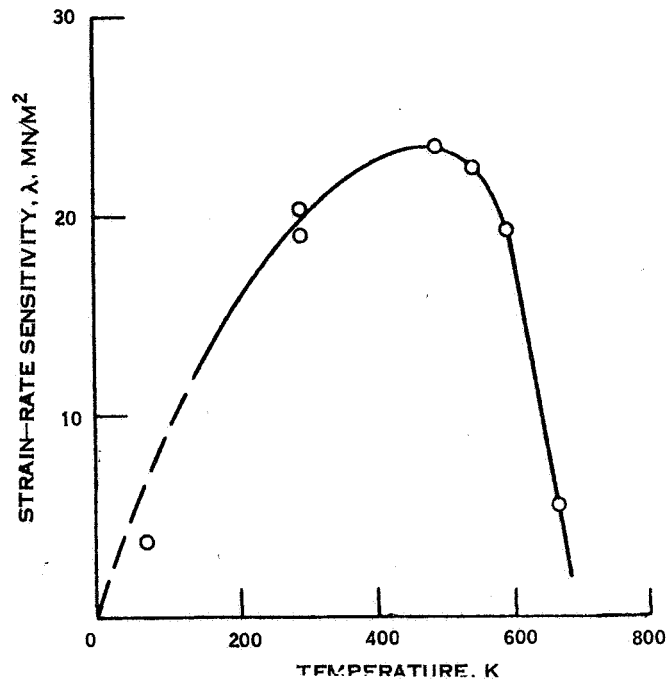


Figure 7 - Strain Rate Sensitivity Of Unalloyed, Arc-melted Tungsten

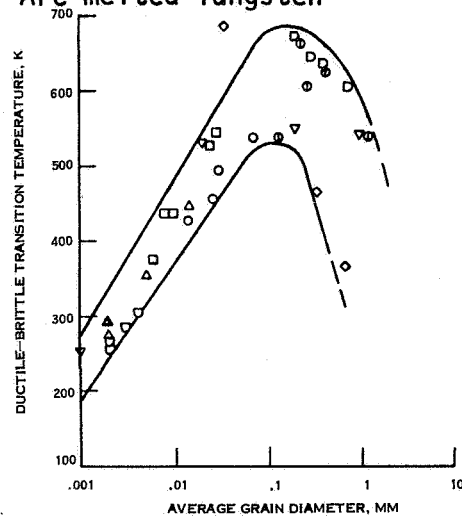


Figure 8 - Effect Of Grain Size On The Ductile-Brittle Transition Temperature Of Tungsten

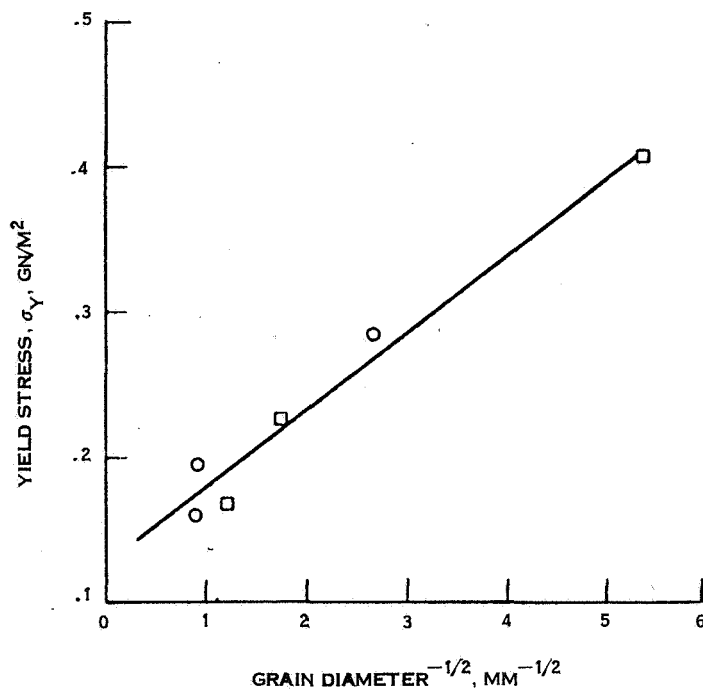


Figure 9 - Variation Of Yield Stress With Grain Size at 500K

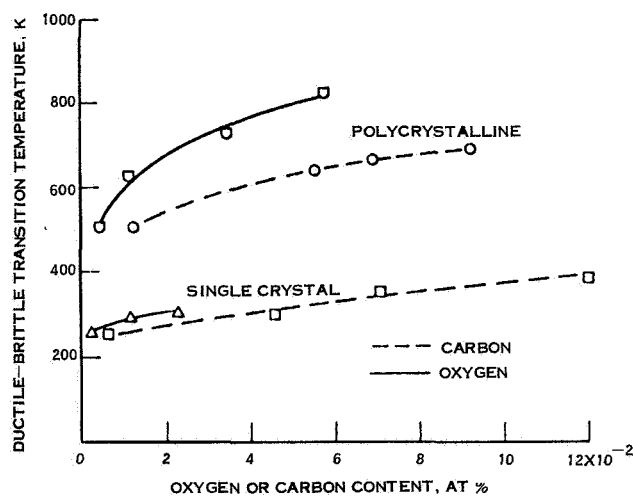


Figure 10 - Effects Of Oxygen And Carbon On Ductile-Brittle Transition Temperature Of Single-Crystal and Polycrystalline Tungsten

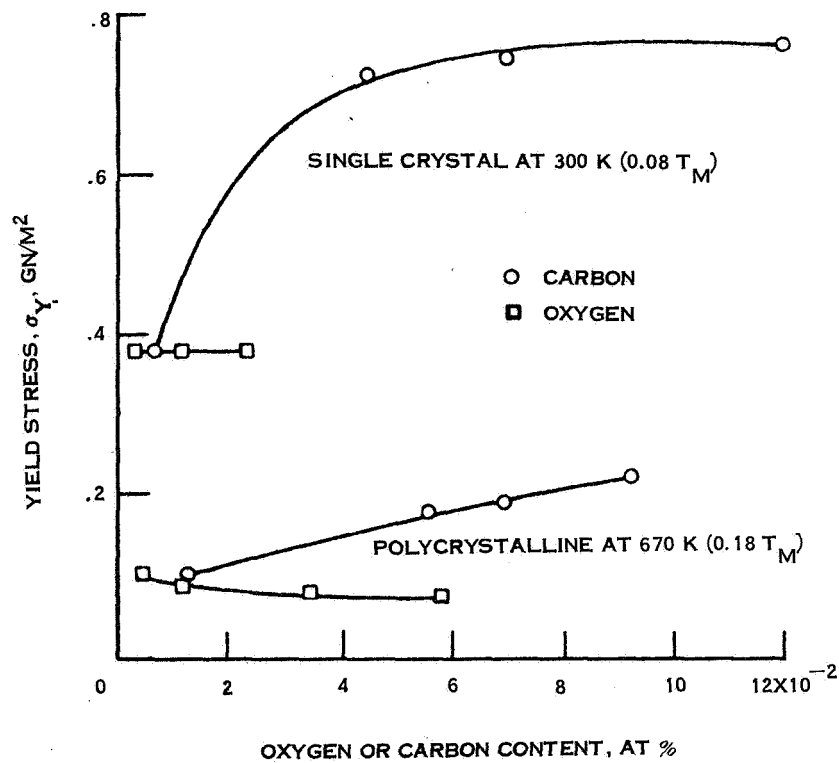


Figure 11 - Effects Of Oxygen And Carbon On Yield Stress Of Single-Crystal And Polycrystalline Tungsten

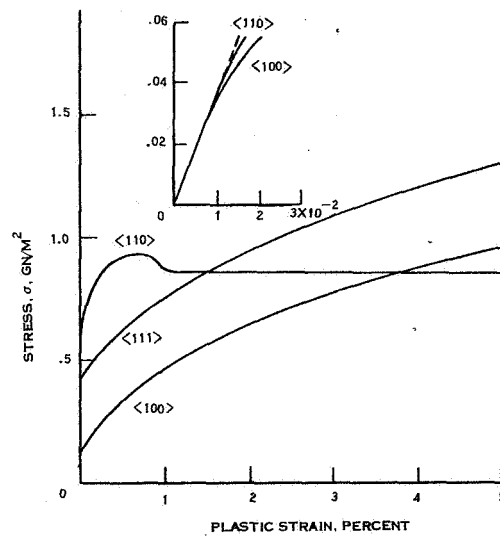


Figure 12 - Stress-Strain Curves For Single-Crystal Tungsten At 300 K

the single crystal and polycrystalline tungsten, elimination of interstitial impurities lowers the DBTT and enhances ductility from these references. The interstitial impurities of carbon and oxygen appear to be most important and it is thought that these impurities are precipitated in grain boundaries where they cause embrittlement in polycrystalline tungsten. High concentrations of these interstitials are typically found in powder metallurgy tungsten.

1.4.5 Intrinsic Factors and Temperatures Below the DBTT

The effect of crystal orientation on the yield stress and dislocation density (Ref. 29,30) is shown in Figures 12 and 13. The insert on Figure 12 is the work of M. Garfinkle (Ref. 31) showing that departures from linearity are similar for the $[100]$ and $[110]$ orientations. The Schmidt factors for slip on particular $(110) \quad [111]$, $(112) \quad [111]$, or $(123) \quad [111]$ slip systems are essentially identical for both orientations (Ref. 31). The insert is necessary for the curves of Figure 12 show that the proportional limit stress is highly orientation dependent and, apparently, does not obey a critical resolved shear stress law. What Garfinkle's work shows is that the critical resolved shear stress criterion is applicable in tungsten crystals.

The microscopic stress-strain curve for the various crystallographic orientations in Figure 12 shows different rates of work hardening for different orientations. The curves of Figure 13 help explain this as for different orientations the dislocation density at different amounts of plastic strain is very different. For $[110]$ orientated crystals, dislocation can glide relatively large distances on parallel planes without intersecting other dislocations and increasing the dislocation density. This means little work hardening for large amounts of plastic strain in this orientation. The discontinuous yield phenomena of $[110]$ oriented tungsten single crystals has been

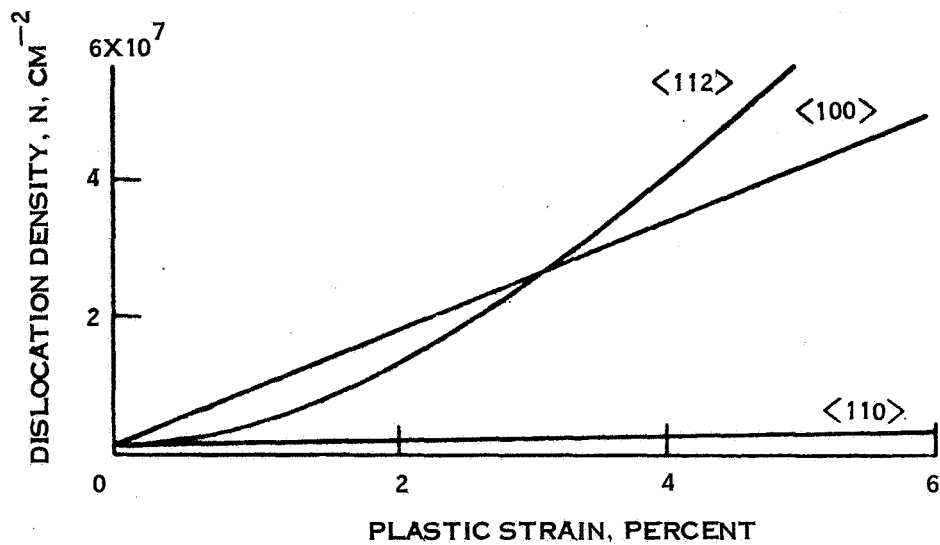


Figure 13 - Increase In Dislocation Density With Plastic Strain For Single-Crystal Tungsten Having Various Orientations

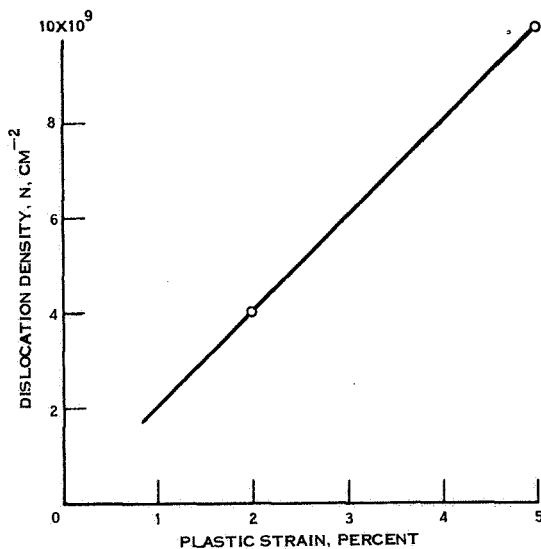


Figure 14 - Variation Of Dislocation Density With Strain For Polycrystalline Tungsten

investigated (Ref. 30) and is an inherent phenomena in tungsten single crystals.

The temperature dependence of single crystals has been discussed above. There is no sharp DBTT. Single crystals exhibit appreciable ductility even at extremely low temperatures, such as 4.2°K. Tungsten is not an inherently brittle metal.

The high stacking fault energy of tungsten means that it is not of much importance in the deformation behavior of tungsten (Ref. 32). Twinning on (112) planes has been associated with fracture after considerable deformation by slip (Ref. 32). Increased purity appears to promote twinning (Ref. 33) at temperatures from 95°K to 180°K. Other work has reported no evidence of twinning initiating fracture and that twins were caused by fracture (Ref. 34). The basic conclusion is that stacking faults of observable widths are unimportant in the deformation of tungsten while twinning under some conditions may play a role in the fracture of tungsten.

The dislocation density variation with strain in polycrystalline tungsten is shown in Figure 14 (Ref. 35) for room temperature. The dislocation structures are reviewed in other works (Ref. 36). It is concluded that, at low temperatures, edge mobility is greater than screw mobility and edge dislocations move through the crystals, leaving behind the long screw segments observed (Ref. 37). At temperatures greater than 340°K (67°C) edge and screw mobilities become equal and both types of dislocations are found. The decrease in screw dislocation mobility with temperature can be correlated to the increasing yield stress with temperature. Higher stresses are needed at lower temperatures to produce dislocation movement after edge dislocations have moved out of the crystal.

1.4.6 Controlling Mechanisms in Tungsten Below the DBTT

For single crystals, an intrinsic lattice resistance to screw dislocation movement, a Peirls mechanism (Ref. 38) controls the deformation behavior at low temperatures. As temperature increases, thermal fluctuations increase screw mobility. Even though ductility is observed in tungsten as low as 4.2°K, the nature of the atomic bonding may make tungsten more susceptible to embrittlement. The statement is made that the high DBTT of tungsten is controlled by intrinsic properties acting indirectly and extrinsic properties playing a direct role (Ref. 39).

The alteration of intrinsic properties by alloying, as alloying with rhenium is very attractive to increasing the ductility of tungsten (Ref. 40). However, if it is desired to work with tungsten directly to preserve other desirable properties, control of extrinsic factors, especially grain size, impurity content, and surface condition is important. Even when alloying control of these extrinsic factors is important for they play a direct role in the deformation behavior at room temperatures.

From the above discussion, it would be highly desirable either to produce a fine-grained, high purity polycrystalline tungsten or to grow very large high purity single crystals of tungsten routinely and cheaply. As will be discussed below, the three routes for achieving this are:

- 1) grain refinement by inoculation or achieving a high degree of supercooling
- 2) growth of high purity single crystals by rapid solidification
- 3) vapor deposition onto a suitable substrate

All of these routes are accessible to containerless processing, as will be discussed below. Further, the development of such structures in tungsten

alloyed with elements, such as rhenium, may also be possible through container-less processing and should be explored.

1.4.7 Service Properties of Tungsten above the DBTT

The service properties of tungsten above the DBTT are of primary importance to its application to devices such as targets for x-ray tubes. Figure 15 (Ref.41) shows the strength of metals including tungsten to 2760°C. The refractory metals: tungsten, tantalum and molybdenum have strengths superior to all other metals above 1500°C. The factors to be considered other than strength are:

- 1) creep resistance
- 2) recovery and recrystallization
- 3) rupture stress
- 4) oxidation resistance

Plots of the ultimate tensile strength, stress rupture vs. temperature for several refractory metals are shown in Figures 16 and 17 (Ref. 41). A summary of the high temperature deformation properties of Group VI-A metals is shown in Figure 18 (Ref. 42) plotted against the ratio of temperature to melting temperature. Figure 19 & 20 (Ref. 42) compare the stress to produce a steady creep rate of 10^{-6} sec^{-1} for melted and P, M, Group VI-A and V-A metals. The Group VI-A metals are stronger than the V-A metals and tungsten with the highest melting point is stronger at all temperatures. The powder metallurgy products are stronger and the obvious structural differences are fine grain size and impurities precipitated at grain boundaries. It is surprising but the finer grained tungsten is stronger than the coarse grained. With metals, such as nickel, the reverse is true at high temperatures (Ref. 43).

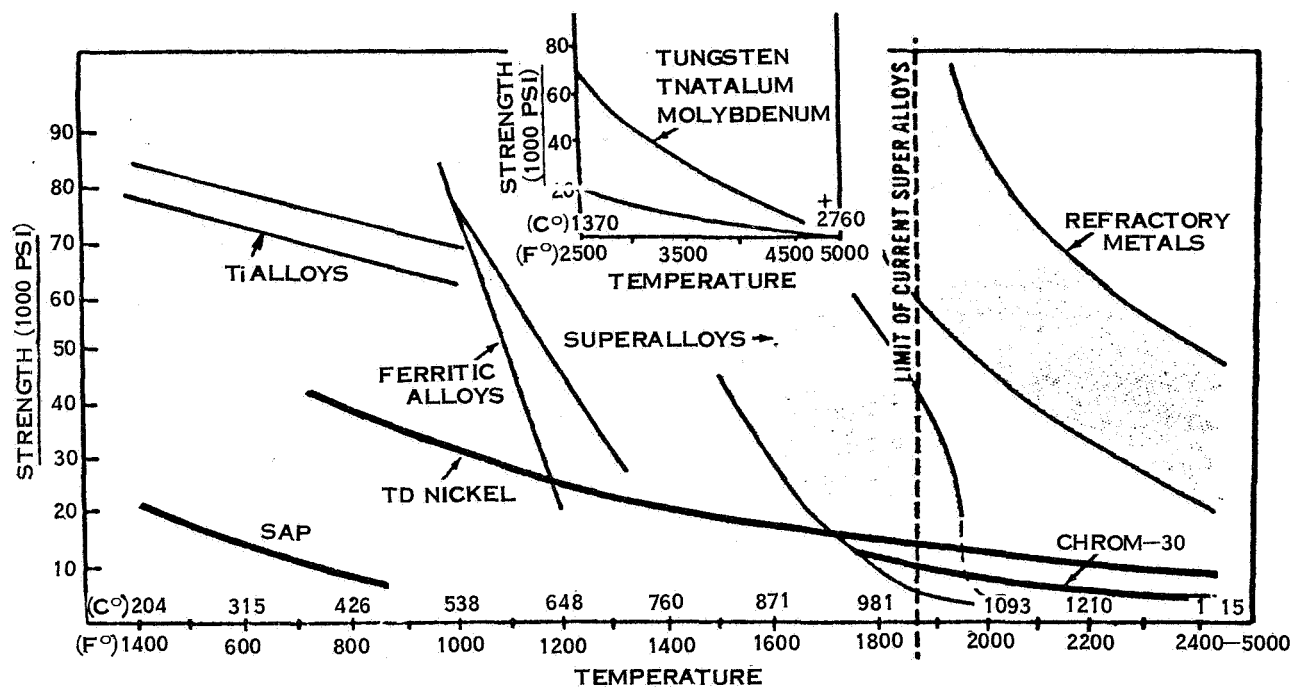


Figure 15 - Strength Of High Temperature Metals

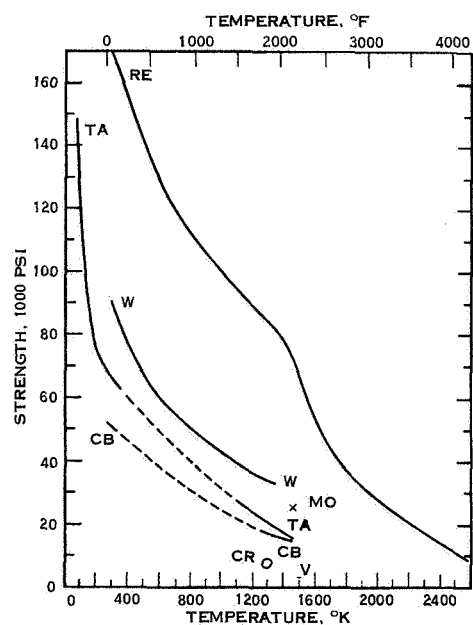


Figure 16 - Ultimate Tensile Stress Of Refractory Metals

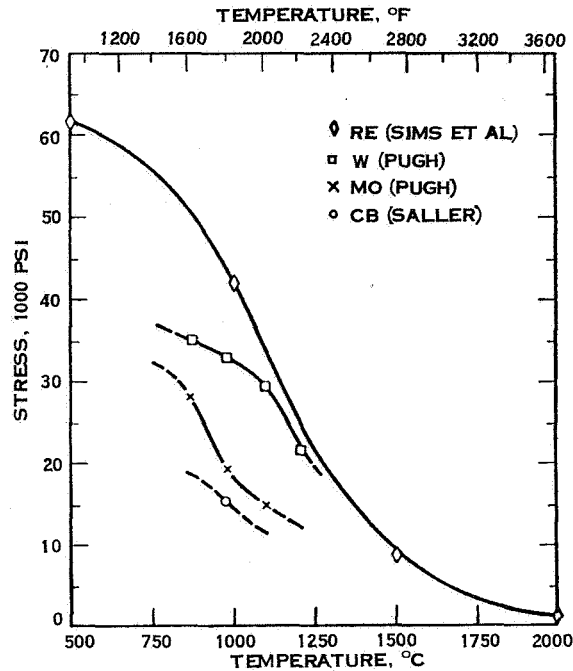


Figure 17 - Stress-Rupture Strength For 10-hr Life

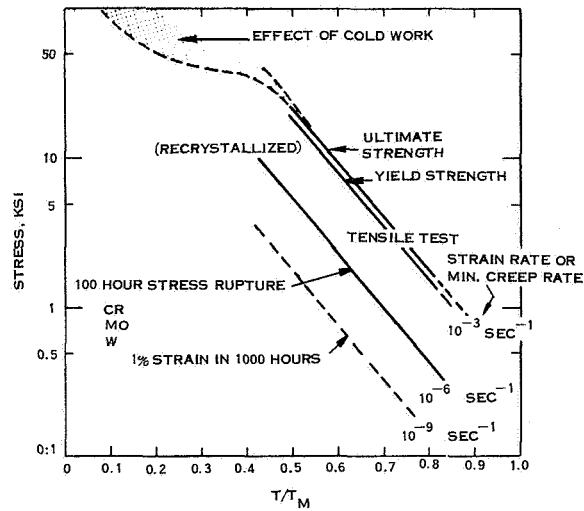


Figure 18 - Summary Of High-Temperature Deformation Of The Group VIA Refractory Metals (Melted Material Only)

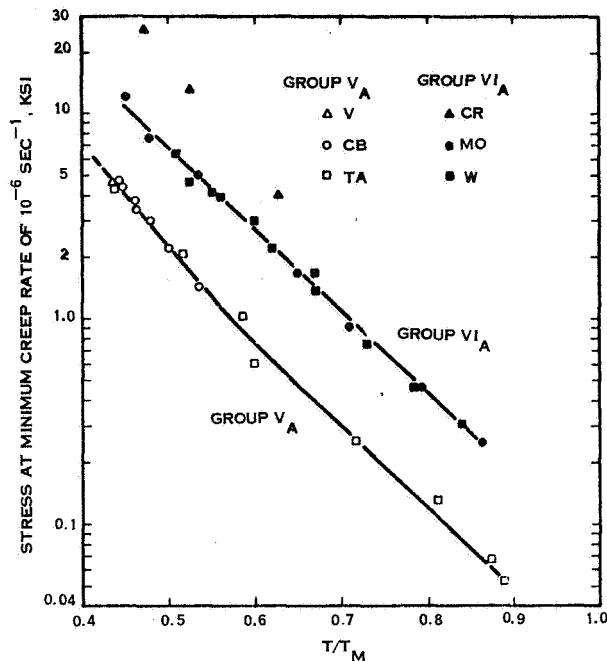


Figure 19 - Stress at $\epsilon = 10^{-6} \text{ Sec}^{-1}$ Vs. T/T_M For Group V_A And Group VI_A Metals (Melted Material Only)

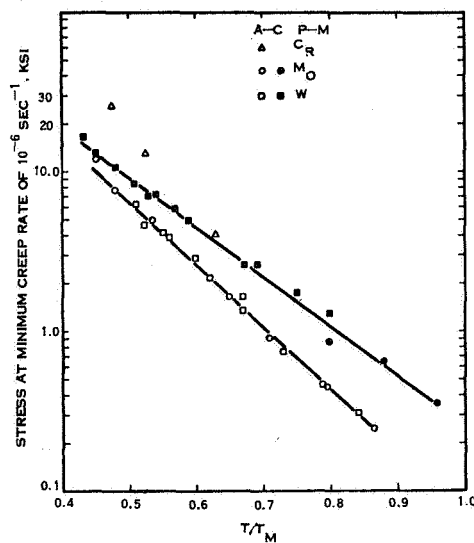


Figure 20 - Stress At $\epsilon = 10^{-6} \text{ Sec}^{-1}$ Vs. T/T_M For Arc-Cast And Powder Metallurgy Group VI_A Metals

Whereas interstitial impurities lower the strength of tungsten below the DBTT, they appear to increase the creep resistance at high temperatures. Cold working lowers the recrystallization temperature and hence weakens the material (Ref.42). It is thought that, as the grain size increases, the creep rate decreases, passes through a minimum, and then increases (Ref. 42). Impurities tend to impede recrystallization and raise the recrystallization temperature for a given stress. It was found (Ref. 44) that electron beam zone melted polycrystalline tungsten deformed 70% had a recrystallization temperature 300°C lower than that of commercial tungsten (1400°C - 1450°C).

Thus, it is difficult to couple high temperature strength enhancement with low temperature strength enhancement. High purity fine grained tungsten, which has good low temperature strength, will recrystallize at lower temperatures under given amounts of stress than fine grained powder metallurgy tungsten with significant interstitial impurities present.

Even available single crystals containing many dislocations, which are as a result weak and exhibit creep strengths superior to polycrystalline metals at high temperatures (Ref. 45). Thus, one route to coupling low temperature ductility with high temperature strength is the elimination of grain boundaries with high purity single crystal tungsten of low defect density.

1.4.8 Enhancing the Service Properties of Unalloyed Tungsten

From the above review, it is evident that below the DBTT, fine grained, high purity tungsten or single crystal tungsten of high purity, low defect content, and good surface condition are structures that will permit fabrication of such device components as x-ray targets at room temperature. Vapor deposited tungsten is another route to fabrication of such components as x-ray targets.

This is discussed below in terms of its applicability to such devices. For structural applications of tungsten, this is not a favorable route, however. Either fine grained, high purity tungsten or single crystal tungsten is the way to go.

At elevated temperatures, recrystallization coarsens the grain size and without interstitial impurities, the creep resistance is lowered. In service, as in a rotating anode x-ray tube, cycled between room temperature and near melting, the high purity, fine grained tungsten is expected to be weaker at both extremes due to recrystallization. The single crystal tungsten is expected to show good high temperature and low temperature behavior under this cycling provided stress centers are not induced. Very fine grained tungsten, vapor deposited onto molybdenum or even amorphous coatings of tungsten may take longer to coarsen under exposures and hence may also be satisfactory for enhancing service lifetime of such components as tungsten x-ray targets.

The question to be resolved in each of the cases discussed is whether rapid cycling between room temperature and near melting will result in recrystallization rapid enough to change the structure discussed so that they fail before the present tungsten x-ray targets for that application.

2.0 LEVITATION SYSTEM APPARATUS

The levitation system for levitation heating and melting of tungsten was assembled in two stages so that experimental work could progress as fabrication and construction of apparatus continued. The first stage used a glass cross as the levitation chamber and so is referred to as the "Glass Levitation System". The second stage used a stainless steel vacuum chamber and is therefore referred to as the "Stainless Steel Levitation System". This was later modified with the addition of a four foot drop tube for studying molten tungsten freely falling.

The Glass Levitation System was used for the levitation and heating experiments with solid tungsten. Within that system tungsten could be levitated and heated to a maximum temperature of 2600°C by induction heating from the levitation coil. Vacuum degassing experiments with levitated tungsten specimens were performed in this system and are reported below. The levitation coil was tested in this system and levitation technique for solid tungsten was tested. This system proved to be very useful during the period of assembly of the Stainless Steel Levitation System.

The Stainless Steel System was used for levitation melting of tungsten, heretofore not reported in the literature. With this system and the additional four foot drop tube the solidification of molten tungsten under a variety of conditions was studied. The results of these experiments are reported on below. The Stainless Steel Levitation System is a unique levitation system utilizing electron beam heating to melt a levitated tungsten specimen. Utilization of this technique has not been reported in the literature before this work but had been discussed as a possible technique for levitation melting of high melting point metals and alloys (Ref. 46). With the perfection of this technique, levitation melting has entered into a new phase of high temperature

chemistry and physics. The perfection of this technique also proves that electron beam heating and melting can be used in the containerless processing of high melting point materials. This is important for space processing of high melting point materials as electron beam heating is a very efficient source for heating and melting.

2.1 GLASS LEVITATION SYSTEM

The Glass Levitation System is shown in Figure 21 . The system consists of the levitation chamber and vacuum system shown centrally, the VEECO GA-4 mass spectrometer with vacuum system and electronics rack shown to the left, the Lepel matching transformer shown to the right and the Lepel 25K.W., 450 Khz r.f. generator shown partially behind the matching transformer. The levitation chamber is air cooled and the blower shown in the photograph is used to cool the glass chamber. Normally the protective plexiglass shield is covered with black paper or gold leaf paper to protect against eye damage from the incandescent tungsten specimen. The photograph of Figure 21 was taken in the light produced by the incandescent specimen through filters and all personnel including the photographer wore protective goggles.

The mass spectrometer has several valves for admission of gases to be analyzed. The one used for this system was a high conductance gold leaf ball valve. Communication to the glass levitation chamber is through a bakeable, flexible stainless steel sample tube terminated in a hoak valve. The sample tube can be evacuated before use by pumping down through the levitation vacuum system and then sealing it off with the hoak valve. The sample tube can thus be used either in the batch mode for collecting gas and analyzing it at a later time or for continuous sampling.

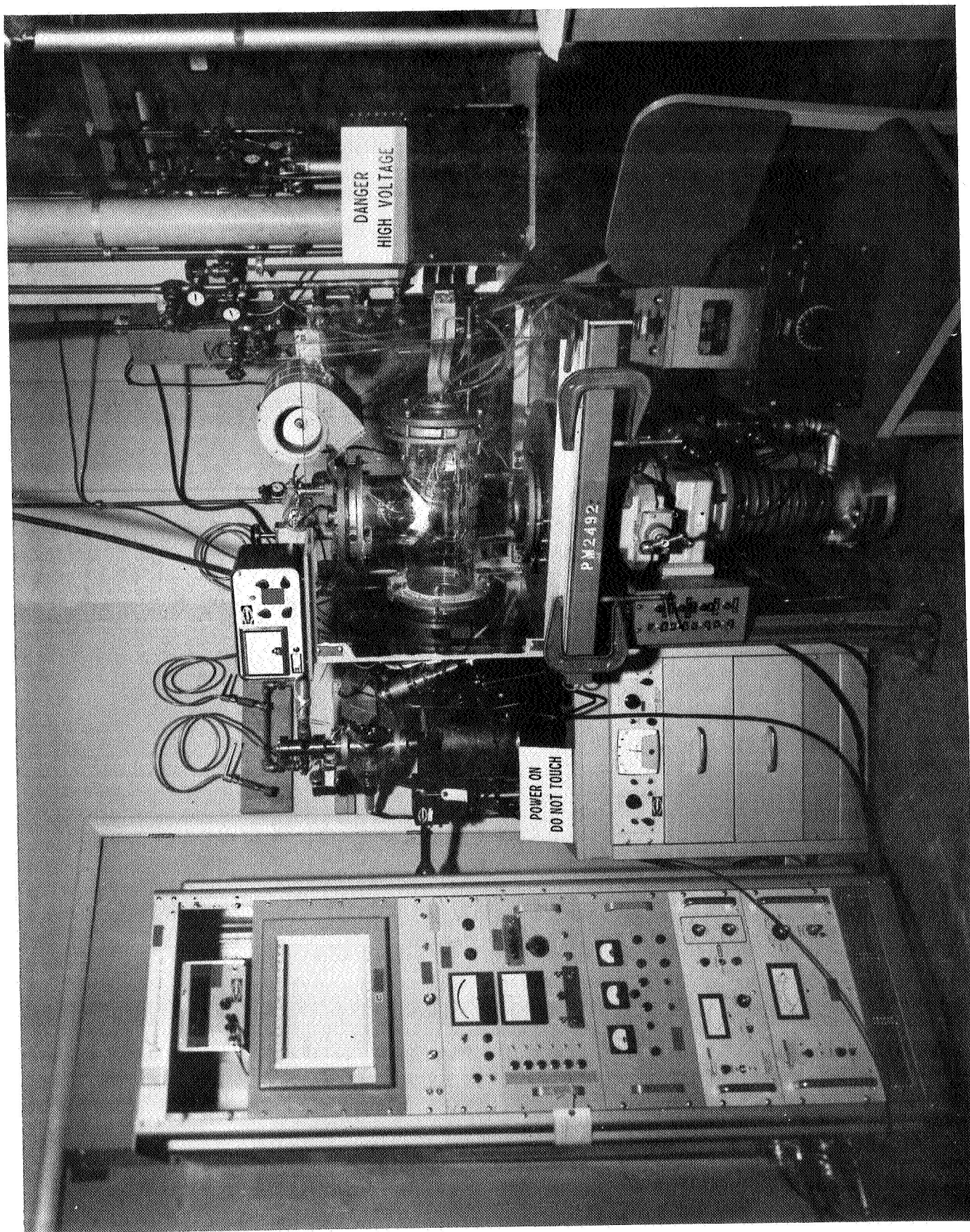


Figure 21 - Glass Levitation System

The power to the levitation coil is supplied through a special copper coaxial feedthrough on the copper end plate shown on the glass cross section to the right. The connection to the feedthrough from the matching transformer is through broad close spaced, water cooled copper strips. The copper endplate in addition also has a pedestal assembly and a coil assembly mounted on it. Figure 22 shows the copper endplate in a transportation fixture as it looks from inside the chamber. The leads to the levitation coil are shorter here because this is as it was used in the Stainless Steel Levitation System. The pedestal assembly is shown with two specimens on it. As many as six have been used and levitation experiments may be conducted serially one after the other. The pedestal assembly slides on the rods shown in the photograph. Figure 23 shows the pedestal assembly with specimen inserted in the levitation coil. Once the specimen is levitated, the pedestal is lowered and the pedestal assembly is slid out from under the levitation coil. With the levitation coil shown, specimens can be dropped through the bottom for free fall experiments or quenching experiments. The ceramic pedestal is made out of boron nitride. The coil consists of a number of turns of copper tubing and is water cooled. Figure 24 shows the copper endplate as it looks from outside the chamber with water lines for cooling. The pedestal assembly is moved by pushing or pulling the rod terminated in an insulated handle and the pedestal itself is raised or lowered by turning the rod. Different coils can be used by removing the one shown and soldering in another so that the levitation coil configuration can be changed.

A levitated tungsten specimen is shown in Figure 25, heated to 2600°C by the rf field. Ten gram tungsten specimens were held levitated at that temperature for as long as 2.5 hours. With the six inch diffusion pump, pressures before below 10^{-6} torr were obtained before starting the levitation and final pressures for long run times approaching this were achieved.

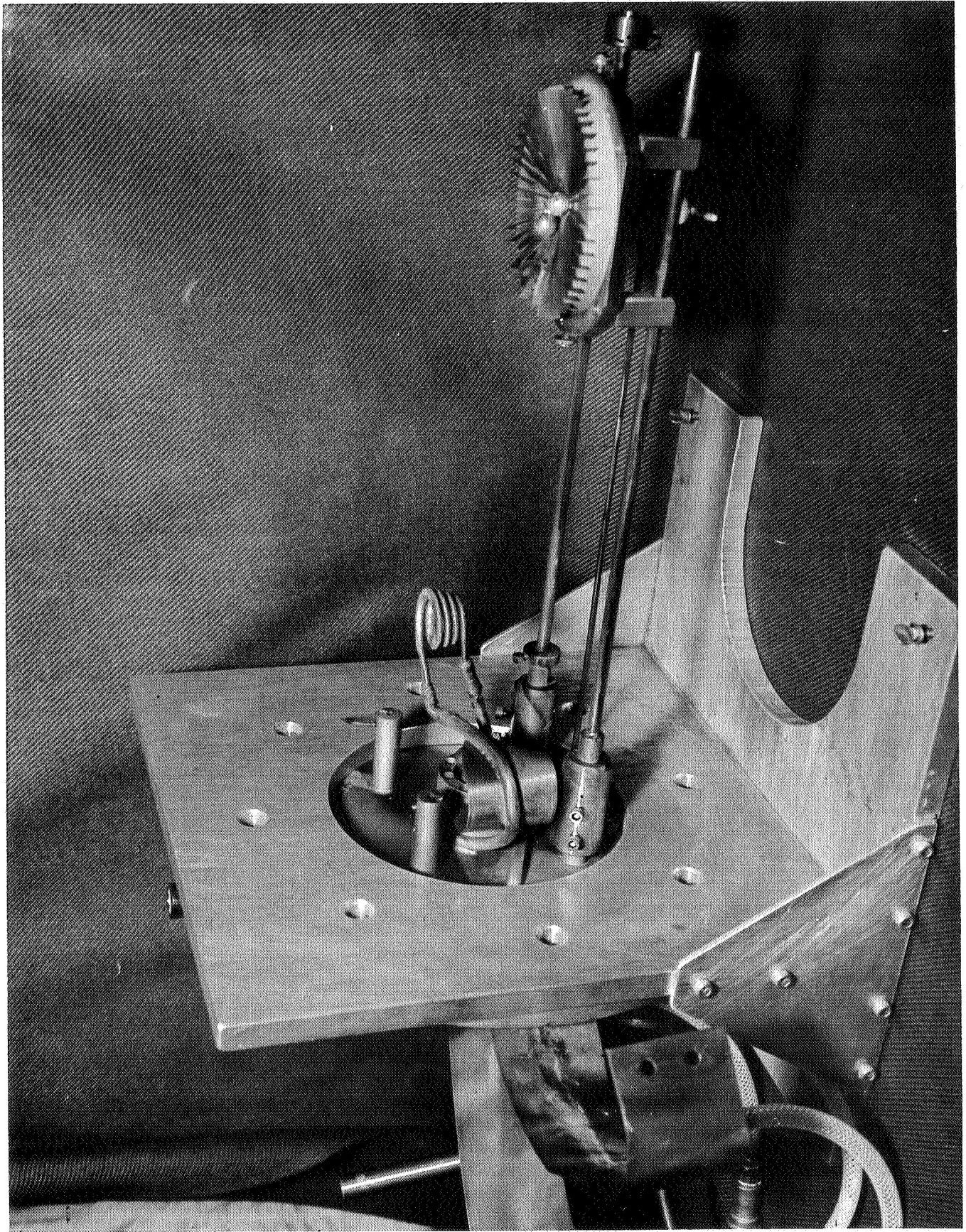


Figure 22 - Copper End Plate With Coil Assembly and Pedestal Assembly

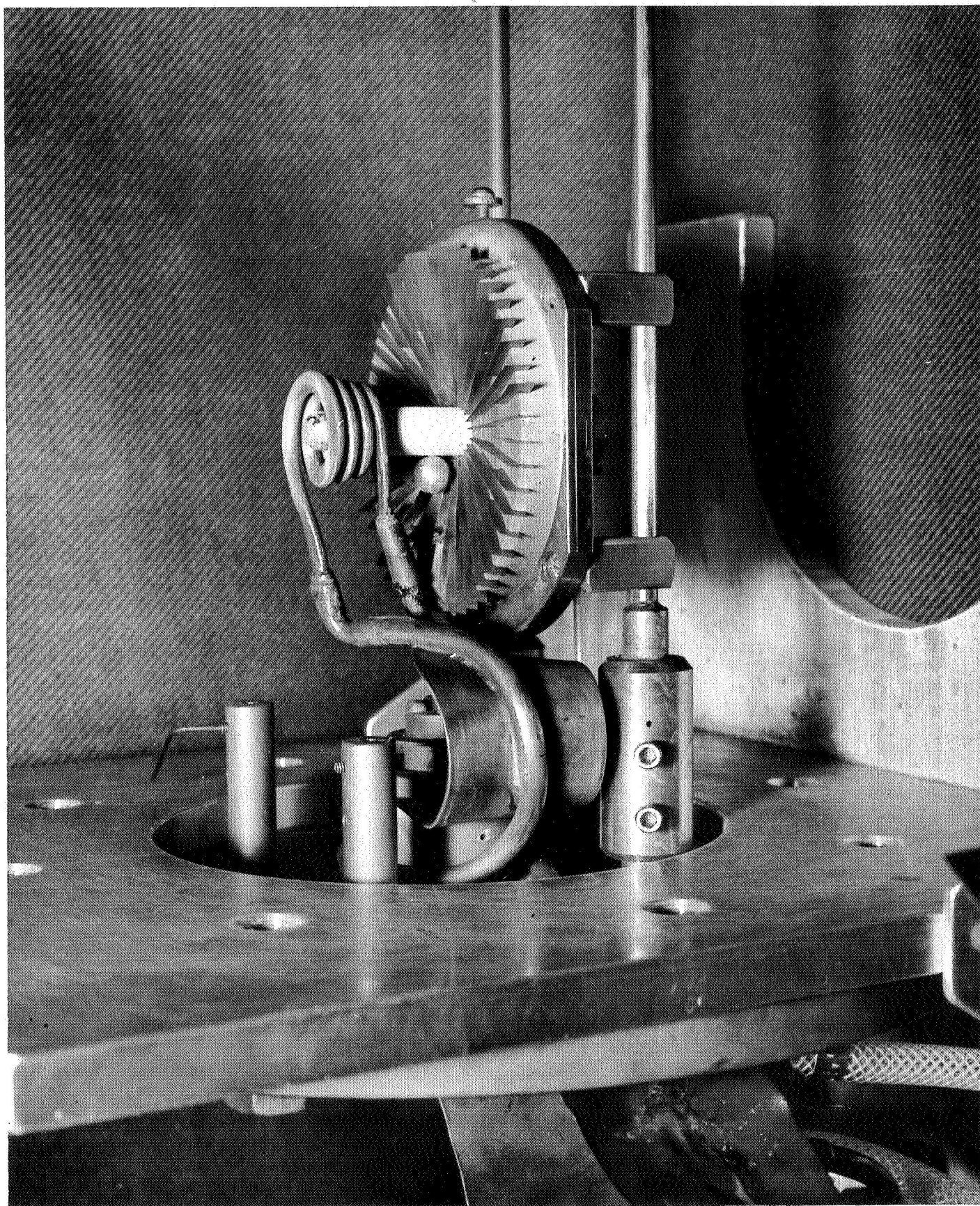


Figure 23 - Pedestal Assembly With Specimen Inserted In Levitation Coil

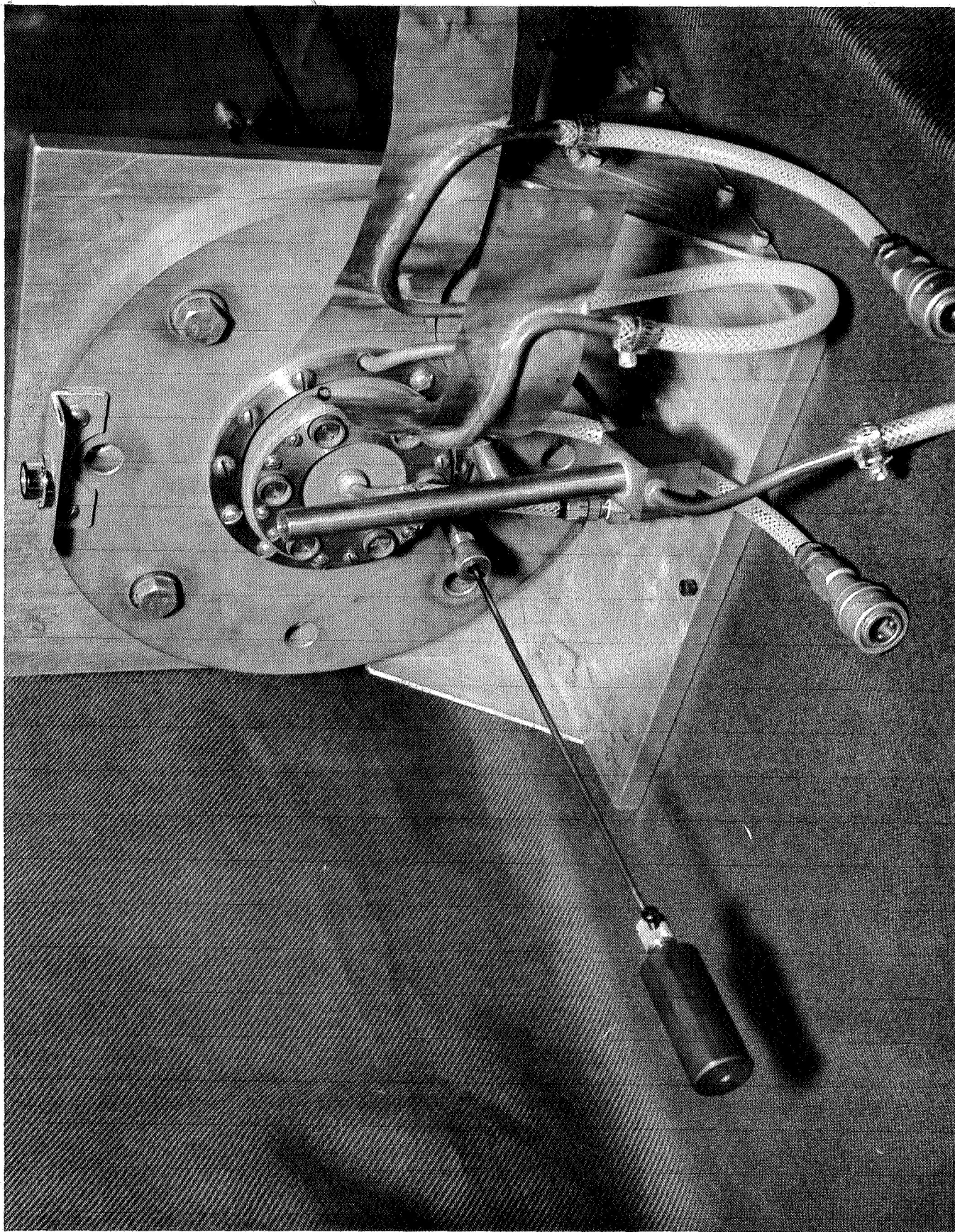


Figure 24 - Copper End Plate Exterior View

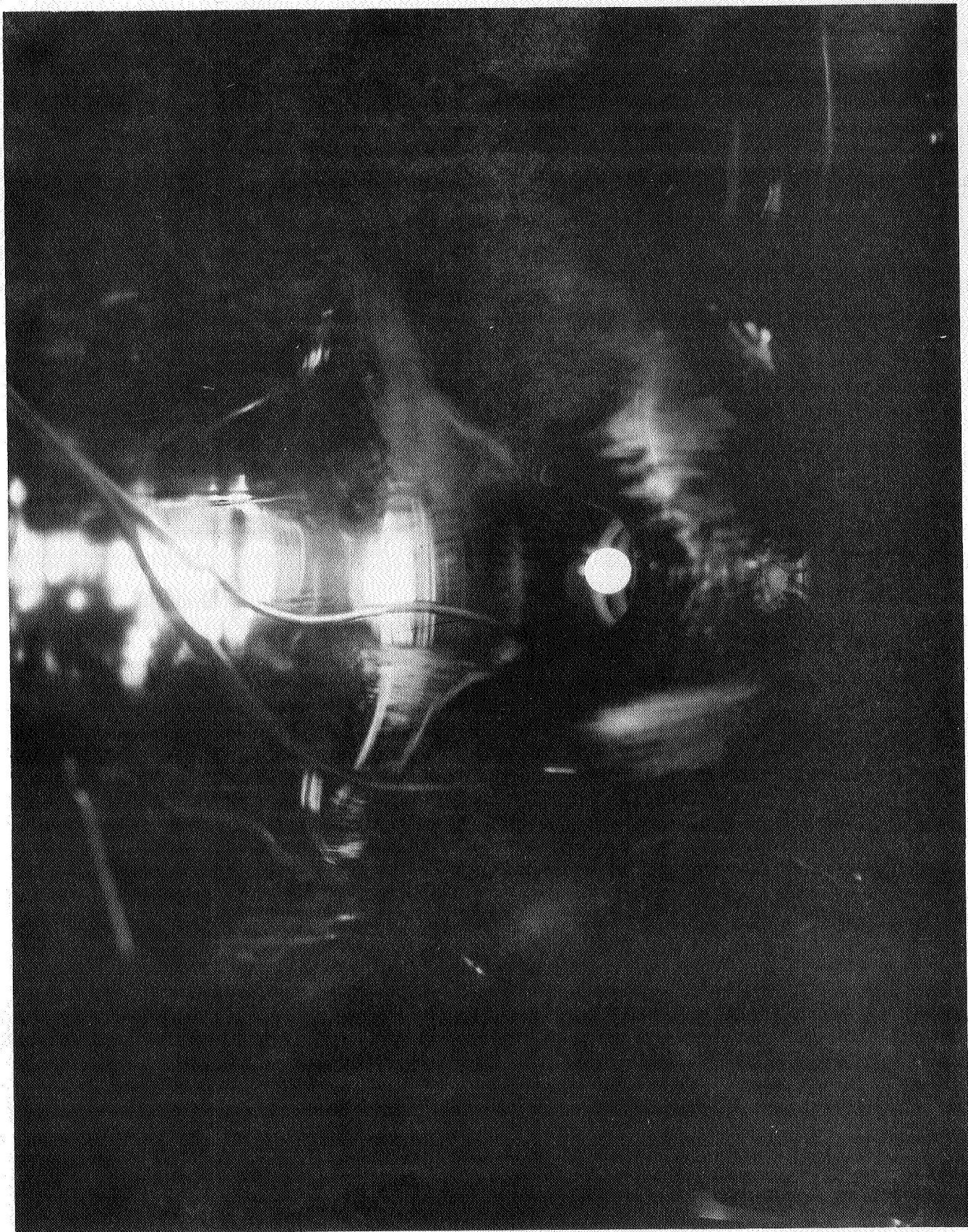


Figure 25 - Levitated Solid Tungsten Specimen (2600°C)

2.2 STAINLESS STEEL LEVITATION SYSTEM

The Stainless Steel Levitation Chamber and electron beam heating unit is shown in Figure 26 . Figure 27 shows the four foot drop tube and six inch diffusion pump below the levitation chamber. The electron beam heating unit atop the vacuum chamber is isolated from the vacuum chamber by an air driven, solenoid actuated valve. The electron beam heating unit has its own vacuum system and one of the two two inch diffusion pumps need to pump the electron gun down is visible. Behind the ionization gauge controllers in Figure 26 the vidicon TV camera is shown. In Figure 28 the solid state imaging array is shown. Figure 29 shows the Stainless Steel Levitation System. The electron beam power supply is shown behind the videotape recorder. The electron beam gun can draw a hundred milliamperes maximum at 40 kilovolts. Generally one hundred miliamperes at 32 kilovolts was employed to melt the levitated tungsten specimens. The rf generator used for this system is a General Electric 25 KW, 450 Khz power supply and is matched to the load through the Lepel matching transformer.

The mate to the flange of the vacuum chamber is the copper plate with coaxial feedthrough, coil assembly, and pedestal assembly shown in Figures 22 , 23 , and 24 . Copper catchbuckets designed for the chamber or the bottom of the drop tube respectively can be used to catch the specimens or quenchpots designed respectively can be used. The entire levitation chamber and drop tube can be evacuated to 10^{-6} torr or better before the experimental work is begun.

With the vidicon camera and solid state imaging array, complete documentation of the runs and temperature data can be obtained. The two viewports permit simultaneous viewing and recording of the specimen levitated in the levitation coil and in free fall through the drop tube. With this unique viewing and

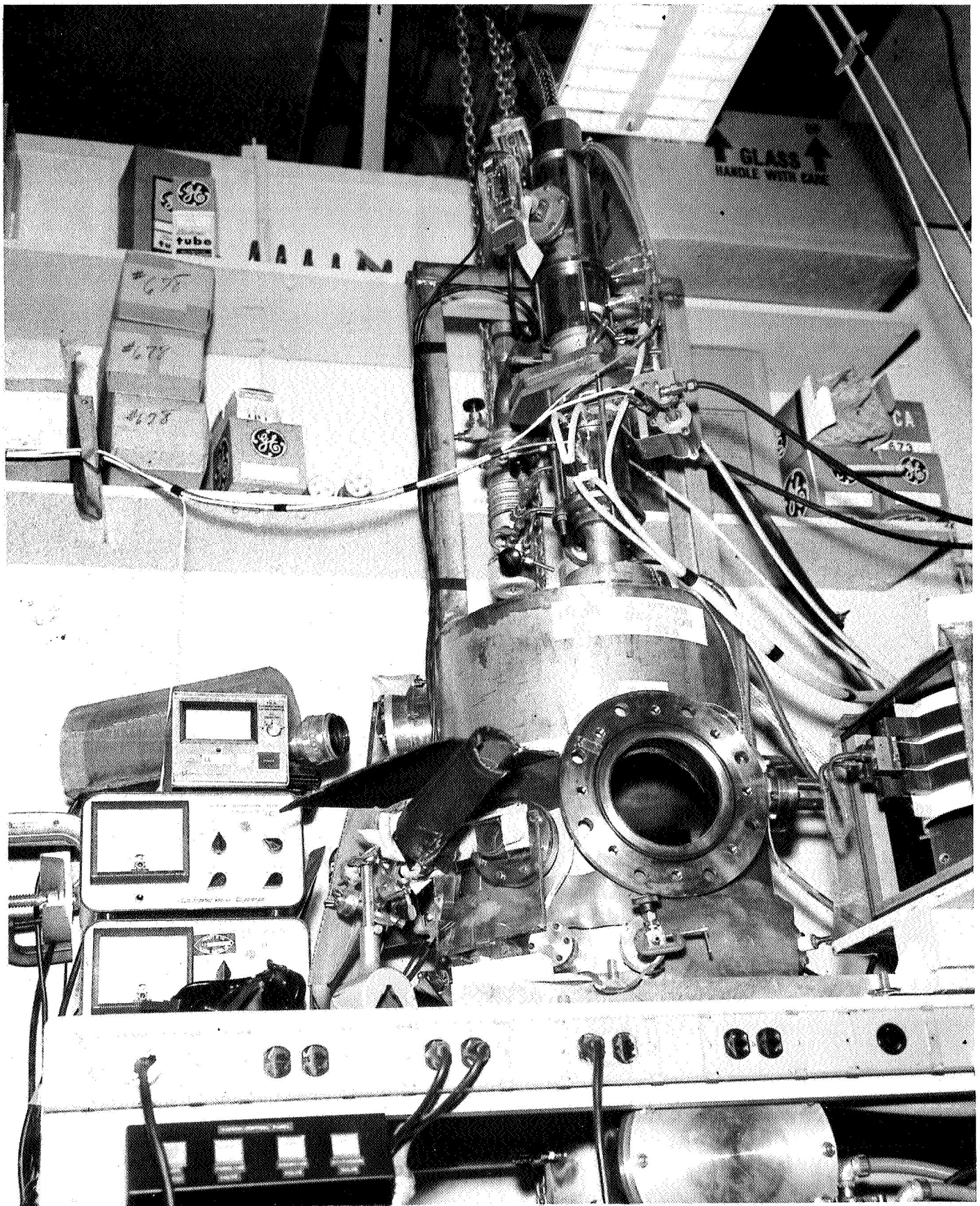


Figure 26 - Stainless Steel Levitation Chamber With Electron Beam Heating Unit

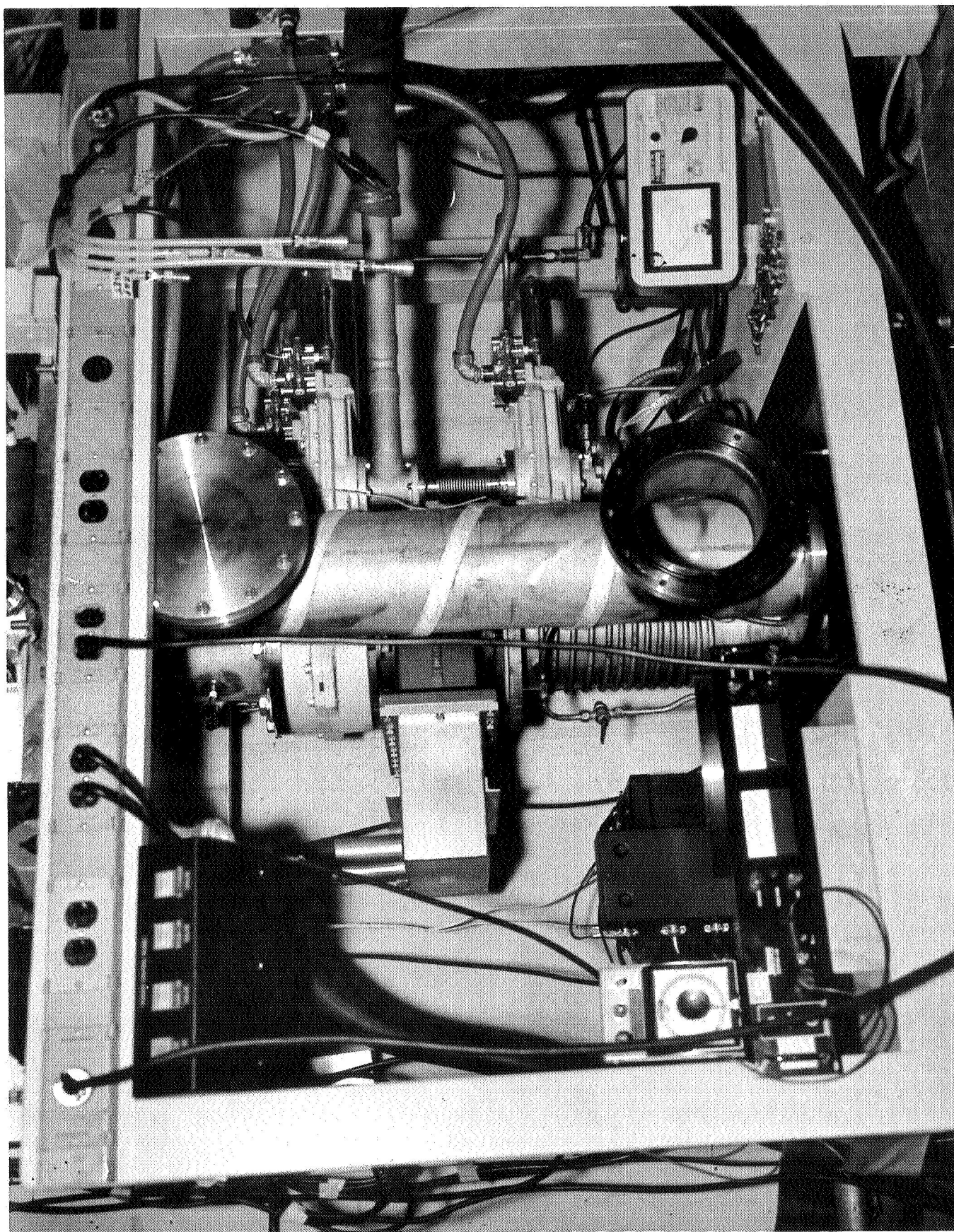


Figure 27 - Four Foot Drop Tube

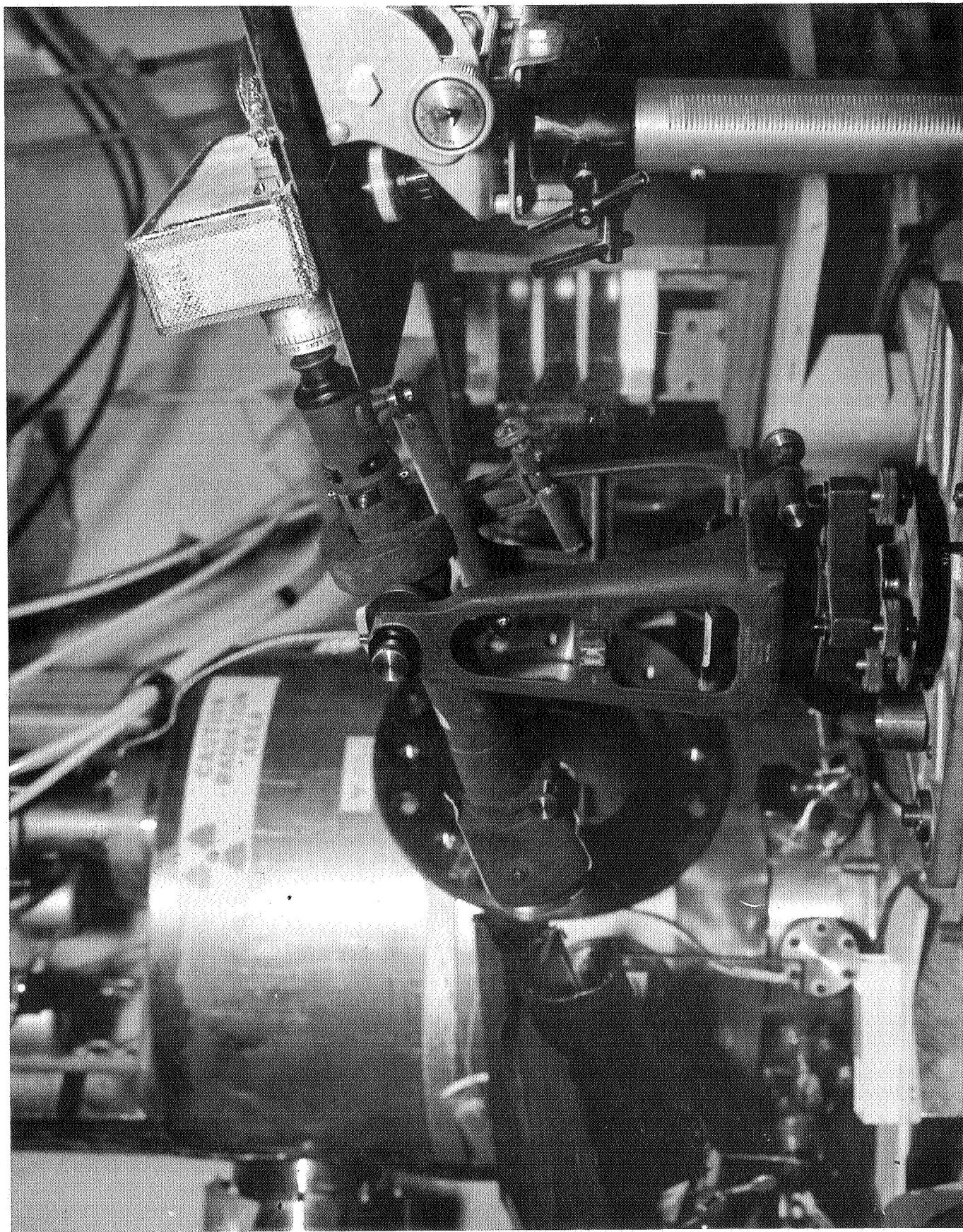


Figure 28 - Solid State Imaging Array

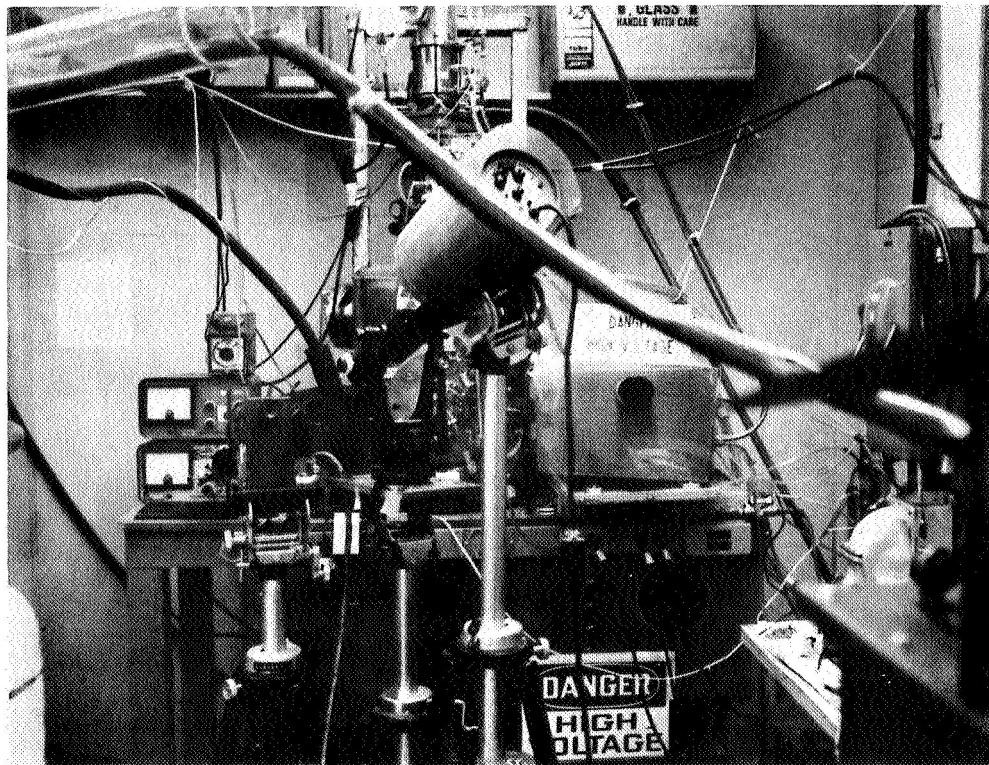
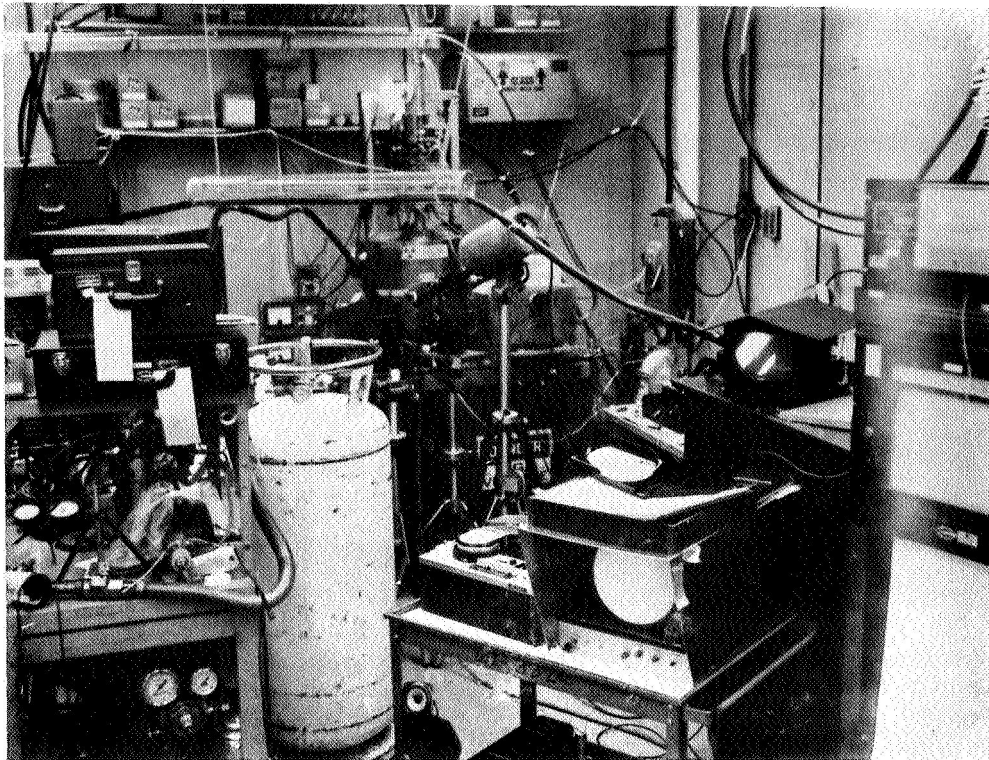


Figure 29 - Stainless Steel Levitation System (Video Display Of Levitated Specimen)

recording system problems associated with the experiments can be viewed and corrected after the actual experiment is performed and the physical situation can be studied at leisure.

A sequence of photographs of a levitated tungsten specimen is shown in Figure 30 . The specimen elongates as melting commences and continues to elongate until the specimen is lost. In the terrestrial levitation 10 gram specimens are typically maintained for periods as long as 2 minutes. In the weightless environment of space no such limitations apply. With terrestrial levitation of 10 grams of molten tungsten, considerable art and skill is required to maintain the specimen levitated and molten for appreciable periods of time. In the weightless environment where objects are naturally levitated, only position must be controlled and this can readily be accomplished (Ref. 4).

The levitation coil assembly used in the Stainless Steel Levitation Chamber is shown in Figure 22 . A thick molybdenum ring acts as a protection for the coil from the electron beam and also is useful for focusing and spot size control. A passive stabilizing ring made from molybdenum is used to shape the levitation field to provide additional stability to the levitated molten tungsten specimen. Without the stabilization ring, specimens tend to jump out of the coil as the levitation force is increased to maintain the molten specimen stably levitated.

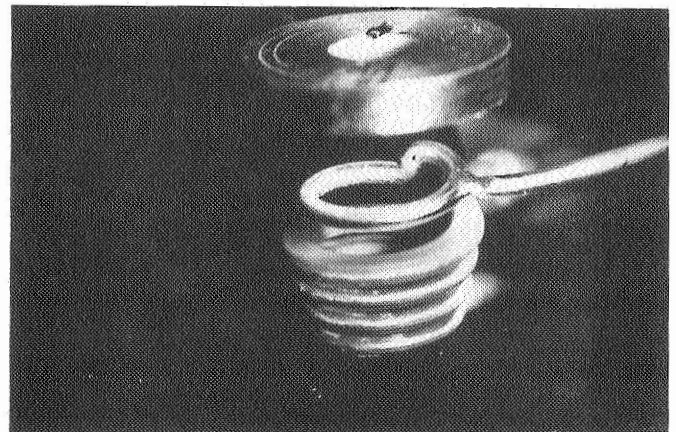
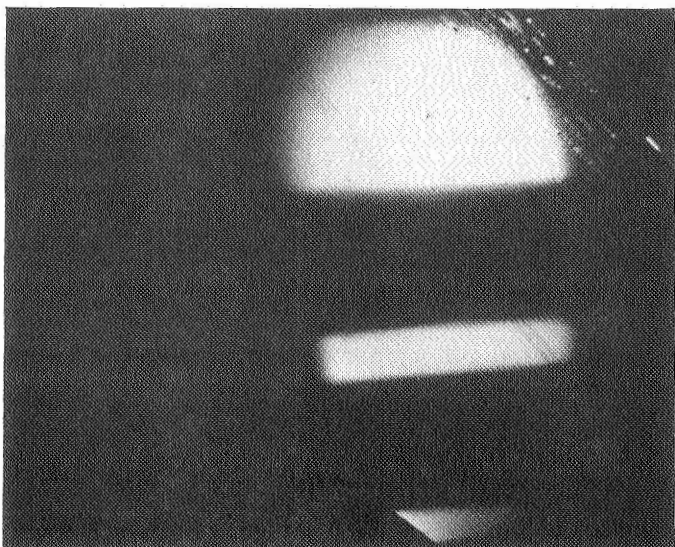
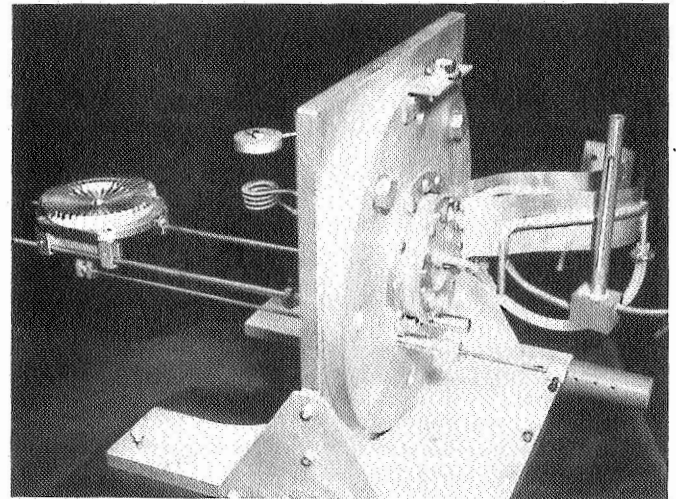
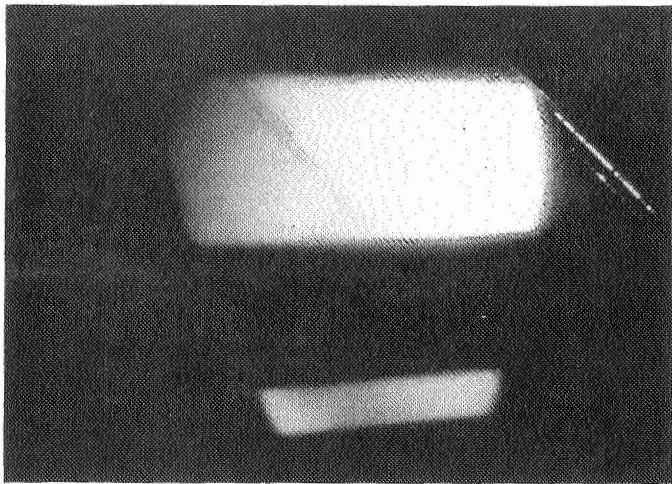
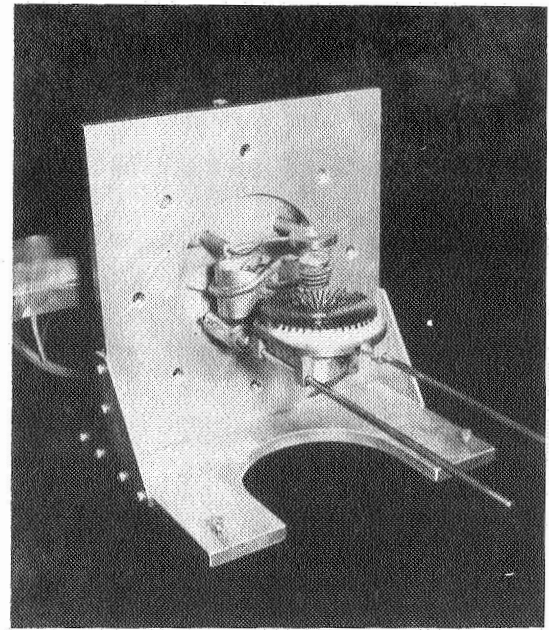
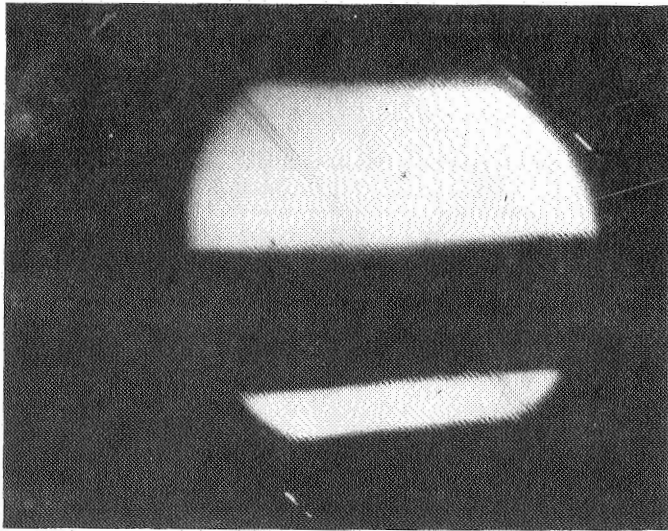


Figure 30 - Melting Sequence With Progressive Elongation of Levitated Molten Tungsten Specimen. Electron Beam Strikes Specimen at Its Top And Melting Progresses Downward.

3.0 LEVITATION EXPERIMENTS: SOLID STATE

3.1 HIGH TEMPERATURE VACUUM DEGASSING

The objectives of these experiments with tungsten in the solid state were:

1. to study the outgassing properties of the commercial wrought tungsten starting material as a function of temperature.
2. To examine the changes in structure of the commercial wrought tungsten as a function of temperature.
3. To develop a technique for levitation and select the levitation coil prior to melting experiments.
4. To test the levitation system prior to melting experiments.

It was initially supposed that the commercial wrought tungsten bar stock purchased, a powder metallurgy product; would contain a high degree of impurities. Therefore it was analyzed by emission spectroscopy to determine the elemental impurities, by vacuum fusion to determine the oxygen, hydrogen, and nitrogen content, and by conductometric analysis to determine the carbon content. These results are presented in the first column of Table I. The weight percentages of carbon, oxygen, hydrogen and nitrogen are typical of this material and convert to 153 parts per million (ppm) of carbon, 57 ppm oxygen, 66 ppm nitrogen, and 183 ppm hydrogen. The rather high percentage of hydrogen is probably due to the sintering process in hydrogen and is not present as an interstitial in the tungsten lattice or in the grain boundaries but is adsorbed into the tungsten and remains held in that form after the sintering. Thus the starting material is a typical commercial stock tungsten. In Figure 31 a photograph of this material is shown. Considerable porosity is observed in this photograph. It is thought that the excess hydrogen is adsorbed onto the surfaces of these pores and hence is not removed during the cleaning procedure before vacuum fusion analysis. As such it represents the hydrogen content of the initial starting material.

Table I
Test Results
(Results in PPM)

<u>Element</u>	<u>Raw</u>	<u>Run 419</u>	<u>Run 420</u>	<u>Run 421</u>
Ba	<10	<10	<10	<10
B	30	24	60	24
MN	<10	<10	<10	<10
Mg	<0.5	<0.5	<0.5	<0.5
Pb	<6	<6	<6	<6
CR	<6	<6	<6	<6
Sn	<6	<6	<6	<6
As	<10	<10	<10	<10
Sb	<10	<10	<10	<10
Bi	<10	<10	<10	<10
Co	<10	<10	<10	<10
Al	<4	<4	<4	<4
V	<4	<4	<4	<4
Be	<0.5	<0.5	<0.5	<0.5
Cd	<10	<10	<10	<10
Ag	3	3	3	3
Zn	<10	<10	<10	<10
Ca	<10	<10	<10	<10
Si	120	120	150	90
Fe	12	15	18	12
Cb	<10	<10	<10	<10
Ni	<4	<4	<4	<4
Mo	60	30	30	24
Cu	1	1	1	1
Zr	<4	<4	<4	<4
Ti	<4	<4	<4	<4

Also sought but not found were the alkali and noble metals.

Table II
(Results in Weight %)

<u>Element</u>	<u>Raw</u>	<u>Run 419</u>	<u>Run 420</u>	<u>Run 421</u>
N	0.0005	<0.0001	0.0004	0.0001
O	0.0005	0.0002	0.0005	0.0002
H	0.0001	0.0001	<0.0001	<0.0001
C	0.0010	0.0012	0.0008	0.0008

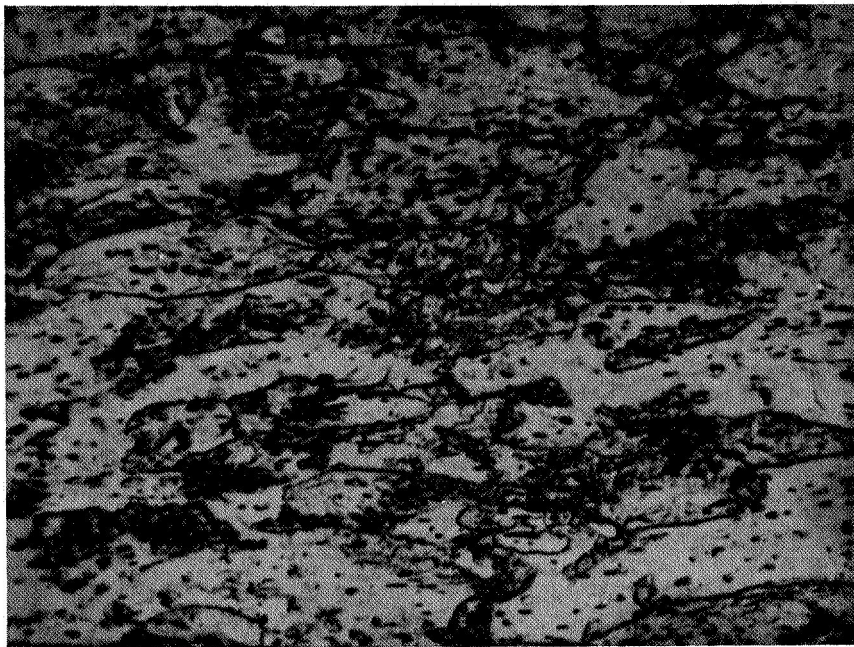


Figure 31 - Micrograph Of Starting Tungsten Material. Magnification Is 150X.

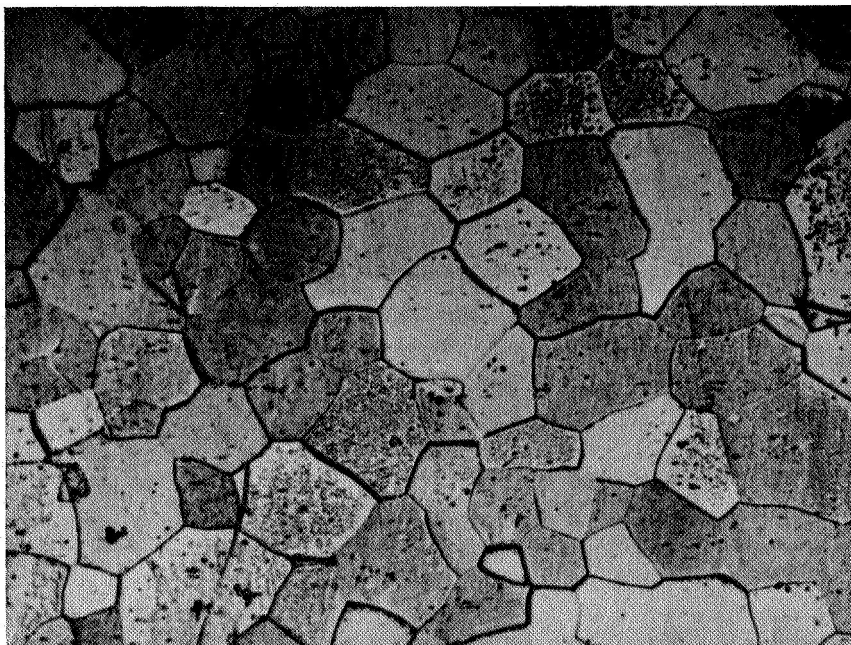


Figure 32 - Micrograph Of Tungsten Specimen Held At 1800°C For One Hour, Magnification at 150x

Using a small vacuum induction furnace, the tungsten was heat treated in a vacuum of 10^{-4} torr to 10^{-5} torr for periods of one to two hours. The results are presented in Table One where run #419 was held at 1800°C for one hour, run #420 was held at 1900°C for two hours and run #421 was held at 2000°C for one hour. For runs #419 and #421 considerable clean up of nitrogen and oxygen is observed. Carbon is not appreciably cleaned up in any of these runs. Because of the high blank of the furnace, meaningful gas evolution data was not obtained. Extensive recrystallization was observed however. In Figures 32 , 33 , and 34 the changes in structure for these runs can be seen. In Figure 35a & b the x-ray Laue patterns for the starting material and the recrystallized tungsten are shown. In Table 3 grain size and Knoop Hardness are compared. Softening of the tungsten from annealing is observed.

The results of these experiments serve as a starting base for the tungsten prepared by levitation processing. They characterize the initial starting material and show that the material behaves typically as expected and is not an anomalous material. The recrystallization of the highly stressed, wrought tungsten at these high temperatures is as expected also. It raises an important question, which is considered below. If the high purity, fine grained tungsten is prepared by containerless processing, what will prevent extensive recrystallization during its service at high temperatures?

Surveying the literature (Ref 47 , and 48) the following conclusions were made:

1. Since a minimum deformation is required to initiate recrystallization at a given temperature, the formation of a fine grained high purity tungsten with a low dislocation density would have a very high recrystallization temperature.

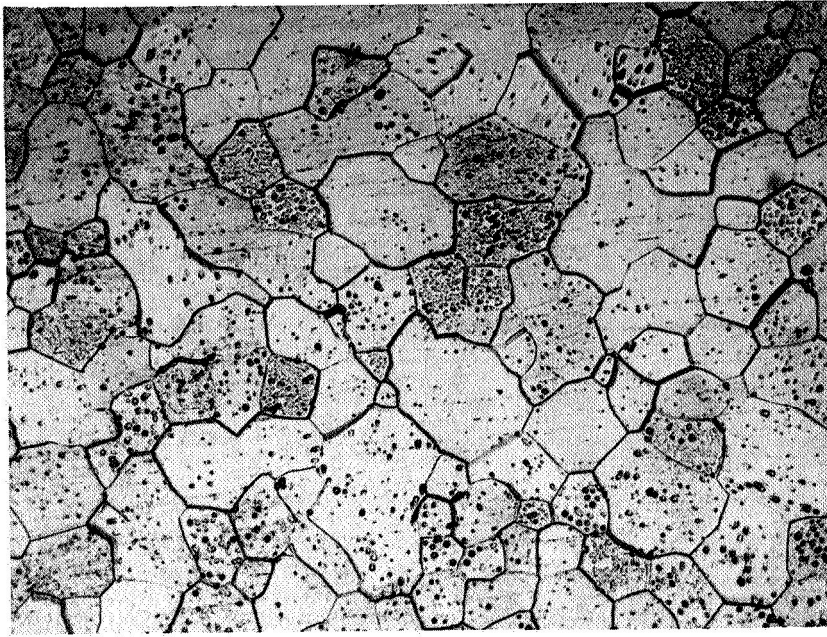


Figure 33 - Micrograph Of Tungsten Specimen Held At 1900°C For Two Hours. Magnification 150x



Figure 34 - Micrograph Of Tungsten Specimen Held At 2000°C For One Hour. Magnification 150x

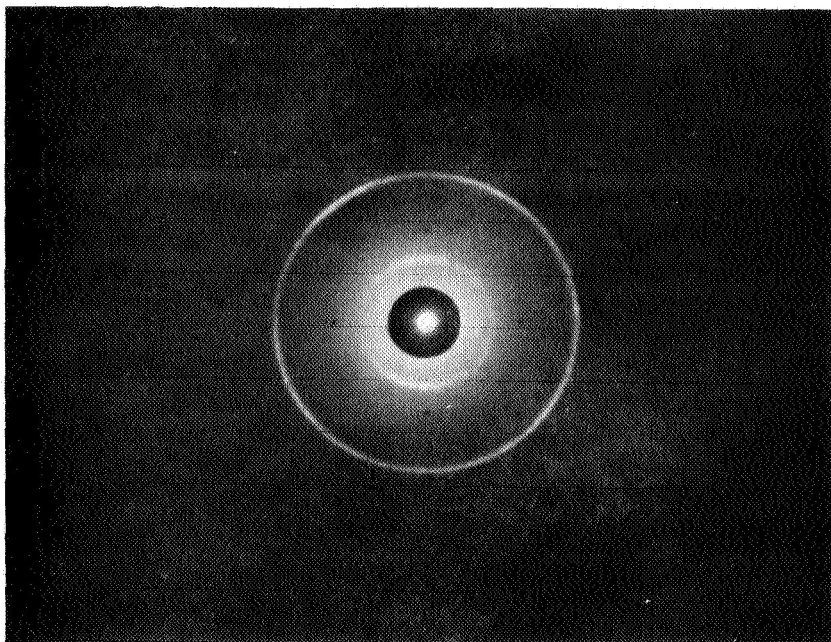


Figure 35a - X-ray Laue Pattern Of Initial Starting Tungsten Material By Back Reflection

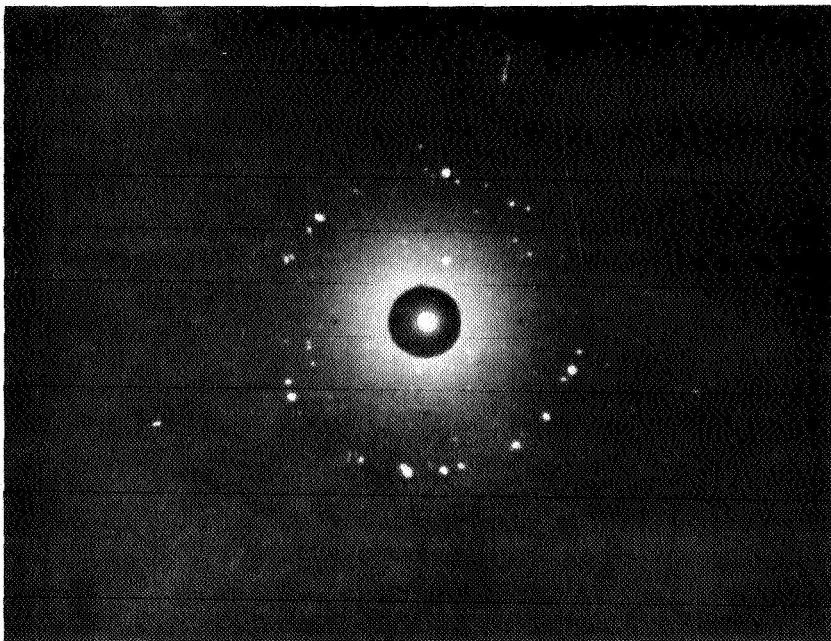


Figure 35b - X-ray Laue Pattern Of Recrystallized Tungsten After Being Held at 2000°C For One Hour.

2. With a very pure metal, however, grain boundary migration and grain growth would not be inhibited and in service grain growth would continue at high temperatures. The extent of grain growth in service would be an important test during the testing contemplated.

3. Work hardening the fine grained metal during fabrication would lower the recrystallization temperature and would result in recrystallization of a fine grained material in service, as the nucleation rate and grain size depends upon the initial grain size and amount of deformation. Grain growth, however, at elevated temperatures, would proceed after recrystallization.

It is concluded therefore, that the production of a fine grained high purity tungsten is a viable route for the production of x-ray targets, provided that in service, excessive grain growth does not limit the service lifetime to the present service lifetime or less. If the service lifetime is lengthened appreciably, even though failure occurs through this mode, then the production of fine grained high purity tungsten for x-ray targets was still highly desirable. Twenty thousand two second exposures is a little over eleven hours but this is not continuous annealing. The problem of grain growth for x-ray targets must be considered in light of the number of exposures per hour and the temperature distribution over the target. Tests of this nature could only be made under actual in service conditions. Thus at this point it is concluded that a high purity fine grained tungsten was one of the routes to explore producing better x-ray targets.

3.2 LEVITATION OF SOLID TUNGSTEN

A series of experiments was performed with 10 gram specimens of tungsten fashioned into either chamfered cylinders or spheroids. It was observed during these and subsequent experiments that irregular shapes could be levitated but that chamfered cylinders and spheroids had greater stability. With the use of the electron beam

only the spheroidal shapes had the required stability.

The basic experiments in the Glass Levitation system were performed to study gas evolution from levitated solid tungsten specimens. Experiments in the Stainless Steel Levitation Chamber with solid tungsten were directed toward recrystallization and grain growth studies and using the electron beam to control temperature. The procedure for these experiments is described below.

3.2.1 Procedure

The procedure for studying the evolution of gases from levitated tungsten in the Glass Levitation System is as follows:

1. The levitation chamber is pumped down to 4 to 7×10^{-7} torr.
2. With the power off, the chamber is sealed by closing off the valve to the vacuum system. The rise in pressure with time is recorded. This is called the leak up test and is a measure of the contribution from surfaces in the chamber other than the hot tungsten ball.
3. The valve to the vacuum system is opened to the point where the pressure reads a fixed value in the range of 10^{-5} to 5×10^{-5} torr. A mass scan is taken with the mass spectrometer at this fixed value to record the contribution of each residual gas specie present.
4. The vacuum valve is opened all the way and the levitation chamber is pumped down to better than 10^{-6} torr again. The specimen is levitated and the pressure rise with the vacuum system pumping is noted. Levitation in a sealed chamber produces a pressure rise initially into the tens of micron range so that this was not attempted due to fear of arcing in the coil.

5. At intervals of 15 minutes leak up rates and mass scans are taken as in procedures 2 and 3 but with the power on and the ball levitated.

The pressure versus time curves are plotted and the mass spectrometer data is analyzed after each run. Solid specimens have been levitated and studied in the Glass Levitation Chamber for periods as long as 2.5 hours.

From the change in slope of the pressure rise curves and the change in residual gas species present with time a picture of what is occurring in the levitation chamber can be evolved. With the levitation chamber air cooled and the levitation coils water cooled, the assumption that the major contributor to the gas load and change in gas species is due to the incandescent tungsten ball at 2600°C is valid.

3.2.2 Experimental Results

Figure 36 shows the pressure rise time curves for a typical 2.5 hour run. The temperature of the levitated tungsten sphere was recorded to be 2743°K or 2470°C. The slope of the rise time curve at the start of the experiment, at room temperature ($\sim 20^\circ\text{C}$), is 2.6×10^{-5} torr/minute. After a half hour, levitated at the above temperature, the slope of this curve is 13.4×10^{-5} torr/minute. Each subsequent pressure time curve from one half hour through 2 hours, 19 minutes levitated shows a decreasing slope, approaching that of the cold measurement. Less and less gas is being evolved as the levitation run is continued.

The mass spectrometer data at intervals given is shown in Table 4. The reduced data is shown in Table 5.

The data was reduced by applying cracking pattern overlays for the gases from the VEECO bulletin on the GA-4R mass spectrometer. Twenty six minutes after levitation, the CO content has fallen by a factor of sixteen and one hundred

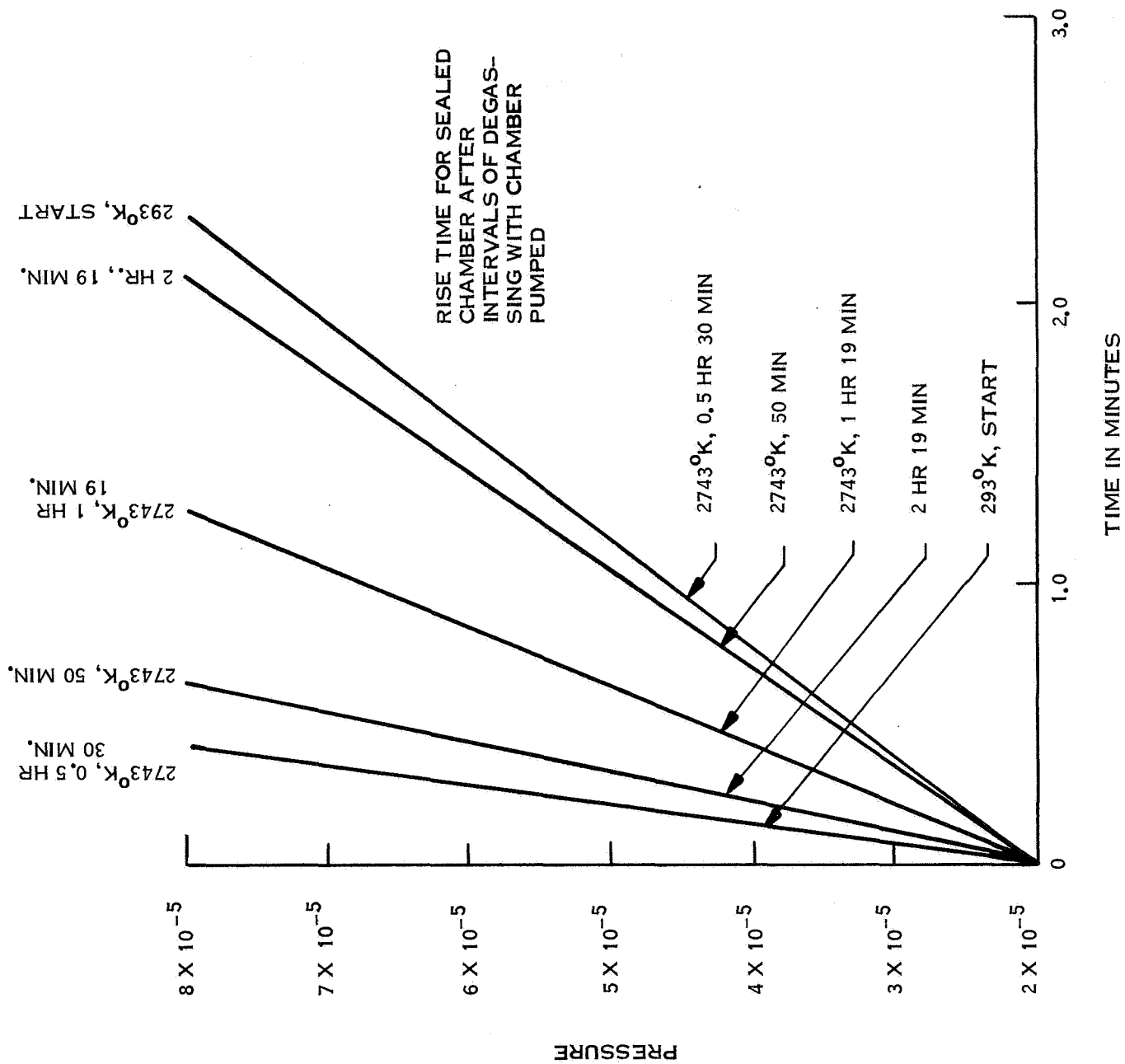


Figure 36 - Pressure Rise Curves For Outgassing Solid Tungsten At 2600°C

Table 3

Specimen Number	Temperature (°C)	Duration hrs	Grain Size (microns)	Knoop Hardness Number
003	Room	0	Wrought	480
004	1800	1	36	390
005	1900	2	66	365
006	2000	1	53	405

Table 4

MASS SPECTROMETER DATA 9/11/74

LABEL	1	2	3	4	5	6
TEMP.	293°K	2723°K	2723°K	2723°K	2723°K	2723°K
TIME	0	26 min.	44 min.	75 min.	100 min.	120 min.
Mass #	Peak Height	Peak Height	Peak Height	Peak Height	Peak Height	Peak Height
40	0.75	0.48	0.50	0.46	0.54	0.48
28	9.79	2.12	2.79	2.17	2.20	1.94
20	0.70	0.31	0.38	0.35	0.38	0.36
18	9.59	2.82	2.89	2.07	1.80	1.54
17	2.69	0.78	0.76	0.60	0.70	0.60
16	3.74	2.62	3.89	3.27	3.60	3.04
15	3.29	2.32	3.49	2.87	3.20	2.74
14	0.75	0.47	0.67	0.59	0.66	0.55
13	0.20	0.15	0.23	0.22	0.25	0.21
12	0.38	0.10	0.14	0.15	0.15	0.17
4	0.42	0.09	0.14	0.17	0.16	0.17
2	248	368	618	519	588	489

Table 5

REDUCED DATA

LABEL	1	2	3	4	5	6
SPECIES	PEAK HEIGHT	PEAK HEIGHT	PEAK HEIGHT	PEAK HEIGHT	PEAK HEIGHT	PEAK HEIGHT
N ₂	3.24	1.72	2.15	2.15	2.20	1.94
CO	6.55	0.40	0.64	0.02	0.00	0.00
CH ₄	3.65	2.6	3.89	3.22	3.58	3.05
H ₂ O	9.59	2.82	2.89	2.07	1.80	1.54
H ₂	248.0	368.0	618.0	519.0	588.0	489.0

Table 6

Temperature	293°K	1933°K	2123°K
N ₂	9.5	2.06	1.04
CO	5	7.34	38
CH ₄	4.44	10.8	8.7
H ₂ O	104	64.8	5.95

minutes after levitation it has a negligible contribution. The hydrogen peak rises to a maximum at 44 minutes. During this run and during repeated runs the glass walls were blackened by a black deposit.

Since the temperature of the levitated tungsten specimens could not be controlled and reached 2473°C to 2600°C upon levitation, a tungsten specimen was suspended by a tungsten wire and heated in the levitation coil to 1933°K and 2123°K (1660°C and 1850°C) respectively. The analysis of gases is shown in Table 5. Nitrogen was evolved rapidly below 1660°C. Carbon monoxide was evolved rapidly at 1850°C.

The pressure rise upon levitation with the vacuum system pumping was typically from 4×10^{-7} torr to 2×10^{-4} torr, a factor of 1000. This prevented experimenting with levitation in a sealed chamber as the pressure would have risen above 1 micron. It was evident that most of the gas was evolved in the first few minutes of levitation as the pressure decreased rapidly. This leads to the conclusion that most of the gases adsorbed on the tungsten are rapidly evolved away during the levitation itself.

The black deposit on the chamber walls is a result of the Langmuir water vapor cycle. Water vapor impinging on the hot tungsten is dissociated into H_2 and O^+ and further to H^+ . The H^+ ions arriving at the glass walls are adsorbed onto the glass. The O^+ ions combine with tungsten to form oxides which stream to the glass. There they are reduced to tungsten and water vapor is regenerated again as a result. Thus the net result is a tungsten deposit on the glass. As the tungsten layer builds up, the process ceases and a rise in hydrogen would be expected. In effect the levitation apparatus is a giant light bulb with the same chemistry involved as described by Langmuir.

The results of these experiments are:

1. Rapid evolution of adsorbed gases upon levitation and heating to 2473°C or higher precludes the necessity of long degassing time before melting. Degassing times of the order of five minutes are sufficient to reduce the gas load to safe levels before the melting profile is begun.

2. The negligible residual gas pressure of oxygen in the initial scan at room temperature and in successive scans at levitation temperature preclude much decarburization. Evolution of adsorbed carbon monoxide is rapid but the carbon monoxide thereafter slowly decreases to a negligible value.

3. The chemistry of reactions occurring with the levitation chamber after initial evolution of adsorbed gases makes it difficult to evaluate the degassing of tungsten. Chemical reactions on the hot tungsten surface and at the levitation chamber walls must be included in any model of degassing of tungsten in good vacuum levels of 10^{-6} torr or below.

3.3 EXPERIMENTS WITH SOLID TUNGSTEN IN THE STAINLESS STEEL SYSTEM

Experiments with tungsten in the Stainless Steel Chamber with electron beam heating yielded important data on continued grain growth at elevated temperatures. Figure 37 shows a one centimeter diameter tungsten specimen which has been taken up to the melting point. Part of the outer surface has melted and a small shrinkage cavity is evident. The melted portion is evident at the top above the shrinkage cavity. This condition is typical of the conditions of near melting experienced during service as an x-ray target. Grain size of the order of 1000 microns is evident in the unmelted portion of this specimen. The duration of this experiment was 15 minutes.

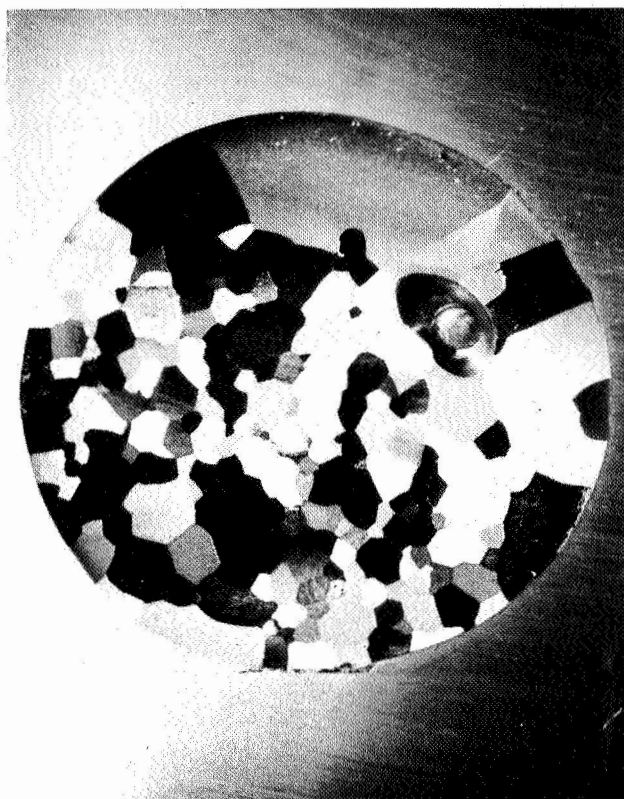
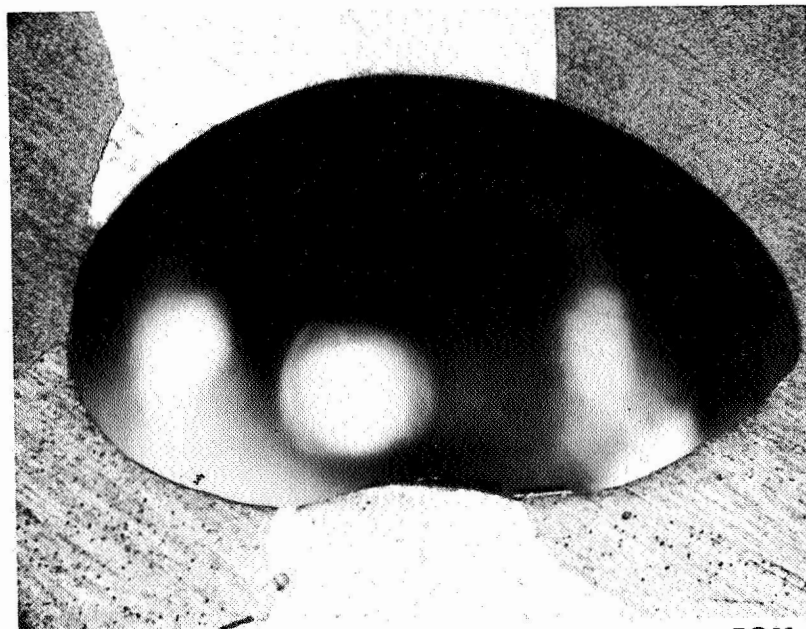
**A****8.5X****B****50X****C****50X**

Figure 37 - Recrystallization At The Melting Point.
Partial Melting Observed at Top

Thus these experiments lead to the conclusion that grain growth at elevated temperatures is to be expected. From the runs at 1800°C to 2000°C which produced grain sizes of the order of 60 microns after long duration, these grain sizes near melting temperature are a factor of 17 larger for a duration of only 15 minutes. The very large grains at the top are the solidified portion that was melted. There is a notable absence of porosity in the large grains compared to that at lower temperatures. From the photograph at 50 x it is evident that grain growth was continuing as the smaller grains were disappearing as the larger grains grew.

The growth of recrystallized tungsten at temperatures near the melting point is as expected. However x-ray targets do not operate at this temperature continuously but for short exposures (2 seconds). Under actual service conditions grain growth would be expected to occur differently and this must be evaluated during the testing of target material under in service conditions. Under conditions of steady heating a fine grained structure could not be maintained at these temperatures. However whether or not this is the limit to service operation for an x-ray target fabricated out of this material can only be determined by actual testing in service conditions.

4.0 LEVITATION EXPERIMENTS: MOLTEN STATE

With successful levitation melting of tungsten, the main phase of experiment work began. Ten grain specimens of tungsten were levitated, melted and solidified under the following conditions.

1. Solidified while levitated in the levitation coil through removal of electron beam.

2. Solidified by dropping while molten onto a water cooled copper plate in the copper catch bucket.

3. Solidified while molten by dropping into a quenchpot with liquid tin as the quenching medium.

4. Solidified after falling freely through a distance of four feet onto a water cooled copper plate in the copper catchbucket at the base of the drop tube.

The major objective of these experiments was initially to achieve a high degree of supercooling and through this to produce a fine grained high purity tungsten with room temperature ductility and enhanced service properties at elevated temperatures. As reported below, appreciable supercooling was achieved only in the case of freely falling molten tungsten. Tungsten solidified while levitated in the levitation coil does not appear to have supercooled any appreciable amount.

As a byproduct of these experiments vapor deposited tungsten on molybdenum with deposits as thick as 3 mils were also obtained. It is thought that fine grained deposits of the order of 6 mils thick would produce x-ray targets with enhanced service properties. This will be discussed below. This may prove to be a viable route to producing better targets.

A variety of structures were produced. The most surprising was the growth of single crystals of tungsten. It had been postulated that with the elimination of sites for heterogenous nucleation, the growth of single crystals of metals

and alloys might be possible (Ref 4) but this had not been seriously considered prior to this work. Upon production of these single crystals, a re-examination of the concept of containerless solidification was initiated. It was clear that a new technique had been discovered for the production of single crystals through rapid solidification. These results have opened up a new area of containerless processing.

4.1 PROCEDURE

The procedure for levitation melting of tungsten is as follows:

1. The stainless steel levitation chamber is pumped down to 10^{-6} torr or better.
2. The specimen is inserted into the levitation coil by raising the pedestal into the coil (see Figure 23).
3. The rf power is turned on and the specimen is levitated.
4. The specimen which has been levitated and heated to 2600°C is allowed to degas for at least five minutes. Usually the time allowed for degassing was longer, sometimes of the order of one half hour.
5. The electron beam is turned on. The beam is focused on the molybdenum protective ring and the spot size is adjusted to about $3/8$ inch ($\sim .95$ centimeter) in diameter or less.
6. The beam is then swung into the hole in the protective ring and impinges on the levitated tungsten specimen.
7. The accelerating potential was preset, usually at 32 kilovolts. The beam current is slowly raised in steps of 10 milliamperes. At each step data for the temperature measurements is recorded. When melting begins or the specimen becomes unstable the beam current is raised until stable melting occurs.
8. Depending upon the experiment the beam may be cut off after an interval molten, to solidify in the coil or the specimen is dropped by cutting off the rf power.

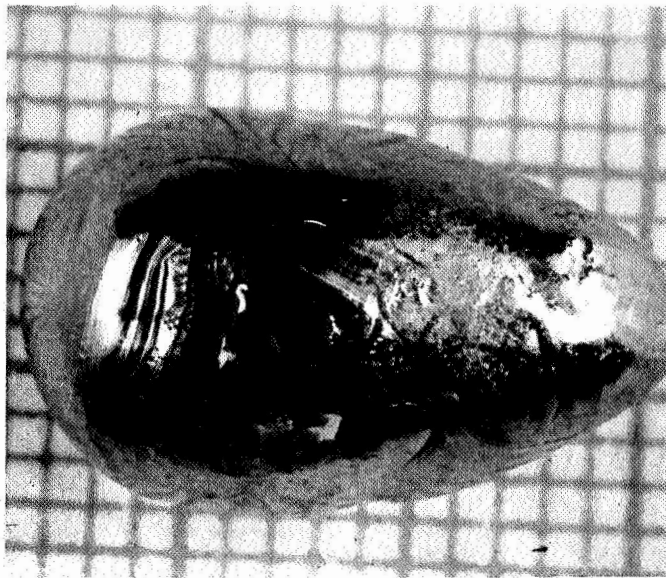
Documentation during the run is obtained through videotape recording of the levitation and/or drop and through written records. A sequence of photographs is shown in Figure 30 . The uppermost is the specimen levitated and solid

at 2600°C. The middle photograph shows stable melting. The lower photograph shows the highly elongated specimen prior to its loss through the coil after two minutes of stable molten levitation. It is an art to keep the molten tungsten specimen levitated by adjusting either rf power or beam power. Quick reflexes are required. Once the specimen has elongated to the extent shown in the lower photograph of Figure 30 it drops through the coil. No dripping or pouring through the bottom of the levitated specimen was ever observed. Specimens were lost through elongation alone.

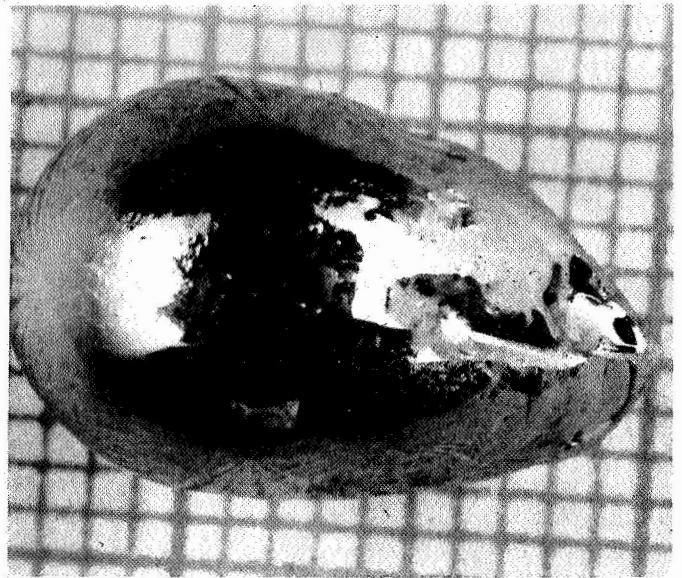
4.2 SPECIMENS SOLIDIFIED WHILE LEVITATED

Specimens solidified while still levitated through turning off the electron beam were either single crystals or bicrystals. Figure 38 is a photograph of a typical specimen produced through solidification while levitated. Figures 39, and 40 are photographs of specimens sliced through the midplane lengthwise and electrolytically etched and polished. The photographs were taken under polarized light (Nomarsky Technique). Figure 39 shows the results of x-ray diffraction analysis. The (211) direction is along the longitudinal axis of the specimen so that the (211) close packed planes are perpendicular to the plane along which it was sectioned. This will be discussed below. There is a low energy grain boundary evident in this photograph. It is low energy because the lattice has the same orientation across the boundary. This was determined by x-ray diffraction. This may be classified then as a sub-grain boundary and the piece is one single crystal of tungsten. There are two shrinkage cavities evident. The large one is near the top and the smaller one is in the subgrain boundary. Since the large shrinkage cavity is near the top solidification must have started near the bottom and proceeded upwards. The smaller shrinkage cavity indicates that at least two nucleation events occurred but that the boundary formed was a low energy rather than a high energy

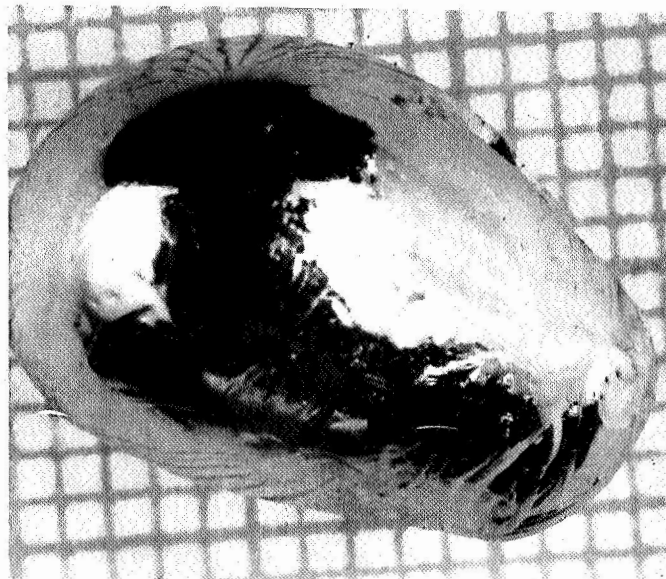
448



A



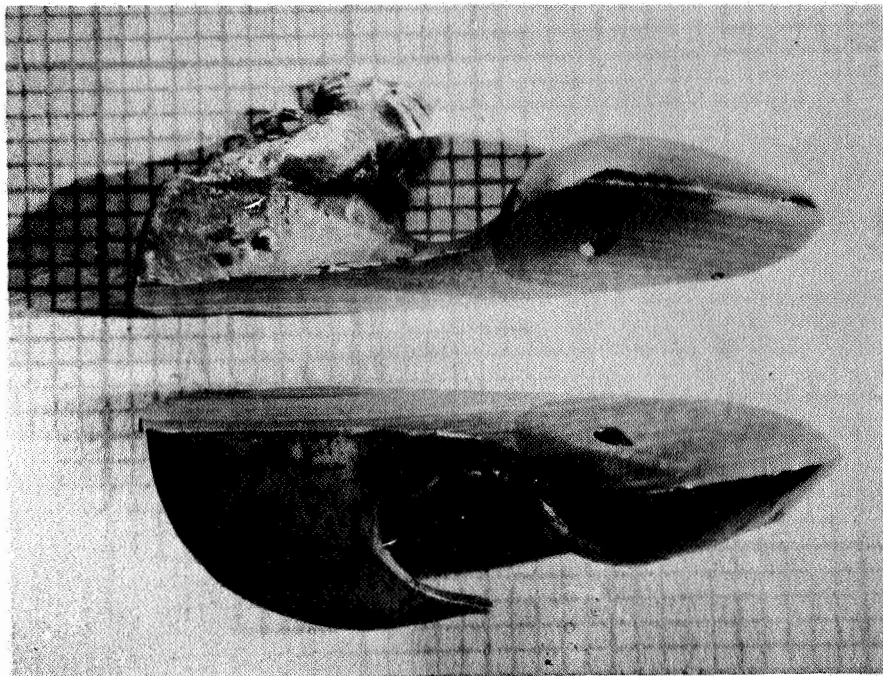
B



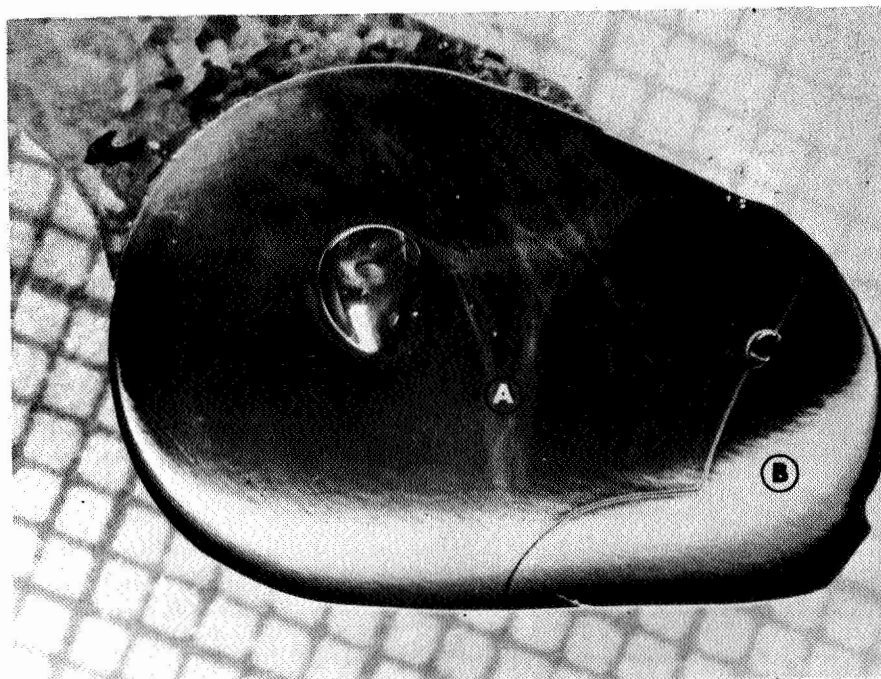
C

Figure 38 - Exterior Of Specimen Solidified While Levitated. The Grid Is A Millimeter Grid To Show True Size

455 B



3.5X



7.5X

Figure 39 - Single Crystal With Low Angle Grain Boundary.
Orientation Determined By Single Crystal Orienter.
Single Crystal Determined By X-ray Diffractometry And
Back Reflection Across Low Angle Grain Boundary

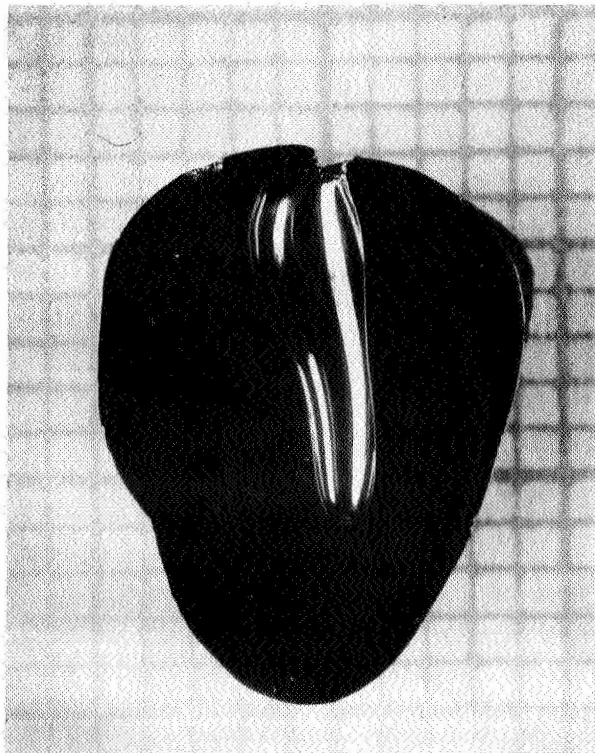
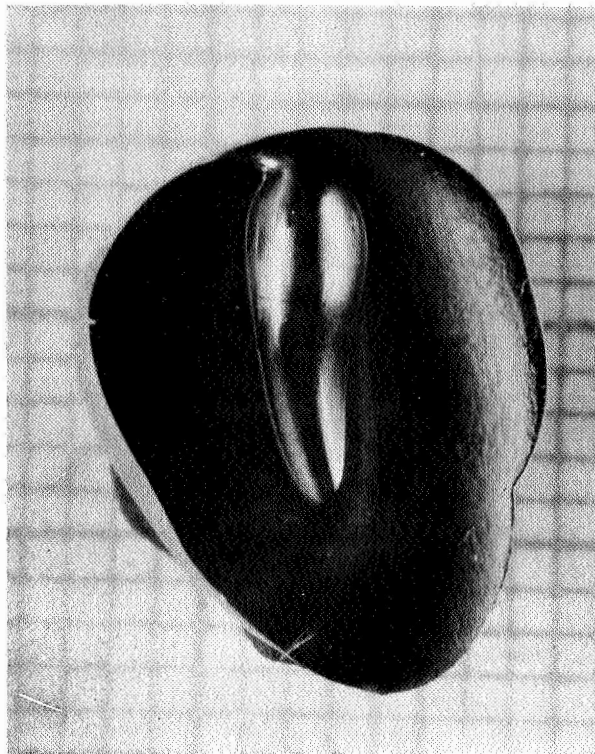


Figure 40 - Single Crystal With No Macroscopic Subgrain Structure Evident

grain boundary. In Figure 40 there are no boundaries, high energy or low energy evident. This is a single crystal of tungsten with no subgrain boundaries evident in the macrograph. The shrinkage cavity is again toward the top indicating that solidification began at the bottom tip. In Figure 41a there are two large crystals evident and three small ones at the bottom. Again evidence points to nucleation at the bottom and by competitive growth two crystals grew out of the three nucleated at the base.

A polycrystalline solid with very large grains was produced when one specimen touched the stabilization loop and solidified there and is shown in Figure 41b. It is evident that nucleation started on the surface of this specimen from the inward columnar shaped grains. It is evident that the impact produced a number of nucleation events. This would tend to indicate that some supercooling had been achieved for otherwise it is hard to explain many inward columnar growth over the surface. If nucleation occurred only at the impact point one would effect a totally different structure.

4.2.1 Characterization of Single Crystals Produced By Solidification While Levitated

The following characterization was performed on these single crystals.

1. Lattice parameter identification through x-ray diffractometry
2. Crystal orientation through X-ray diffractometry
3. Crystal perfection using optical microscopy
4. Deformation under compression
5. Asterism in Laue Pattern after deformation by Back Reflection X-ray technique.

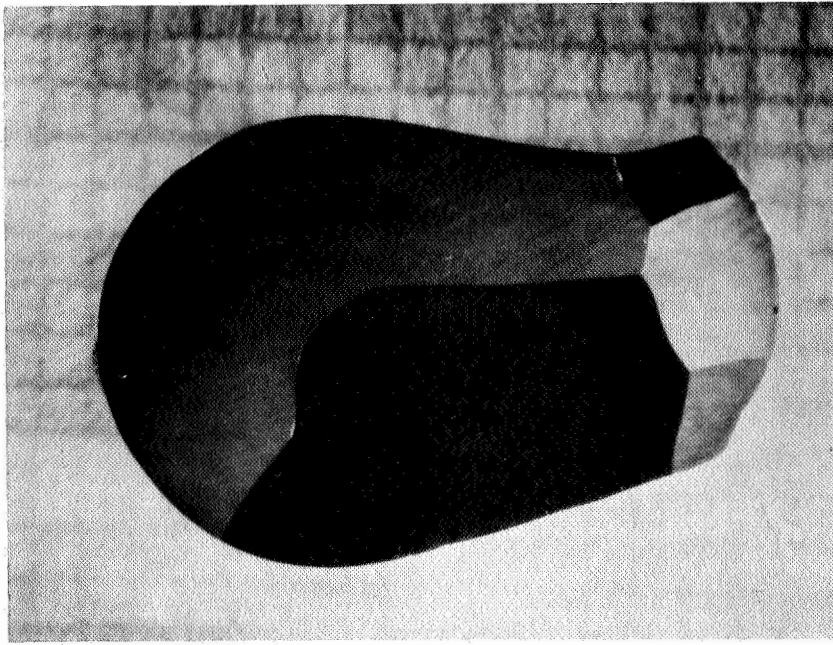


Figure 41a - Bi-crystal With Evidence Of Nucleation Starting At Tip.

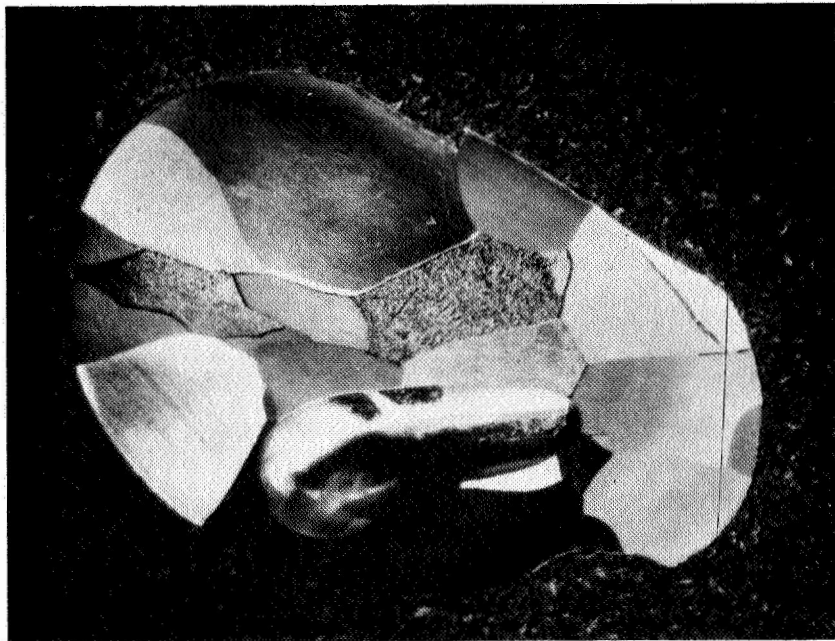


Figure 41b - Polycrystalline Specimen Solidified By Impacting Stabilizing Ring

Crystal orientation was determined using a single crystal orienter. The orientation typical of these crystals has been discussed and shown in Figure above. Crystal perfection was studied through etching and polishing and optical microscopy. In Figure 42 the typical mosaic pattern of tungsten single crystals is evident. In Figure 43 a subgrain (low energy) boundary is evident. In Figure 44 the typical Laue pattern of an undeformed single crystal of tungsten is evident. In Figure 45a the asterism or elongation of spots after deformation is evident. Figure 46 shows the compression stress-strain curve for both the raw polycrystalline wrought tungsten and the single crystal tungsten. In Figure 45b, slip in the single crystal specimen produced by this deformation is evident.

Results of this characterization show:

1. That single crystals of tungsten can be produced by rapid solidification while levitated. These single crystals are of good quality exhibiting substructure consisting of large subgrains within which there is a mosaic pattern of microscopic subgrains of dimensions of the order of 10 microns. The shape of these microscopic subgrains is not cellular and resembles subgrains produced through dendritic growth (Ref. 49). This dendritic growth may be produced by constitutional supercooling and in experiments with other metals (Ref. 50) only a small amount of impurities ($\sim .05\%$ by weight) can produce this growth structure. Dendritic growth could also be produced by achieving a large amount of supercooling. These single crystals resemble crystals produced by zone refining in microscopic subgrain features but do not show the cellular growth patterns of microscopic subgrains, which is also due to the presence of minute impurities. The difference is thought to be in the growth rate of the single crystals produced by solidification while levitated, which is less than 2 seconds, while zone refining takes much longer.

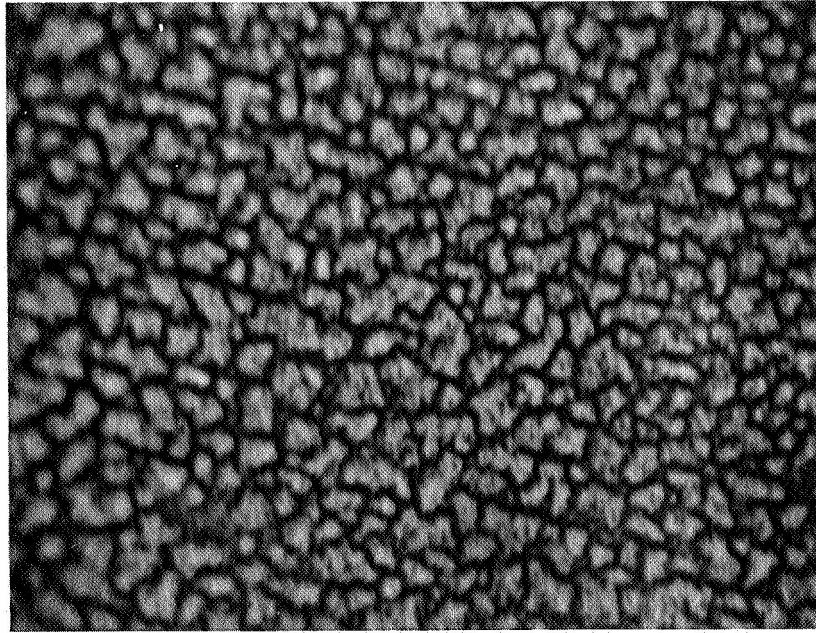


Figure 42 - Micrograph Of Figure 39 Specimen Showing Subgrain Structure After Etching And Polishing. Magnification 1000x.

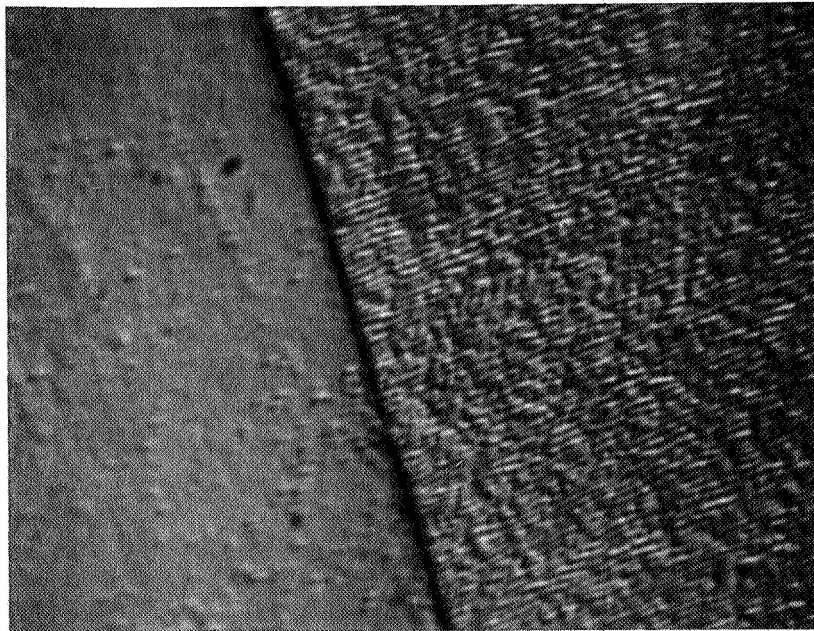
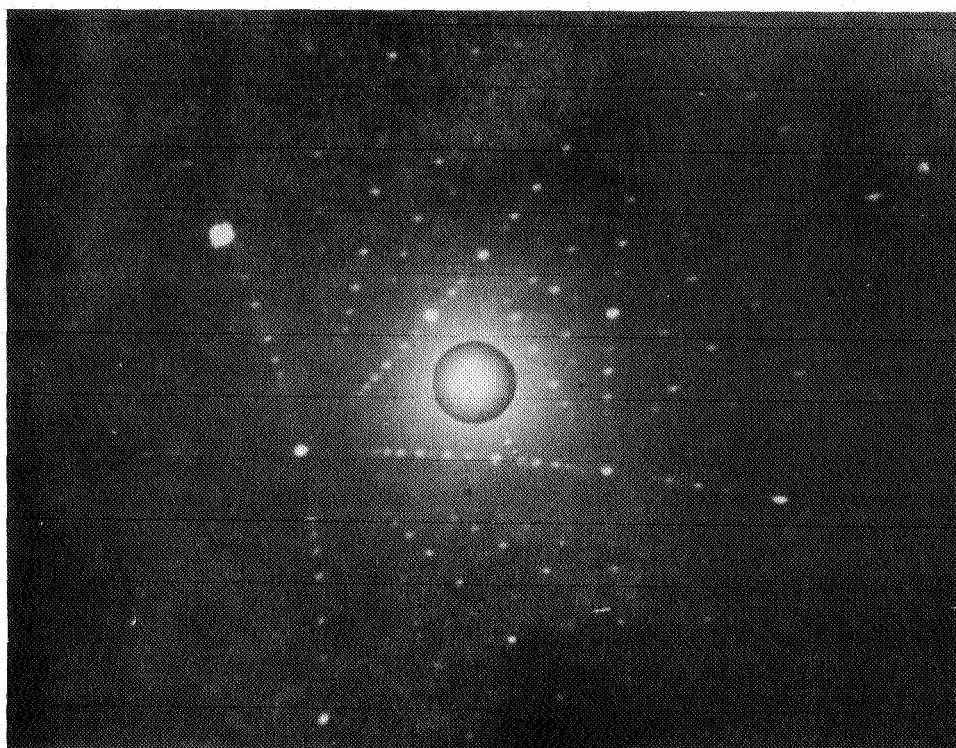
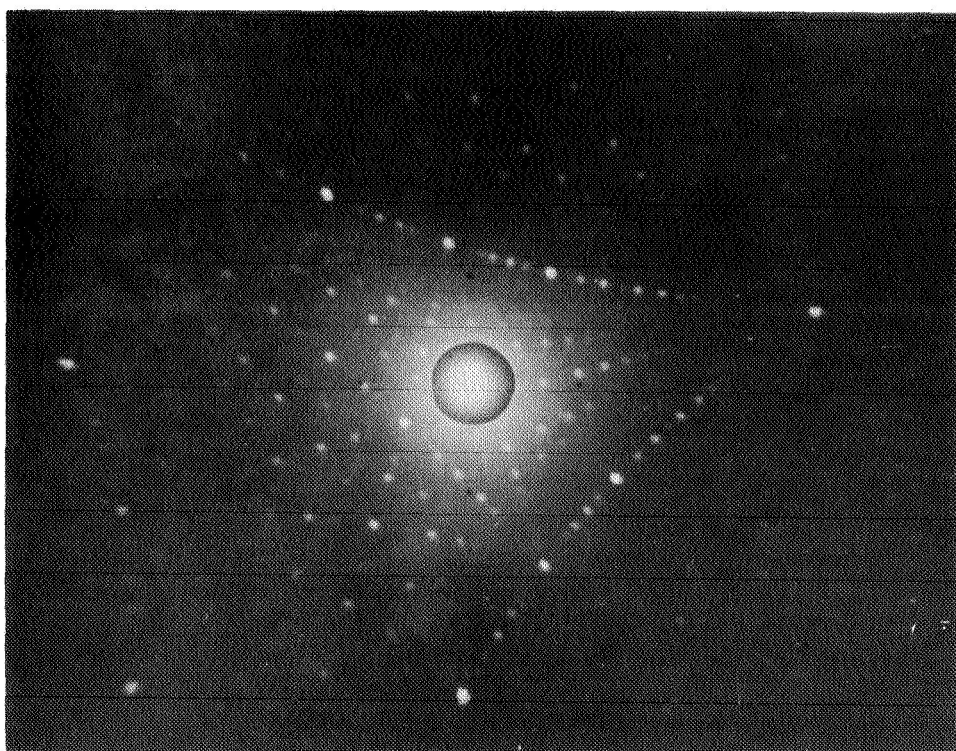


Figure 43 - Micrograph Of Figure 40 Specimen After Etching Showing Low Angle Grain Boundary. Magnification 1230x.



A



B

Figure 44 - Single Crystal Laue Patterns By Back Reflection.

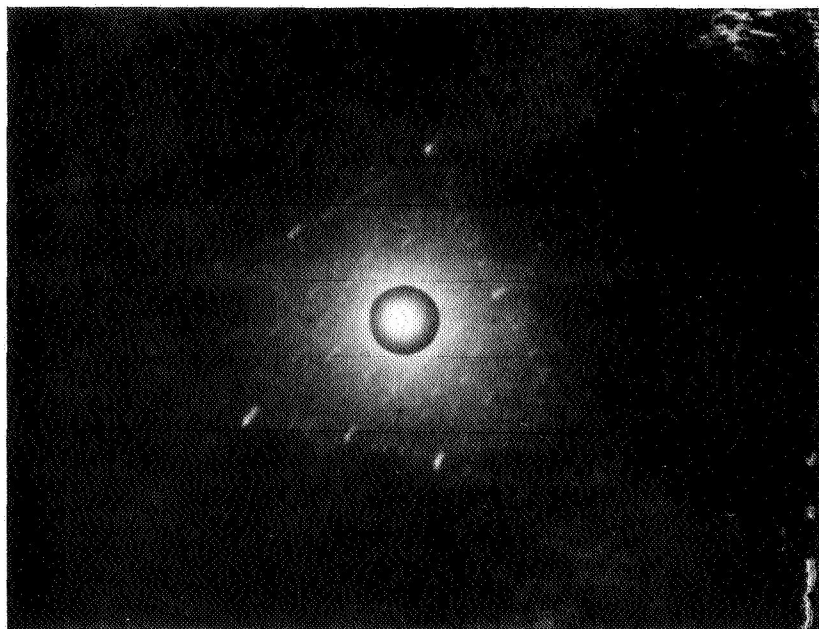


Figure 45a - Asterism In Laue Pattern After Deformation
By Compression

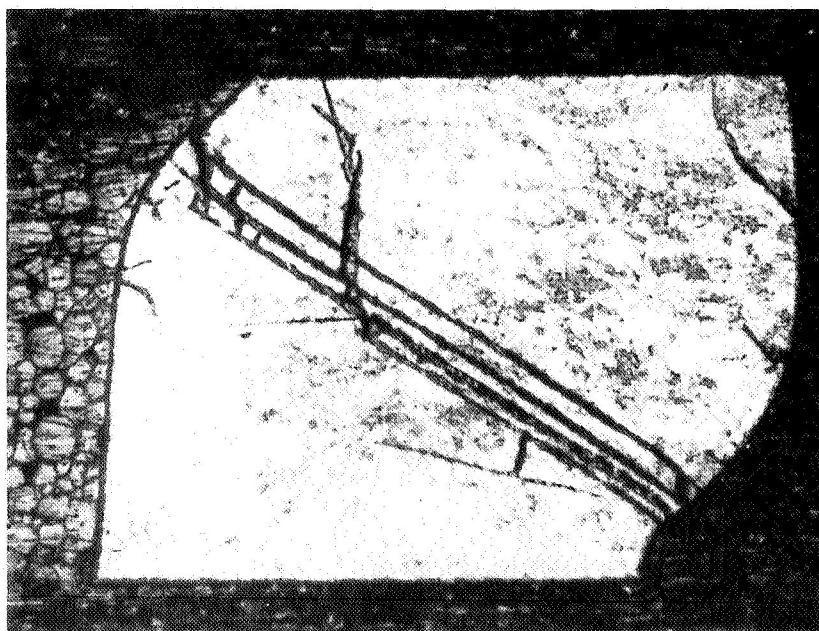


Figure 45b - Slip Produced By Same Compressive Deformation

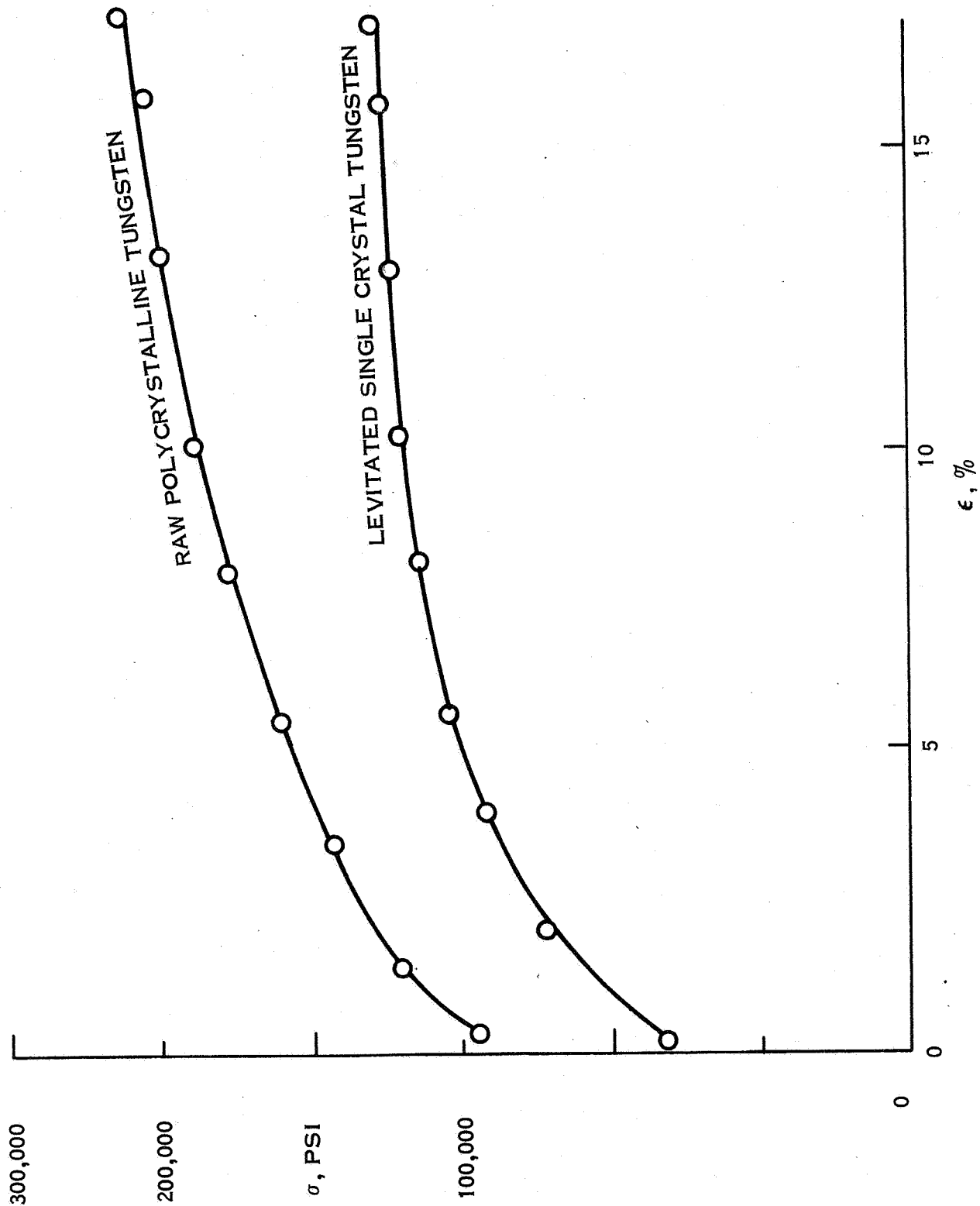


Figure 46 - Stress-Strain Curve Incompression For Starting Material
And Single Crystal Produced By Levitation

2. Compression testing shows that the single crystal tungsten produced is much easier to form, exhibiting the ductility of single crystals. Compression testing was terminated with the onset of slip so the % glide at fracture was not determined. There is no question though that the flattening of single crystal stress-strain curve component to the steady rise of the raw wrought tungsten shows greater formability for the single crystal tungsten.

4.3 SPECIMENS SOLIDIFIED THROUGH FALLING ONTO A WATER COOLED COPPER PLATE WHILE MOLTEN

The specimens were polycrystalline. Examination of one of the small satellite drops shown in Figures 47 and 48a&b shows grain sizes of the order of 300 microns. From these examinations it was concluded that chill casting by dropping a levitated molten tungsten specimen into a water cooled crucible would not produce the fine grained material initially sought. What is interesting here is the columnar growth inward from the surface. This is similar to the growth exhibited when a levitated drop touched the stabilizing ring and solidified. The shrinkage cavity is where the last liquid solidified and almost breaks the surface. That growth started at several sites on the surface is evident in these photographs. There is also no chill zone evident so that where the drop impacted is difficult to define.

4.4 SPECIMENS SOLIDIFIED BY DROPPING INTO MOLTEN TIN

These specimens are shown in Figures 49 and 50. Figures 51 and 52 are regions of fine grained material exhibiting grain sizes of the order of 25 to 100 microns. By and large however these specimens are largely single crystal. It is thought that molten tin may have nucleated the fine grains but that further growth favored only a few nucleation events.

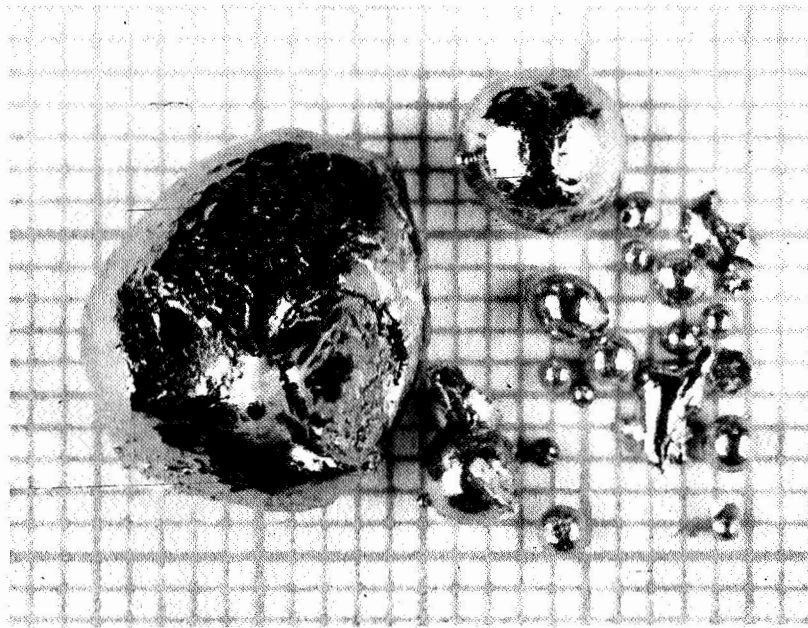
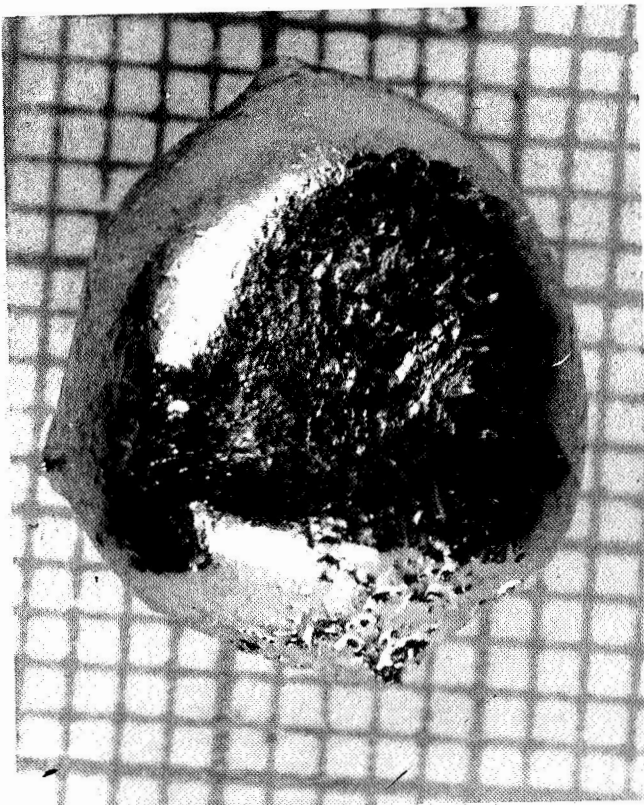
**A****B****C**

Figure 47 - Specimen Solidified Through Falling Onto A Water Cooled Copper Plate While Molten

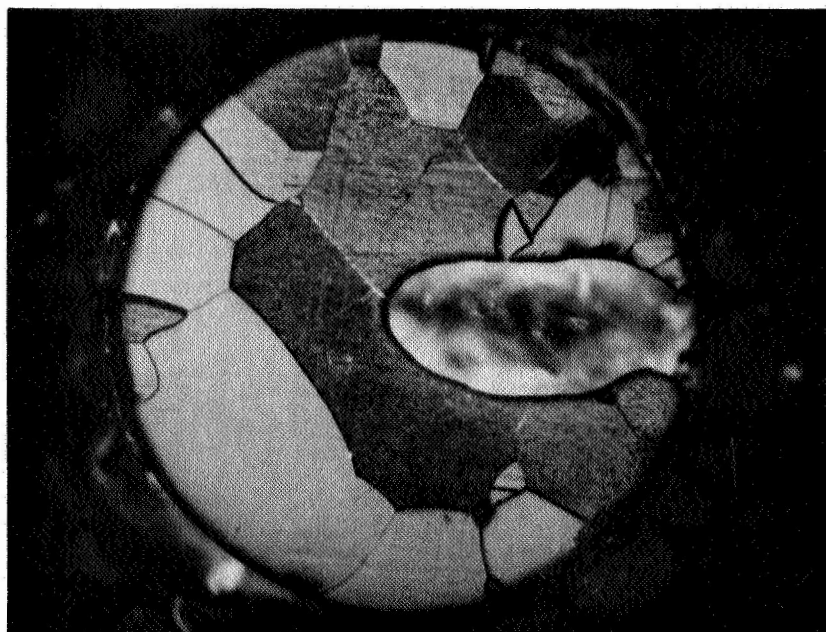


Figure 48a - Small Satellite Drop Sectioned, Etched, And Polished. Magnification 50x

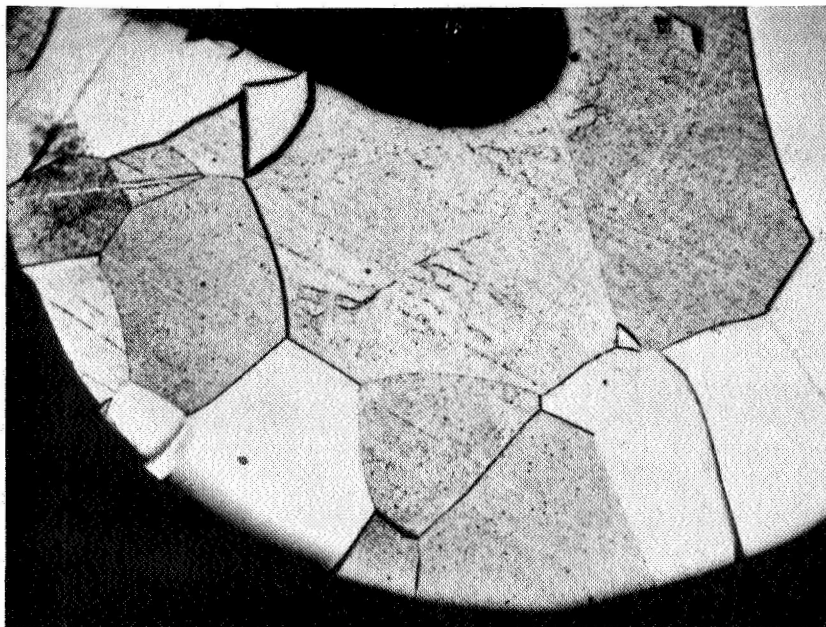
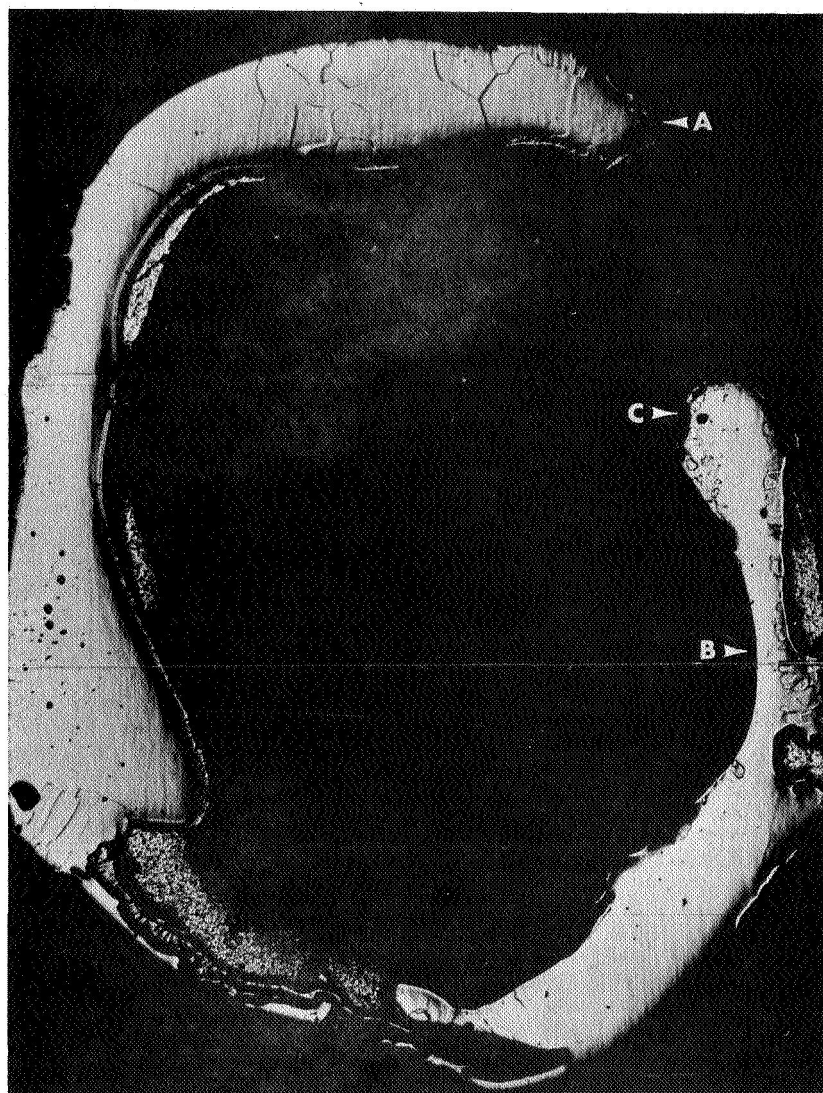


Figure 48b - Small Satellite Drop Sectioned, Etched, And Polished. Magnification 150x

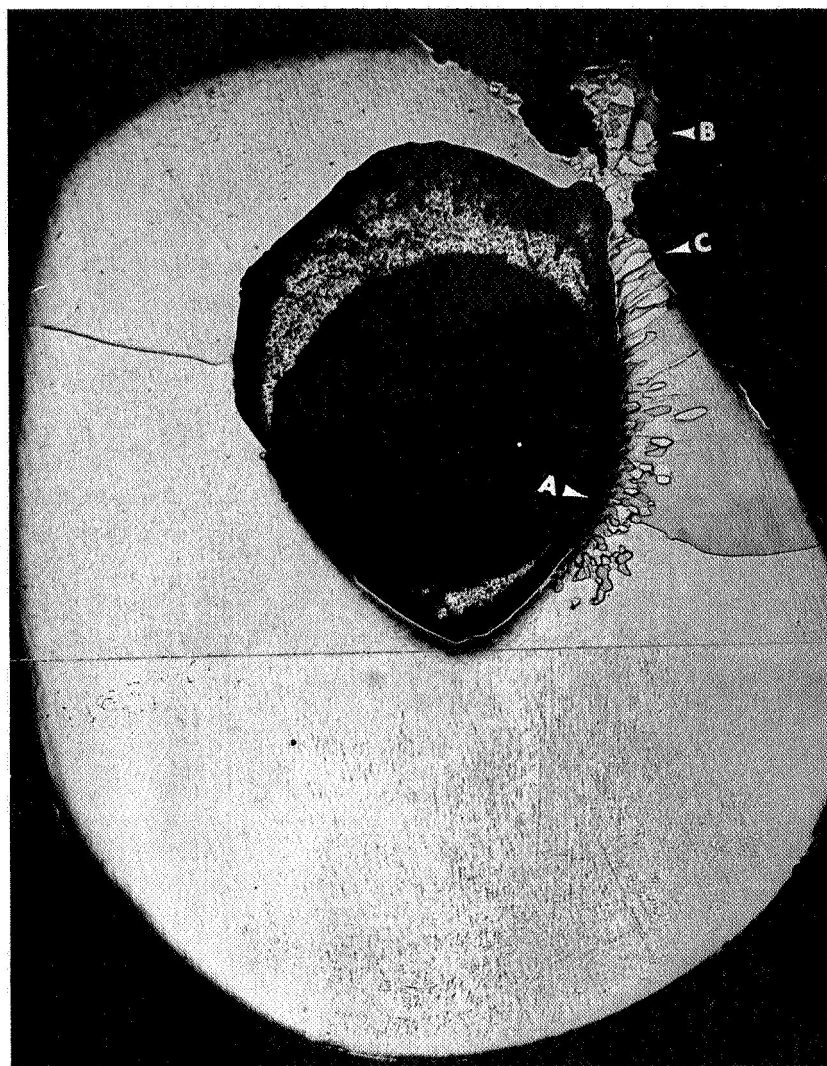
406A



M=11.5X

Figure 49 - Specimen Solidified By Falling Into Molten Tin

406B



M=11.5X

Figure 50 - Specimen Solidified By Falling Into Molten Tin

406A

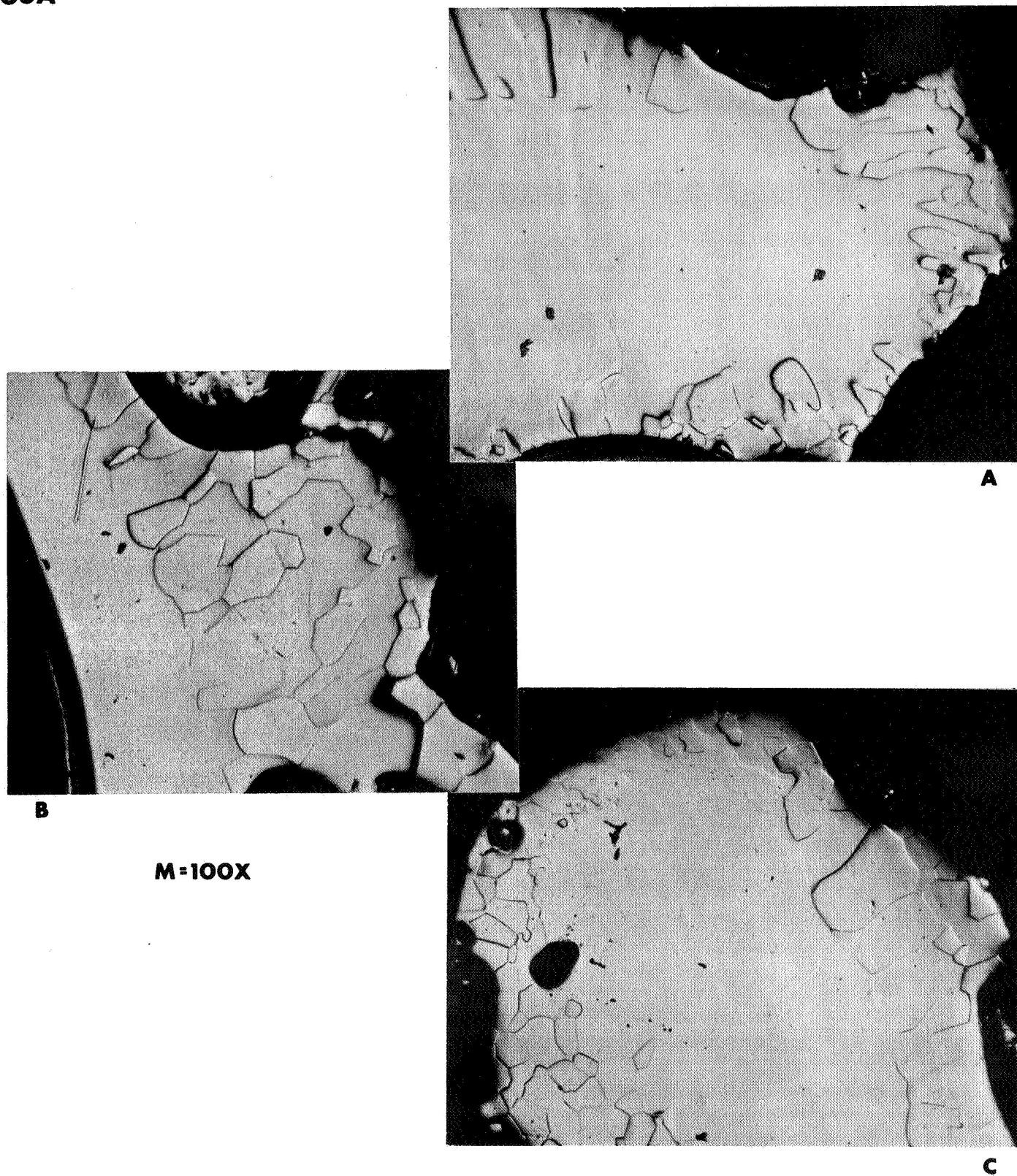


Figure 51 - Fine Grained Regions Of Specimen Solidified
By Falling Into Molten Tin

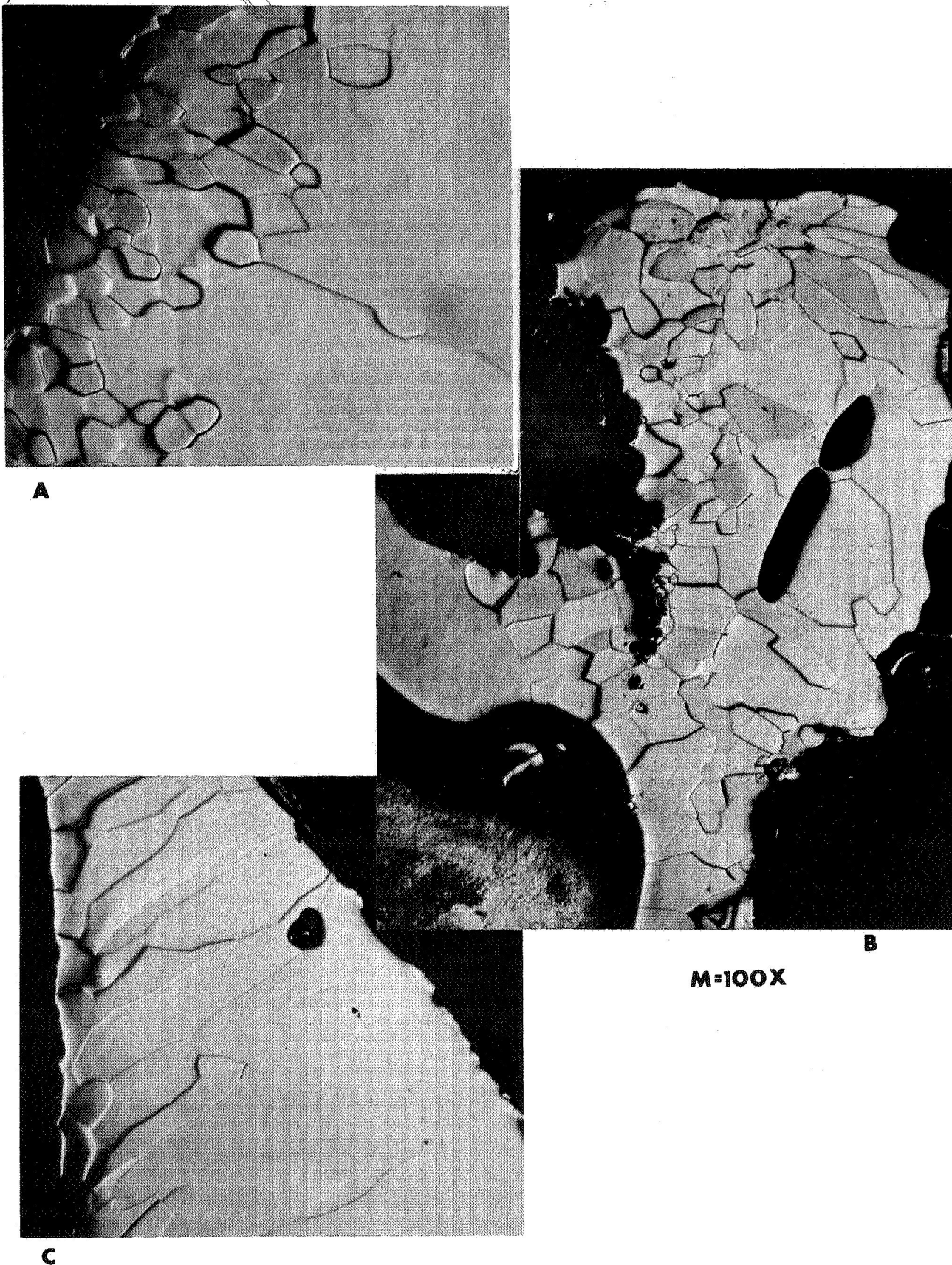


Figure 52 - Fine Grained Regions Of Specimen Solidified By Falling Into Molten Tin

Thus by dropping molten tungsten into a liquid tin quenching medium, large single crystals were again produced with some portions of fine grained material. It was concluded that this was not a viable technique to producing fine grained tungsten in bulk quantities.

4.5 SPECIMENS FREELY FALLING

Specimens which were dropped molten in the four foot drop tower were still molten upon impact at the bottom. These tests showed that with a freely falling molten tungsten specimen, large amounts of supercooling can be obtained. As the specimens were not solid when they impacted, more supercooling could be obtained by lengthening the drop tube to the 16 feet originally contemplated.

These tests show that in the weightless environment of space, free from the influence of the levitation coils, large amounts of supercooling may be expected. The amount of supercooling obtained in the four foot section, from a theoretical standpoint would not produce grain refinement but the amount that could be obtained in the 18 foot drop tower might. Therefore it is felt that continuation of this work is necessary either in the complete drop tower or in the weightless environment of space. The results of these tests can only lend to the conclusion that there is a difference between results produced by terrestrial levitation and in the weightless environment with regard to amount of supercooling achieved. Therefore these tests have served to point out the need for further work in the weightless environment.

4.6 CONTAINERLESS VAPOR DEPOSITION

Vapor deposition from specimens levitated molten produced dense deposits of tungsten up to 3 mils (76.2 microns) thick on molybdenum substrates after a half hour of depositing. A photograph of one of these coatings is shown in Figure 53. There is no evidence of the long dendritic needles characteristic of tungsten deposits produced by chemical vapor deposition. It is thought that

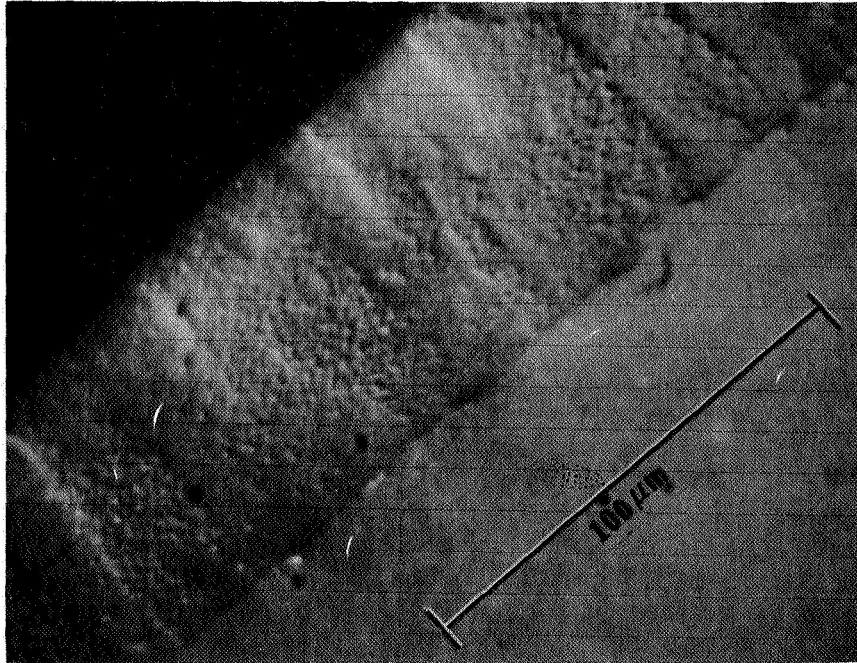


Figure 53 - Vapor Deposited Tungsten Onto Molybdeum Substrate
From Containerless Melt

coatings as thin as 6 mils (152.4 microns) might be suitable as x-ray targets.

Fundamental limitations encountered during this work were the inability to superheat the tungsten to temperatures high enough for rapid vapor deposition. Progressive elongation as shown in Figure 30 resulted in loss of the molten specimen before two hundred degrees centigrade of superheating was obtained. Calculations show that at least six hundred degrees centigrade of superheating above the melting point would be required for practicable vapor deposition onto large target areas. Thus to overcome these limitations, the weightless environment of space, where objects are naturally levitated, offers definite advantages. The economics of this have been discussed above.

Production of x-ray targets by vapor deposition of tungsten onto molybdenum substrates is thought to be one of the more viable routes to enhanced exposure lifetime targets. Although it was not considered originally within the scope of this contract, the results obtained as byproducts during experimental runs are very encouraging and represent one of the more promising areas to be pursued in future work.

5.0 EVALUATION AND ANALYSIS

It is evident from this work that single crystals of tungsten can be produced through solidification while levitated. Consider the levitated molten specimen with electron beam impinging on the top as shown in Figure 54 . By



Figure 54 - Molten Drop With Electron Beam Impinging At Top

observation the bottom tip is at most only a few degrees centigrade above the melting temperature of tungsten because by observation often the tip solidifies and has to be remelted by lowering the specimen a little into the coil upon elongation when first melted. The top where the beam impinges can be one to two hundred degrees centigrade above melting.

When the beam is removed the top with higher temperature and broader surface area for radiation cools faster than the tip but the tip is already at the melting point and can supercool while the top has to still cool down to melting. Thus it is postulated that solidification begins at the bottom tip and proceeds upward with heat being extracted from the surface through radiation and through the solid through conduction to the solid surface where it is radiated away. The solid tungsten has greater thermal conductivity than the liquid and this increases as its temperature falls. The situation is almost like one dimensional solidification except for the rapid extraction of heat through radiation from the surface.

If the melt surface is curved as shown in Figure 55, then stray nuclei at the surface will not grow into the melt and the specimen will be a single crystal. Where more than one nucleation

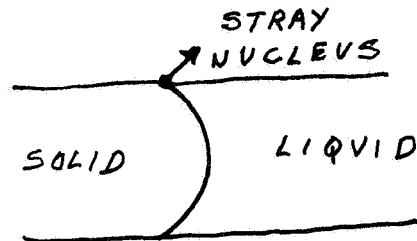


Figure 55 - Solid-Liquid Interface Shape Which Prevents Stray Nuclei From Growing Into Melt

is produced at the tip a bicrystal may be produced. The evidence for this is in Figure 41a. In Figure 41a the shape of the low angle grain boundary is convincing evidence for the melt solid interfacial shape.

This model qualitatively explains the growth morphology observed. If the amount of supercooling is small, then as shown in Figure 56, where the nucleation rate and grain growth rate are plotted qualitatively for amount of supercooling, the growth rate is very large and would account for rapid solidification with production of single crystals or bicrystals. This model would also permit the microscopic subgrain boundary morphology to be explained for even a small amount of supercooling or constitutional supercooling due to minute impurities would promote dendritic growth.

This qualitative explanation fits the observed facts. Coupled with the fact that the specimens remained molten when in free fall, there is convincing evidence that the particular levitation melting technique used for terrestrial containerless processing does not allow appreciable supercooling but that in the weightless environment considerable supercooling can be obtained. From this it can be concluded that in the weightless environment of space achievement of large amounts of supercooling could be expected with resultant grain refinement upon solidification

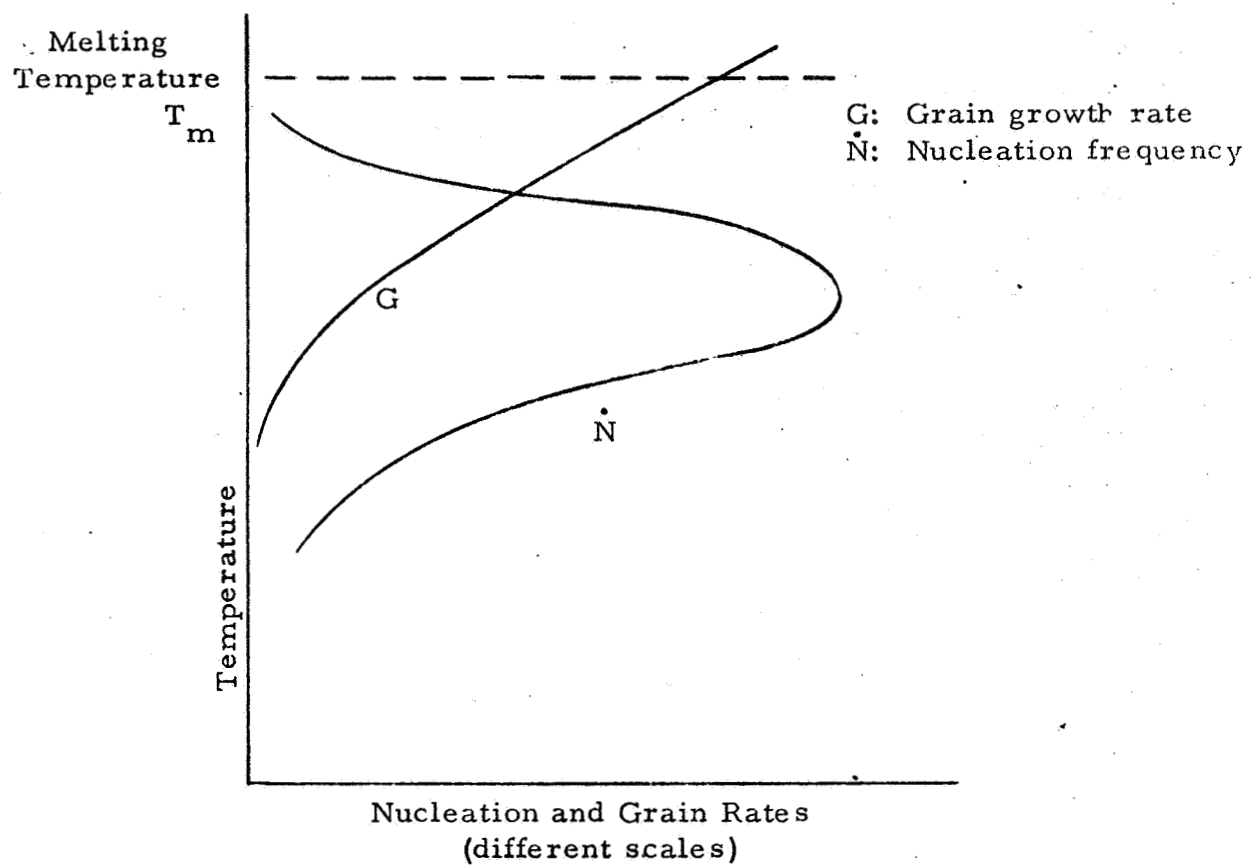


Figure 56 - Nucleation and Grain Growth Versus Degree of Supercooling

5.1 Re-evaluation of BUS Study of Tungsten Targets Produced in Space

The Phase III Beneficial Uses of Space Study (BUS) indicated that prospects were marginal for a business involving space produced tungsten x-ray targets where the business had to bear as much as 1/2 the development costs for an electromagnetic levitation production facility. This study showed that one assumption which would bring the economic measures of return on investment and break-even point within the acceptable range is the assumption of the major cost of the development by the government or other users. During the course of the present contract the effect of changing the assumed cost of electric energy in space was assumed. The Phase III BUS assumption for this energy cost was \$40 per kilowatt hour such as might be produced by a nuclear electric plant.

Since energy costs are a major element in total production cost for this high temperature process example, the effect of a lower energy cost such as could be provided by a solar collector if assumed during the present work. A preliminary study assumed a one million dollar investment in a 32 square meter collector delivering 32 kilowatts at the focus for a 5 year period and showed that a cost of \$1.42 per kilowatt hour might be representative. The effect of this assumption was carried through the tungsten target business calculations with the following results quoted from that study:

Taking the assumption that \$1/KWH could be achieved, the unit cost of a tungsten target could be reduced to \$134, with a resultant doubling of net income and tripling of percent return on investment. The breakeven point would be reduced from 10-12 years to 6-8 years and the venture present value would increase from \$1.6M to \$12.7M. Cumulative cash flow (1975 to 1992) would increase from \$7.7M to \$45.6M. In summary, a dramatic improvement in venture acceptability could be achieved by this reduction in energy costs.

Because of the requirement of operating very near to the tungsten melting temperature in practical evaluation tests, it was concluded that further testing without a highly regulated electron gun would not lead to definitive results. Since such a facility is not available at the Corporate Research and Development Center, a decision was made to turn the actual evaluation tests back to the X-ray Tube Department where such facilities do exist. Present plans are to incorporate improved specimen materials as patches on standard rotating molybdenum target wheels and to carry out the testing in full scale model tubes.

Since the range of 100 Kev electrons in tungsten is less than 10μ , calculations of the minimum tolerable thickness of tungsten on the molybdenum substrate have been carried out by M. German of the Applied Mechanics Branch of the Corporation Research and Development Center. These calculations indicate that the minimum thickness of tungsten, if based upon thermal considerations, is about 6 mils. This result would indicate that vapor deposition might be an attractive method of formation of targets provided that the crystal structure is suitable and if sufficient superheat could be furnished to the evaporation source to achieve practicable deposition rates on surfaces of reasonable size. With this process it is considered that deposition would be carried out on thin large area molybdenum sheets which would then be cut and bonded to the target wheels. Since a time of the order of an hour was required to lay down a 3 mil layer at about 1 inch distance, it is clear that higher superheats will be required to make the process practicable. The elongation and subsequent loss of the levitated tungsten melts observed in the laboratory may indicate a fundamental limit to the superheat which can be achieved for long times in the terrestrial environment. This would indicate the possible viability of this process as a space processing candidate provided the vapor deposited material proves suitable for x-ray target application.

5.2 General Electric Effort on Specimens Characterization

Funded partially by the General Electric Medical Department, Dr. T. Devine at the Corporate Research and Development Center in Schenectady initiated a program for evaluation of potential improved tungsten specimens as x-ray target materials. This effort consisted of designing and constructing a special test device which allows simulation of conditions in the region of electron impact on the x-ray target by duplicating these conditions for a small representative area. The beam size chosen at the point of impact on the specimen materials was 3 mils in diameter. Typical beam energies were 100 Kev at currents on 0.3 milliamperes corresponding to a power density of $30 \text{ watts}/4.4 \cdot 10^{-5} \text{ square cm} = 0.68 \text{ megawatts cm}^{-2}$ which is typical of full scale x-ray tubes. The tungsten target specimen was given a transverse oscillation so that the electron track described an ellipse on the specimen surface, thus simulating the effect of target rotation. Experiments were carried out at a pressure of 10^{-6} torr which is considered sufficient for short term evaluation. (Life testing however will require pressures of 10^{-8} torr which are typical of single crystal tungsten produced in the levitation apparatus. Difficulties in regulation of beam current caused partial melting of the specimen as the power density was adjusted to values which would give tungsten surface temperature near to melting. Despite fluctuations in beam current which exceeded these values, due to poor beam regulations, no gross cracking of the single material was evident. This contrasts with earlier tests using single crystal tungsten produced by zone refining which led to cracking and rejection of single crystal material as a candidate target material,

5.3 CONCLUSIONS

The conclusions to be made from this work are:

1. That single crystals of tungsten can be produced by rapid containerless solidification. The conditions favorable to this result are small supercooling. In the weightless environment of space this could be obtained by controlling the cooling rate. This can easily be accomplished with much larger specimens in the weightless environment of space with independent positioning and heating.

2. Containerless vapor deposition to deposit tungsten onto molybdenum substrates will be enhanced by the ability to superheat the tungsten independent of positioning to temperatures of 4000°C where rapid deposition of fine grained, dense tungsten deposits is expected of as high as 60 mils per hour.

3. Achievement of large amounts of supercooling in the four foot drop indicate that with more time as in the contemplated 16 foot drop tower much more supercooling ($\sim 700^{\circ}\text{C}$) could be achieved. This experiment is worth performing to test the concept of grain refinement through solidification of a highly supercooled melt. In the weightless environment of space, much larger specimens could be supercooled so that scale up in space is necessary for production of pieces large enough to produce x-ray targets.

4. Containerless vapor deposition of tungsten onto molybdenum substrates in the weightless environment of space appears to be the most viable process with single crystal tungsten a close second. The fine grained high purity tungsten should be investigated as a viable route for production of tungsten x-ray targets with respect to grain growth after recrystallization at high temperatures.

5. Containerless single crystal growth as a technique to grow other materials may be one of the most important by-products of this work.

6. Containerless vapor deposition of other materials may also be another most important by-products of this work.

5.4 RECOMMENDATIONS

It is evident that the results obtained during the contract work have provided a firm foundation for future experiments with containerless processing.

In that light it is also evident that only a beginning has been made in the new areas of containerless single crystal growth and vapor deposition that came into being as a result of this work. It is felt that at the present stage of development it would be desirable to pursue this work further not only in single crystal growth and vapor deposition but in supercooling and nucleation as well.

A suggested work statement for a follow-on contract is submitted with this final report. It is hoped that the work can continue as it has much relevance not only to producing better x-ray targets by space processing but to space processing itself. It is also hoped that others will be stimulated by these results to conduct experiments terrestrially and in the weightless environment of space in containerless processing of materials. In that way the results of this work can be furthered to the point where products produced in the weightless environment of space result.

REFERENCES

1. Muck, O., German Patent No. 422,004, October 30, 1933.
2. Bedrod, B.D., Peer, L. H. B., and Tonks, L., "The Electromagnetic Levitator", General Electric Rev. 42, 246-247, 1939.
3. Okress, E. C., Wroughton, D.M., Comenetz, G., Brace, P. H., Kelly, J. C.R., "Electromagnetic Levitation of Solid and Molten Metals", J. Appl. Phys. 23, 545-552, 1952.
4. Frost, R. T., Bloom, H. L., Napaluch, L. J., Stockhoff, E. H., and Wouch G., "Electromagnetic Containerless Processing Requirements and Recommended Facility Concept and Capabilities for Space Lab", Final Report, Contract No. NAS8-29680, NASA Contract.
5. Wouch, G., Okress, E. C., Frost, R. T., and Rutecki, D. J., "Electromagnetic Levitation Facility Incorporating Electron Beam", Rev. Sci. Instrum., Vol. 46, No. 8, August 1975
6. Sell, H. G., "Advanced Processing Technology and High Temperature Mechanical Properties of Tungsten Base Alloys" from "Refractory Metal Alloys, Metallurgy and Technology", edited by Machlin I., Begley, R. T., Weisert, E. D., Plenum Press, New York, 1968.
7. Mueller, C. P., "Economics of Metal Melting with Electron Beams", from "Electron Beam Metallurgical Processing Seminar", Universal Technology Corporation, 1971
8. Lawley Alan, "Electron Beam Refining", from "Introduction to Electron Beam Technology" edited by Bakish, R., John Wiley and Sons, Inc., 1962.
9. Rugh, J. W., Proc. First Symp. Electron Beam Tech., J. Hetherington, Editor, Boston, Mass, p.89, 1959.
10. Bechtold, J. H., and Shewmon, P. G., "Flow and Fracture Characteristics of Annealed Tungsten", Trans. ASM, Vol. 46, 1954, pp 397-408.
11. Wronski, A. and Fordeux, A., "Slip Induced Cleavage in Polycrystalline Tungsten", J. Less-Common Metals, Vol. 6, 1964, pp 413-429.
12. Hull D., Beardmore P., and Valentine, A. P., "Crack Propagation in Single Crystals of Tungsten", Phil. Mag, Vol. 12, No. 119, Nov. 1965, pp 1021-1041
13. Biggs, W. D., "Fracture", Chapter 20 of "Physical Metallurgy" R. W. Cahn, Editor, North Holland Publishing Company-Amsterdam, 1965

14. IBID Ref. 10
15. Beardmore, P., and Hull, D., "Deformation and Fracture of Tungsten Single Crystals", J. Less-Common Metals, Vol. 9, 1965, pp 168-180
16. Oku, T., and Galligan, J. M., "Plastic Deformation of Zone-Refined Tungsten Between 4.2 and 300K". Rep. Jaeri-Memor 4124, Japan Atomic Energy Research Inst., Augu 1970.
17. Das, G., and Radcliffe, S. V., "Effects of Hydrostatic Pressure on the Mechanical Behavior of Tungsten", Trans. Japan Inst. Metals, Vol. 9, Supplement, 1968, pp 334-342.
18. Das, G., and Radcliffe, S. V., "Pressure-Induced Development of Dislocations at Elastic Discontinuities", Phil. Mag., Vol. 29, No. 165, Sept. 1969, pp 589-609.
19. Wronski, A.S., and Chilton, A. C., "The Effects of Temperature and Pressurization on the Tensile and Compressive Properties of Polycrystalline Cast Tungsten", Scripta Met., Vol. 3, No. 6, June 1969, pp 395-400.
20. Verbraak, C. A., "Effects of High-Energy Rate-forming on Properties of Refractory Metals", From "The Science and Technology of Tungsten, Tantalum, Molybdenum, Niobium, and their Alloys", N. E. Promisel, Editor, Macmillan Company Distributor for Pergamon Press, Ltd, 1964 21.
21. Stephens, J. R., "An Exploratory Investigation of Some Factors Influencing The Room-Temperature Ductility of Tungsten," NASA TND-304, 1960.
22. Stephens, J. R., "Effects of Oxygen on Mechanical Properties of Tungsten", NASA TND-1581, 1963
23. Bechtold, J. H., "Strain Rate Effects In Tungsten", J. Metals, Vol. 8, No. 2, Feb. 1965, pp 142-146
24. Chilton, A.C., and Wronski, A. S., "The Effects of Strain Rate And Pressurization on the Ductile-Brittle Transition Temperature of Polycrystalline Sintered Tungsten", J. Less-Common Metals, Vol. 17, Apr. 1969, pp 447-450.
25. Seigle, L. L., and Dickinson, C. D., "Effect of Mechanical and Structural Variables on the Ductile-Brittle Transition In Refractory Metals" Refractory Metals II, I. Perlmutter and M. Semchyshen, Editors, Interscience Publ., 1963 pp 65-116.
26. Thornley, J. C., and Wronski, A. S., "The Effects of Grain Size and Annealing Temperature on the Mechanical Properties of Cast Tungsten", Materials Science Research Final Report, Univ. Bradford, England, 1970.

27. Stephens, J. R., "Effects of Interstitial Impurities on the Low-Temperature Tensile Properties of Tungsten", NASA TND-2284, 1964.
28. Savitsky, Ye. M., Tsarev, G. L., "Investigations of Effect of Interstitial Impurities on the Structure and Properties of Tungsten Single Crystals, NASA TTF-10157, 1966
29. Rose, R. M., Ferriss, D. P, and Wulff, J., "Yielding and Plastic Flow in Single Crystals of Tungsten", Trans. AIME, Vol. 224, No. 5, October 1962, pp 981-990
30. Argon, A. S., and Maloof, S. R., "Plastic Deformation of Tungsten Single Crystals at Low Temperatures", ACTA Met, Vol. 14, No. 11, Nov., 1966 pp 1449-1462
31. Garfinkle, M., "Proportional-Limit Stress of Tungsten Single Crystals", Trans. AIME, Vol. 236, No. 9, Sept. 1966, pp 1373-1374
32. Wolff, Ursula E., "Twinning and Fracture in Tungsten Single Crystals at Room Temperature", Trans AIME, Vol. 224, No. 2, APR. 1962, pp 327-333
33. Koo, R. C., "Effects of Purity on the Tensile Properties of Tungsten Single Crystals From -196°C to 29°C", ACTA Met., Vol. 11, No. 9, Sept. 1963, pp 1083-1095.
34. Ibid Ref. 15
35. Stephens, J. R., "Dislocation Structures In Slightly Strained Tungsten, Tungsten-Rhenium, and Tungsten-Tantalum Alloys, Trans-Aime, Vol. 242, No. 4, Apr. 1968, pp 634-640.
36. Stephens, J. R., "Dislocation Structures In Single-Crystal Tungsten And Tungsten Alloys" Metallurg-Trans-, Vol 1, No. 5, May 1970, pp 1293-1301.
37. Arsenault, R. J., Crone, C.R., and Carnahan, R. D., "Dynamic Microplasticity of BCC Metals And Solid Solutions", EMG Rep. No. XXIII, University Maryland 1970
38. Ibid 36
39. Crutchley, D. E., and Reid, C. N., "Mechanical Properties of Chromium Single Crystals", High Temperature Materials, F. Benesovbky, Editor, Metall Werk Plansee Ag., 1969, pp 57-66
40. Ibid 36
41. Promisel, N.E., "Why Refractory Metals", From "The Science And Technology of Tungsten, Tantalum, Molybdenum, Niobium and Their Alloys", N.E. Promisel, Editor, Pergamon Press, 1964.

42. Bergley, R. T., Harrod, D. L., and Gold, R. E., "High Temperature Creep and Fracture Behavior of the Refractory Metals", from "Refractory Metal Alloys, Metallurgy and Technology", I. Machlin, R. T. Bergley, and E. D. Weisert, Editors, Plenum Press, New York, 1968.
43. Conrad, H., "The Role of Grain Boundaries In Creep and Stress Rupture", from "Mechanical Behavior of Materials at Elevated Temperatures", J. E. Dorn, McGraw-Hill Book Company, Inc., 1961.
44. Rieck, G. D., "Tungsten and Its Compounds", Pergamon Press, 1967, pp 62
45. Weinberg, F. "Grain Boundaries In Metals", from "Progress In Metal Phycis", 8, Pergamon Press Ltd., 1959
46. Rony, P. R., UCRL Report 11411 (1964)
47. Cahn, R. W., "Recovery and Recrystallization", from, "Physical Metallurgy", Cahn, R. W., Editor, North-Holland Publishing Company, Amsterdam, 1965.
48. Vandermeer, R. A. and Gordon, P., "Recovery and Recrystallization of Metals", Interscience Publishers, New York, 1963.
49. Ovsienko, D. E., "On The Nature of the Formation of Dislocation Structure in Metallic Crystals During Growth From the Melt", from "Growth and Imperfections of Metallic Crystals, D. E. Ovsienko, Editor, Consultants Bureau, New York, 1968.
50. Flemings, M. C., "Solidification Processing", McGraw-Hill, Inc., 1974